A FIELD INVESTIGATION TO STUDY THE RESPONSE OF BURIED POLYETHYLENE NATURAL GAS PIPELINES SUBJECTED TO GROUND MOVEMENT

by

Jeremy F. Groves

B.A.Sc., The University of British Columbia, 2009

A THESIS SUBMITTED IN PARTIAL FULFILLMENT OF

THE REQUIREMENTS FOR THE DEGREE OF

MASTER OF APPLIED SCIENCE

in

THE FACULTY OF GRADUATE AND POSTDOCTORAL STUDIES

(Civil Engineering)

THE UNIVERSITY OF BRITISH COLUMBIA

(Vancouver)

March 2014

ABSTRACT

The performance of buried natural gas pipelines located in areas prone to ground movement is a major concern for utility owners since the failures of such pipeline systems during service is extremely serious due to the potential for loss of life, as well as the associated environmental and economical impacts. With plastic pipes now the industry standard for most utility distribution systems (e.g., medium density polyethylene (MDPE) pipes for natural gas distribution), understanding the response of these extensible pipes when subjected to ground movements is an important consideration and critical for their integrity.

Through previous research work conducted at the University of British Columbia (UBC) on the subject of extensible natural gas pipelines subject to relative ground movements, a new analytical model was developed to account for the soil-pipe interaction mechanisms for buried MDPE pipes. The new approach can be used to estimate the relative ground surface movements needed for pipe failure, which is an important consideration for evaluating the field-performance of pipe systems in areas prone to landslide movements.

In order to further validate the new analytical model, a large-scale field-testing program was implemented that consists of five MDPE pipeline alignments buried at a site which is part of a slow-moving landslide. The pipelines were instrumented with over 200 strain gauges that provide pipe strain data induced due to continuing ground movements at the research site. Along with the pipe strain data, close monitoring of the system for overall pipe and ground surface movements is ongoing, and the collected information is expected to provide a reliable database of ground movement and associated pipe strain to further validate the new analytical model.

Laboratory element-level testing was conducted to investigate the effects of strain gauge stiffening on local strain readings on the MDPE pipes used in this study. The results indicate that the strain gauge installation procedures used throughout this research have minimal stiffening effects on the pipes.

In addition to implementing the field experiment, a framework for using the field data to predict the axial pipe strain for the pipes in this study using the new UBC model is presented.

PREFACE

This master's thesis contains details of the research program conducted at the University of British Columbia during the period of September 2011 to March 2014. All of the experimental and analytical work presented in this thesis was carried out by the author under the supervision of Professor Dharma Wijewickreme. The author acknowledges the comments provided by the second thesis reviewer, Professor Tony Yang.

A version of Chapter 3 has been published in the proceedings of the 2013 Canadian Geotechnical Society annual conference and is listed below.

Groves, J. and Wijewickreme, D. (2013) Field monitoring of buried polyethylene pipelines subjected to ground movement, Proceedings of the 66th CGS Conference September 29-October 5, 2013, Montreal, Quebec.

TABLE OF CONTENTS

LIST OF TABLES

LIST OF FIGURES

NOMENCLATURE

A_p	The cross sectional area of the pipe
a, b, c, d	Constants that can be determined by fitting the stress-strain responses obtained from uniaxial extension or compression tests
D	Outside diameter of the pipe
D_i	Inside diameter of the pipe
d_{50}	The average grain size of the soil
$G_{(\gamma)}$	Shear modulus of soil at a shear strain of γ (N/m^2)
H	Depth from ground surface to pipe springline (m)
K_0	Coefficient of lateral earth pressure of the soil backfill around the pipe (non dimensional)
N_{qh}	Dimensionless horizontal bearing capacity factor
P_U	Ultimate lateral soil resistance per unit length (N/m)
T	Axial soil load on the pipe per unit length of pipe (N/m)
Δt_d	Thickness of the soil shear zone outside of the buried pipe diameter
$(\sigma_n')_{av}$	Average normal soil load
δ	Interface frictional angle between soil and pipe
γ_t	Effective soil total unit weight (i.e. the average unit weight that would lead to the computation of soil effective stress at the pipeline springline (N/m^3)
ε_θ	Strain on the inside surface of the pipe
ε_{axial}	Axial strain of the pipe

ACKNOWLEDGEMENTS

The research work presented in this thesis is not the work of just one author, rather it is a collaboration of efforts put forth by a wide range of individuals and I am pleased to extend my appreciation to all of those who have been involved.

First, I would like to thank my supervisor Dr. Dharma Wijewickreme for the opportunity to work on this project as it has greatly enhanced my perspective on the field of geotechnical engineering with specifics on soil-pipe interaction. The value of the time and effort that you spent throughout this projects inception, implementation and ongoing data collection have contributed hugely to its success and my appreciation cannot be overstated.

None of this research would be possible without the technical and financial contributions from FortisBC Energy Inc., of Surrey, BC. I would like to extend my particular thanks to Bassam Saad for your ongoing support and consultations, as well as Frank Mostad and Mujib Rhaman for your contributions.

With specific reference to the preparation for the fieldwork portion of this research, I would like to thank all of those involved at the UBC civil engineering workshop, including Scott Jackson, Herald Schremp, Bill Cheung, Doug Hudnik and Mark Rigolo.

Thanks are due to Mike Gray, Ryan Teesdale and their crew from Canadian Utility Construction Corp. for helping with the pipe installations, Wayne Moseanko with the City of Chilliwack for allowing provisions to the site, Dr. Alex Sy for information pertaining to historical ground movements at the site, Professor Ian Moore and Professor Richard Brachman (Queen's University, Kingston, Ontario) and FortisBC Energy Inc. survey crews for your ongoing ground monitoring efforts.

I owe particular thanks to Dr. Lalinda Weerasekara for your ongoing technical support and your keen interest with this research.

Last but certainly not least, a special thanks is owed to my family who has provided me with enduring support and encouragement throughout my years of education.

CHAPTER 1: INTRODUCTION

Prior to 1940, natural gas distribution pipeline networks were primarily made from wrought and cast iron pipes. Just as the 1940s and 1950s saw a shift to steel pipeline materials, the 1970s brought a transition from steel to plastic services, except for the larger diameter installations that continued to rely on steel.

Through more than 100 years of application in a variety of industries, steel pipe properties became well established and standardized. Early steel pipeline failures led to stricter and more safety conscious design standards for all types of pipes, which are reflected throughout industry standards such as ASCE (1984) and ALA (2001). Furthermore, in the last few decades, a significant amount of research has been completed to develop pipe performance models for high capacity steel transmission lines. A relatively comprehensive knowledge base regarding the soil-pipe interaction for steel pipes has been developed through research ranging from full-scale models to centrifuge testing and monitoring, analytical and numerical modeling.

Soil-pipe interaction models for modern day polyethylene (PE) pipelines however, are not as well established compared to steel pipes mainly due to the more recent adoption of PE pipes to the industry. The capabilities and characteristics of PE, however, have greatly improved since their initial implementation more than 40 years ago, and PE pipeline networks have established an impressive safety record over the past few decades. Today's natural gas distribution companies install PE services confidently as a result of continued industry attention and education involving better materials and a better understanding of the performance of these materials for both immediate and long term system integrity. Unlike steel pipes, however, very few experimental studies have been performed to evaluate the performance of PE pipes subjected to soil loading. Consequently soil-pipe interaction models used for steel pipes are often considered for analyzing PE pipeline systems.

Despite this limited knowledge on soil-pipe interaction aspects, today's PE pipes are well engineered and are considered to provide a good balance of strength, stiffness, toughness and durability meeting the demands of the gas distribution industry. For the gas distribution industry, the choice of using PE pipes over steel pipes offers a number of advantages including, but not limited to: low material cost, light weight design (ease of transport and handling), high volume

manufacturing (extrusion, injection moulding), design flexibility (easily shaped), flexibility (ease of transport and handling, use of conjunction with trenchless technologies and resistance to seismic activity), relative ease of jointing, corrosion and chemical resistance, toughness, impact resistance, abrasion resistance and long term durability, technical lifetime of >50 years, low maintenance costs and environmental benefits (recyclable) (O'Connor 2012).

Maintaining the safety and reliability of PE natural gas pipeline systems are important across all areas of the industry, from production to transport, to the delivery of gas to residential and commercial users. PE pipeline failures, however, can occur for a range of reasons including: system design deficiencies, errors in manufacturing and installation, accidental damage, incorrect material selection, thermal exposure, stressing beyond anticipated design stress, point loading, weathering, chemical exposure, and soil conditions (O'Connor 2012).

The research program presented herein considers the performance of buried PE pipes subjected to ground movement in natural gas distribution systems. The ground movements in question have the potential to put significant strain on buried PE piping systems. While PE piping materials are generally, as a ductile material, very resistant to strain, there are limits to the material performance at large strains where mechanical failure could occur. It is therefore important to understand the response of the pipe to these applied strains to define a safe operating window for the pipeline owners.

1.1 Problem statement for the present study

The performance of buried natural gas pipelines located in areas prone to ground movement is a major concern for utility owners since the failures of such pipeline systems during service is extremely serious due to the potential for loss of life, as well as the associated environmental and economical impacts. With plastic pipes now the industry standard for most utility distribution systems (e.g., medium density polyethylene (MDPE) pipes in natural gas distribution), understanding the response of these extensible pipes when subjected to ground movements is an important consideration and critical for their integrity.

Natural gas distribution pipeline networks are exposed to a wide variety of natural hazards since they cover such large areas. According to PHMSA (2010), post-failure analyses revealed that the

majority of gas distribution pipeline failures are attributed to excavation damages. However, when the excavation and intentional damages to pipelines are taken aside, ground movements cause more than 10% of the accidents.

In many instances, ground movement hazards that pose a risk to pipeline networks can be identified with good confidence and monitoring these ground movements can be done relatively easily before the actual occurrence of the pipe failure takes place. Correlating these ground movements to the pipe deflection and the loads applied on the pipe, however, can be challenging without reliable models to correlate such displacements to the conditions of the buried pipe (typically the strain in the pipe). The pipe deflection cannot be considered equal to the ground movement as a result of the differences in the stiffness of the pipe and the soil surrounding it, the soil-pipe interaction (which depends on the pipe and the soil properties) and the pipe relaxation over time. It is therefore important to develop analytical and numerical methods to correlate the pipe performance to the measured ground movements.

With this background, a research program was initiated at the University of British Columbia (UBC) in collaboration with FortisBC Energy Inc. of Surrey, BC, to investigate the performance of buried MDPE pipelines subjected to ground movements. During the earlier stages of this research, a full-scale soil-pipe testing facility was developed and several full-scale pipe pullout tests on selected diameters and configurations of MDPE pipes were performed (Anderson, 2004; Weerasekara, 2007). During more recent stages of this research (Weerasekara, 2011), a field-testing program was conducted on five axial pipe pullout tests with different burial depths, pullout rates and loading regimes. The laboratory and field pullout tests led to the development of a new analytical model to determine the response of pipes subjected to axial and lateral soil loading. The model was derived using an advanced interface friction model to account for the soil dilation and interface friction aspects, and combined with the MDPE pipe nonlinear stress-strain pullout resistance, displacement and mobilized frictional lengths obtained from the experimental data.

The present study is a continuation to the previous research work that has been carried out at UBC on this subject.

1.2 Objectives of the thesis

The main purpose of the current research is to further validate the new analytical model that was developed at UBC using a full-scale field test established to monitor the performance of MDPE pipelines subjected to ground movement. The ultimate goal of this research is to provide further contributions to the previous research work on this subject to help develop guidelines and criteria to determine the amount of ground displacement associated with the safe operational limits of buried natural gas distribution pipelines. Accordingly, the key objectives for the current thesis are highlighted below:

1. Design and implement a full-scale field testing program to monitor the performance of buried MDPE pipelines subjected to ground movement.

2. Develop a reliable database of ground movement and associated pipe strain data from the full-scale field test that can be used to further validate the new UBC model.

3. Conduct laboratory tests on MDPE pipe samples to determine the reliability of the strain gauge instrumentation used throughout the field test.

4. Provide a general framework for using the field data from this study to calculate the pipeline axial strain for the buried pipes installed for this research using the new analytical model developed at UBC.

1.3 Scope of the thesis

In order to accomplish the research objectives outlined above, the following scope of work was carried out:

1. A full-scale field testing program was designed and implemented, which consisted of burying five MDPE pipeline alignments in a slow moving landslide located in Chilliwack, BC. Prior to the installations, the pipes were instrumented with over 200 strain gauges to provide pipe strain data as they are induced to deformations caused by the continuing ground movement at the selected research site.

2. Established a data collection program for the field study, which includes regular acquisition of the buried pipe stain, pipe deformation and ground surface movement data.

3. Carried out thermally induced contraction tests on four MDPE pipe specimens to determine the effects of strain gauge stiffening on local strain readings for the MDPE pipes used in this study.

4. Provided a general framework for using the field data from this study to calculate the pipeline axial strain for the buried pipes installed for this research using the new analytical model developed at UBC.

1.4 Organization of the thesis

Chapter 1 provides the background information pertaining to the research problem and highlights the key objectives, the scope of work and the organization of this thesis.

Chapter 2 presents a concise summary of the published literature that has contributed to the current understanding of soil-pipe interaction for MDPE pipes, which includes the analytical techniques contributed from UBC that can be used for analyzing the response of buried MDPE pipes subjected to ground movement. This chapter also includes a detailed discussion of the mechanical properties of MDPE.

Chapter 3 outlines the details associated with the field installation and instrumentation of the pipeline alignments employed for this research and also highlights the data collection methodology established for the study. Results from the first six months of data collection for the field experiment are also presented.

Chapter 4 provides the background, methodology, and results from eight laboratory tests performed on four MDPE pipe samples to investigate the effects of strain gauge stiffening on local strain readings for the pipes used in this research.

Chapter 5 discusses a framework for the selection of input parameters for use in the new UBC analytical model to predict the axial strain of the buried pipeline alignments in this study. Projected model results for these pipelines based on a hypothetical scenario of landslide-induced movement is also presented

Chapter 6 provides a summary of the research carried out for this study and a discussion on future research considerations and needs.

Appendix A provides a series of photos taken at the research site throughout the field program implementation.

Appendix B provides a detailed description of the strain gauge installation procedures used for this project.

Appendix C provides a detailed presentation of the installed strain gauge locations and labels for the buried pipeline alignments.

Appendix D provides a detailed summary of the locations of the survey monument points established at the site for monitoring the ground surface movements as well as the pipe deflections.

Appendix E presents experimental observations of field data from the subject research site collected between May 23, 2013 (study implementation) and December 31, 2013.

Appendix F presents the results from the laboratory tests conducted to investigate the effects of strain gauge stiffening on local strain readings for the MDPE pipes used in this research.

CHAPTER 2: LITERATURE REVIEW

Although the design approaches for the installation of buried MDPE gas pipes are well established, these approaches are based on a stable, at rest, soil-pipe system. The soil-pipe interaction becomes a more complex and important consideration when the buried pipeline is located in areas of significant ground movement. Upon a review of the literature available on this subject, no standard design approaches for accounting for the performance of buried MDPE pipelines subjected to ground movement conditions were identified. The following sections, however, provide a summary of the available information related to this problem and include the guidelines presently used in the current design practice.

2.1 Current design practice for buried pipelines subjected to ground movement

The initial step to determining pipeline response due to ground movement is to carry out a regional-level pipeline risk assessment to determine the regions of the pipeline that are most vulnerable to permanent ground deformation from hazards such as faulting, landslides, liquefaction or seismic settlements. Once the vulnerable regions are identified from the regional assessment, a more detailed site-specific soil-pipe interaction analysis can be carried out on local pipe segments (Wijewickreme et al. 2005). Four basic pipe loading mechanisms can be identified based on the orientation of the pipeline segments with respect to the direction of the ground movement, namely:

1. Pipe is subject to axial tensile loading,
2. Pipe is subject to axial tensile loading and pipe bending,
3. Pipe is subject to axial compressive loading, and
4. Pipe is subject to axial compressive loading and pipe bending.

Both analytical and numerical methods can be used to estimate the performance of the pipe for each of the above loading scenarios. Closed-form analytical models can be derived when giving consideration to the equilibrium and compatibility conditions of the pipe at an element-level, and numerical models use traditional soil-spring analysis to estimate the loading situations. Soil-spring analyses represent the soil loading in three basic directions, namely, along the pipe axis (axial), perpendicular to the pipe axis (lateral), and upward or downward directions. The pipe

performance (strain) is estimated by solving the equilibrium and compatibility equations using built in algorithms in the numerical model with the selected pipe material properties. When using either analytical or numerical techniques it is important to understand the soil loading characteristics in each direction of the soil spring model to estimate the pipe performance.

The soil-pipe interaction problem can be discussed using a three-component framework in the analytical and numerical formulations (ASCE 1984):

1. Determine the external soil loads on the pipe due to relative ground movements,
2. Determine the stress-strain behaviour of the pipe material, and
3. Combine the soil loading and the stress-strain behaviour to derive an overall pipe performance model based on the element-level equilibrium and compatibility conditions.

The current design approach to calculate pipe pullout resistance and the soil-pipe interface shearing resistance in cohesionless soils consider the effects of the unit weight of the backfill material, depth of the pipe burial, the coefficient of lateral earth pressure, the friction angle of the soil and the friction angle of the pipe interface. The basic concept is that the frictional resistance along the outside of the pipe depends directly on the normal stress acting on the pipe and the frictional characteristics of the soil-pipe interface. It should be noted that this approach does not consider the effect of temperature or strain rate on the interface shearing resistance.

This approach has been adopted by various guidelines for the design of buried pipelines subjected to ground movement, such as ASCE (1984) "Guidelines for the Seismic Design of Oil and Gas Pipeline Systems," American Lifeline Alliance (2001) "Guidelines for the Design of Buried Steel Pipe," and PRCI (2009) "Guidelines for the Seismic Design and Assessment of Natural Gas and Liquid Hydrocarbon Pipelines,"

The average normal soil load, $(\sigma'_n)_{av}$, acting on the pipe under "at rest conditions" is given by:

$$(\sigma'_n)_{av} = \frac{(1+K_0)}{2}\gamma_t H$$

Where:

K_0 is the coefficient of lateral earth pressure of the soil backfill around the pipe

γ_t is the effective soil total unit weight (i.e., the average unit weight that would lead to the computation of soil effective stress at pipeline springline)

H is the depth to the pipe springline

This equation ignores any interactions, such as soil arching, taking place between the pipe and its surrounding soil (Petroff 1990). Then, using the equation for the average normal stress above, the axial soil load on the pipe per unit length of pipe, T, is given by:

$$T = \frac{\pi D H \gamma (1 + K_0) \tan\delta}{2}$$

Where:

D is the outer pipe diameter

δ is the interface friction angle between soil and pipe

As mentioned above, this equation is widely used for pipeline performance design. Newmark and Hall (1975) used this equation to calculate axial soil loads on pipes subjected to strike slip fault movement, and Kennedy et al. (1977) used it to assess pipelines subject to large deformations that eventually form into a cable-like profile closer to the fault crossing.

Using this equation to estimate the axial pullout resistance of MDPE pipes is not a trivial task as the accuracy of the calculations becomes complicated due to the complexities associated with the input parameters. Although this equation has been widely used in practice for the design of buried pipelines, several pipeline studies have shown discrepancies between the measured experimental pullout resistance during axial pipe pullout and the calculated axial pull out resistance using this equation and using the best estimated input parameters (Paulin et al 1998; Anderson 2004; Wijewickreme et al. 2009; Karimian 2006). In addition to the interface friction at the soil-pipe interface, the main factors that have been noted to influence the discrepancy between the measured and the calculated pullout resistance are the shear-induced dilation of soil at the soil-pipe interface and frictional degradation behaviour of soils under large shear displacements.

In consideration to soil loads acting perpendicular to the buried pipeline axis, the current recommendations for calculating the ultimate lateral soil resistance per unit length, P_u, for soils with no apparent cohesion can be expressed as:

$$P_u = N_{qh} \gamma H D$$

Where:

N_{qh} is the dimensionless horizontal bearing capacity factor

This equation is recommended by the ALA (2001) guidelines using the analytical model by Hansen (1961) to calculate N_{qh}. The N_{qh} values recommended by PRCI (2009), based on Yimsiri et al. (2004), are considered the state of the art in assessing soil loads on pipelines subjected to relative lateral soil movement.

In other research studies attempting to define the performance of buried pipelines, particularly for earthquake induce ground movements, approximate analysis procedures for both segmented and continuous buried pipelines are presented for axial and lateral loading conditions (O'Rourke 1989; O'Rourke and Nordberg 1990). Analytical relationships were developed for the longitudinal strain in continuous pipes, which were subsequently compared with finite element results based on information on the geometry of earthquake induced lateral spreads in Japan. It has been shown that these approximate analytical results compare well with the finite element model results.

Researchers also investigated the field performance of buried pipelines following the permanent ground displacements resulting from the earthquake-induced liquefaction during the 1971 San Fernando and 1994 Northridge Earthquakes (O'Rourke and Tawfik 1983; O'Rourke and O'Rourke 1995; Nishio 1995). For the large diameter steel pipelines that were investigated, it was found that for large displacement events, the geometry of the lateral spread had a greater influence on the magnitude of the strains induced in the pipe than did the soil type.

Ranji et al. (1995) develop two analytical solutions, one for transverse movements and another for longitudinal movements, based on the concept that the soil resistance reaches an ultimate value as the soil reaches failure and develops plastic strains. Non-dimensional relationships were developed and presented in the form of charts permitting hand calculations and rapid verification of structural design of the pipeline in areas with ground instability.

2.2 Research on buried PE pipelines subjected to ground movement

To date, only a limited number of research studies have been performed to evaluate the performance of PE pipelines subjected to ground movements. Although numerical models and

analytical approaches can help in understanding soil-pipe interface behavior during ground movement in the field, due to the large number of influencing factors, physical models simulating the field situations play a key role in calibrating and validating the analytical approaches and numerical models. Some of the large soil chambers for full-scale testing of soil-pipe interaction problems are available at Cornell University (Trautmann and O'Rourke 1983), Center for Cold Oceans Resources Engineering (Paulin et al. 1997), Queen's University (Brachman et al. 2000; Brachman et al. 2001), and UBC (Wijewickreme et al. 2009, see Figure 2.1 below). Physical model tests are also performed by private companies for specific uses and the results are neither published nor generalized for other cases.

This literature review will look at some of the work completed at Cornell University, Queen's University and UBC. The following sections provide a summary of the research contributions from each of these universities that are pertinent to the present research topic.

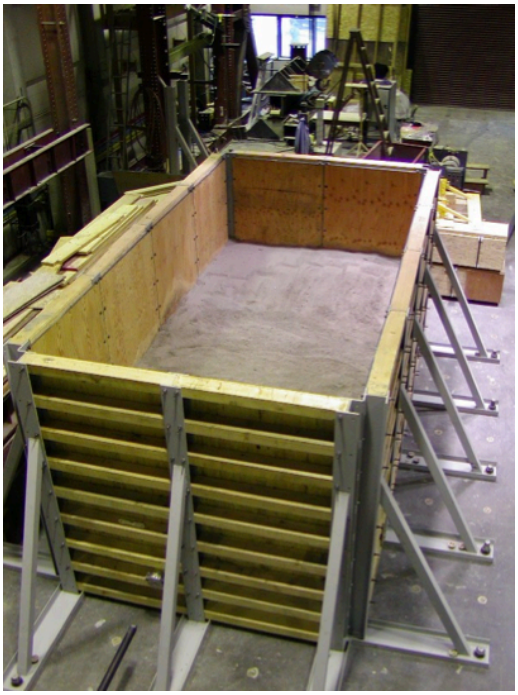

Figure 2.1 Photo of the soil-pipe testing chamber at UBC (Karimian 2006)

2.2.1 Findings from research at Cornell University

Stewart et al. (1999) and Bilgin and Stewart (2009) noted that the current methods used to determine the pullout capacity of PE pipes commonly used in pipeline systems do not consider the effects of diameter changes and cyclic movements that the pipelines may experience due to

temperature changes. As such, a series of full-scale laboratory tests were performed to study the interface shearing resistance of these pipes under varying conditions. Pull/push and cyclic tests were performed in a temperature-controlled room and the results indicated that reductions in pipe diameter affect the interface shear resistance that develops between the soil and pipe. As the pipe diameter gets smaller, the normal contact stresses at the interface decreases, causing a reduction in the interface shearing resistance directly proportional to the normal stress changes. Cyclic pipe movements also caused significant reduction in the pipe pullout resistance. They suggested that the long-term design of polyethylene systems should consider that interface shearing resistance changes with both temperature change and with repeated pipe movement.

Bilgin et al. (2007) performed laboratory tests to study the thermal and mechanical properties of polyethylene pipes to account for the complex viscoelastic nature of these pipes. Mostly MDPE specimens of the type used by utility companies in their distribution systems were used throughout these tests. The testing program included stress relaxation tests at various temperatures and temperature ramp tests to show material modulus and relaxation behaviours over the full range of temperature expected in the field. The results showed that within the range of temperatures expected for field applications, the pipe behaves in a manner consistent with linear viscoelastic theory, suggesting that linear visco-elastic models can be used in the design of polyethylene pipelines for thermal loads, and that temperature has a significant effect on polyethylene modulus.

O'Rourke et al. (1990) also studied the effect of surface hardness on the interface friction of several materials (HDPE, MDPE, and PVC pipes and HDPE and PVD lining) and found that the interface resistance increases as the surface hardness decreases. They also reported that the sliding motion of soil particles occurs at relatively harder material surfaces while the rolling motion occurs at softer material surfaces.

2.2.2 Findings from research at Queen's University

In recognition that one of the design situations that has similarities with the condition of a buried pipeline subjected to ground movement is horizontal directional drilling (HDD), a review of the available information on this subject from the Queen's University, in Kingston, Ontario, Canada, was considered relevant.

Researchers form Queen's University have undertaken several studies to investigate the soil-pipe interaction between HDPE pipelines installed using HDD methods (Chehab 2008; Chehab and Moore 2004, 2010; Chehab and Moore 2012). "HDD is a technique for installing pipes or utility lines below ground using a surface-mounted drilling rig that launches and places a drill string at a shallow angle to the surface and has tracking and steering capabilities" (ASTM 1999).

Queen's researchers recognized that estimating the pulling forces during HDD installations is an important step in successfully designing an HDD project and that estimating the post-installation loads are important for the prediction of the long-term performance of the installed pipe. A new one-dimensional computer model, HDDPIPE, was developed that can be used to calculate the short and long term response of steel (elastic) and polymer (viscoelastic and viscoplastic) pipes installed using HDD. The new model employs a mechanism to account for the adhesion, friction, and the stiffness of the soil medium for the pipe-soil interaction. The axial strains and deformations in the pipe are calculated based on the axial stresses using the constitutive model selected in the program. Linear elastic models can be used for steel pipes or plastic pipes that are not expected to experience a time-dependent response, and for materials where the response is nonlinear and/or time-dependent such as HDPE, linear viscoelastic (Moore and Hu 1996), nonlinear viscoelastic (Zhang and Moore 1997), viscoplastic (Zhang and Moore 1997), linear viscoelastic-viscoplastic (Chehab and Moore 2004), and nonlinear viscoelastic-viscoplastic (Chehab and Moore 2006) models can be used.

A parametric study using HDDPIPE was carried out by Chehab and Moore (2010) to examine the short and long term response of HDPE pipes installed by HDD methods. The results from this study showed that the stresses and strains continue to change along the pipe throughout its service life and that some installation parameters have significant effects on the short term installation loads, as well as the long term axial stress and potentially influence the expected service life of the pipeline. Additionally, it was shown that the pipes experienced cyclic response during installation and a combination of creep and stress relaxation in the long term.

2.2.3 Findings from research at the University of British Columbia

Researchers at UBC have conducted extensive studies on soil-pipe interaction on steel pipes to understand the interface friction between them as well as studying the performance of buried

MDPE natural gas distribution pipelines subjected to ground movements. The main objective of this work has been to investigate the contributing factors and key parameters influencing this soil-structure interaction response. As part of Anderson's (2004) M.A.Sc. research, a full-scale testing facility comprised of a 3m x 5m soil chamber (shown in Figure 2.1 above), with the capacity to test pipeline segments with up to one meter of displacement, was developed. Axial pullout tests performed on straight 60 mm and 114 mm outer diameter MDPE pipe configurations using this chamber indicated that the axial resistance to pipe pullout increased with pipe displacement in a relatively non-linear manner up to a peak value, after which the pullout resistance gradually decayed with increasing pipe displacement. The behaviour was attributed to the changes in interface frictional resistance that occur in the shearing zone adjacent to the pipe due to a number of factors that are considered to change the normal soil stresses on the pipe: i.e., shear volume coupling response of soils, potential arching of the soil outside the shearing zone, and tensile strain-induced reduction of the diameter of the pipeline. It was also observed that the peak axial pullout resistance of straight pipeline section estimated using published design equations, such as ASCE (1984) and ALA (2001), tended to over predict the pullout force for the pipes in uncompacted sand, and significantly underestimated pullout resistances in dense sand. The measured axial displacement required to mobilize the peak axial force for straight sections (in the order of 20 mm) was also significantly larger than the displacements suggested in existing design guidelines (i.e. 2-3 mm for steel pipes). Generally, the research indicated that there are significant limitations in the applicability of the currently available equations developed for steel pipelines for the prediction of axial pullout resistance of MDPE pipelines. Furthermore, tests conducted by Anderson (2004) on branched MDPE pipeline configurations showed that the anchoring effect of branched pipes generates significant strain concentrations in both the trunk line and in the branch pipes.

Weerasekara (2007) carried out further pipe pullout tests on various MDPE pipe configurations using the same soil chamber developed by Anderson (2004). The results from these tests further confirmed that buried MDPE pipes subjected to relative soil movements in the axial direction cannot be predicted using the simplified equations, primarily due to the complex soil-pipe interaction arising from the flexibility and the non-linear response of PE pipes, combined with dilation and arching effects from the soil around the pipe. In addressing these complexities,

Weerasekara and Wijewickreme (2008), derived a new closed-form solution providing the framework for analysis of straight pipe sections undergoing permanent ground movement and the solution was capable of capturing the response observed in the full-scale pullout tests. The new closed-form solution accounts for the nonlinear material response of MDPE pipes allowing the user to obtain the response of the pipe (strain, force and the mobilized frictional length along the pipe) for a known relative displacement of the pipe. The analytical solution also incorporates the influence of soil dilation and frictional degradation.

In addition, Weerasekara (2011) performed five large-scale field tests at the south end of the UBC Vancouver campus designed to capture different MDPE pipe responses at various burial, loading and pipe conditions encountered in practice. In each test, the pullout resistance, strain, displacement and elapsed time were directly recorded and similar to the pullout tests performed in the soil chamber (Anderson 2004; Weerasekara 2007), highly nonlinear pipe responses were observed in these tests. The field pullout tests indicated that the overall pipe response depends on the pipe properties (e.g. pipe cross-sectional area, stress-strain behaviour) and the soil characteristics (e.g. burial depth, density, friction angle, lateral earth pressure coefficient), which in turn highlighted the need to incorporate these parameters into any analytical model to capture the pipeline response.

Additional work by Weerasekara (2011) was undertaken to further refine the analytical solution to model the response of MDPE pipes due to relative axial soil loading. The analytical solution included a soil-pipe interface friction model that captures the increase in friction due to constrained soil dilation, the impact of mean normal stress on soil dilation and the subsequent decrease in friction (frictional degradation), and the stress-strain behaviour of the pipe material using a strain-rate dependent hyperbolic formulation and derived considering the equilibrium and compatibility conditions at the pipe element-level. The analytical solution provides the framework to relate the displacement, axial strain, axial force and mobilized frictional length along the pipe. With the knowledge of the measured ground displacement, the solution provides a method to estimate the pipe strain and mobilized frictional length along a pipe during axial loading.

The pipe response estimated using the new analytical solution was validated using data from the field pullout tests combined with those from previous laboratory pullout tests. The validations were undertaken using a consistent set of input parameters used in the analytical solution and these parameters were obtained with reasonable accuracy through independent experiments or direct field measurements. It was found that there was an excellent agreement between the analytical and experimental results for tests conducted with different pipe diameters (60 mm and 114 mm), soil density conditions (loose and dense), burial depths (0.54 m to 0.98 m), burial lengths (3.8 m, 5.0 m and 8.5 m) and under a range of axial pullout displacement rates. The new analytical model was extended to account for the combined response of axial tensile load and bending in the pipe for the case of soil loading acting perpendicular to the pipe axis. The solution allows relating the measured ground offset at the location of abrupt ground movement to the bending moment, shear force and axial force at any location along the length of the pipe.

2.3 Properties and mechanical behaviour of MDPE natural gas pipes

PE piping material consists of a polyethylene polymer (commonly designated as the resin). Small quantities of colourants, stabilizers, anti-oxidants and other ingredients are added to enhance the properties of the material, which protect it during the manufacturing process and throughout storage and service. PE piping materials are classified as thermoplastics because they soften and melt when sufficiently heated and harden when cooled. Because PE is a thermoplastic, pipes and fittings can be fabricated by simultaneously applying heat and pressure. In the field, thermal fusion processes can join pipe segments where matching PE surfaces are permanently fused together when they are brought together at a temperature above their melting point (PPI 2007).

When buried in moving ground, the MDPE pipes under consideration are subjected to a number of different, complex, possible loading scenarios. The loading scenarios will typically induce strain in the pipe. The MDPE pipe material, being a viscoelastic material, would further respond to this induced strain in a time-dependent manner where stress, creep and stress relaxation can all occur. If sufficient strain is applied to the pipe, the pipe can undergo yielding, necking in draw down and ultimate rupture.

As indicated by Weerasekara (2011), having a reasonably accurate representation of the stress-strain behaviour of the pipe material is one of the key factors to understanding the overall

response of the buried pipeline, especially when attempting to develop an analytical solution to represent the overall pipe response. Unlike the linear elastic stress-strain behaviour that is commonly assumed to represent steel pipes, the stress-strain behaviour of MDPE pipes is known to be nonlinear and governed by viscoelastic properties.

Figure 2.2 (a) illustrates the typical uniaxial stress-strain behaviour of polyethylene under a constant rate of loading. Figure 2.2 (b and c) show the effect of temperature and strain rate on the stress-strain behaviour. The behaviour shown in Figure 2.2(a) can be divided into three separate zones, where Zone I shows linear elastic behaviour at small strains (instantaneous recoverable strains), Zone II deformations are viscoelastic (still recoverable but not instantaneously), and Zone III is visco-plastic (inelastic response with irrecoverable strains).

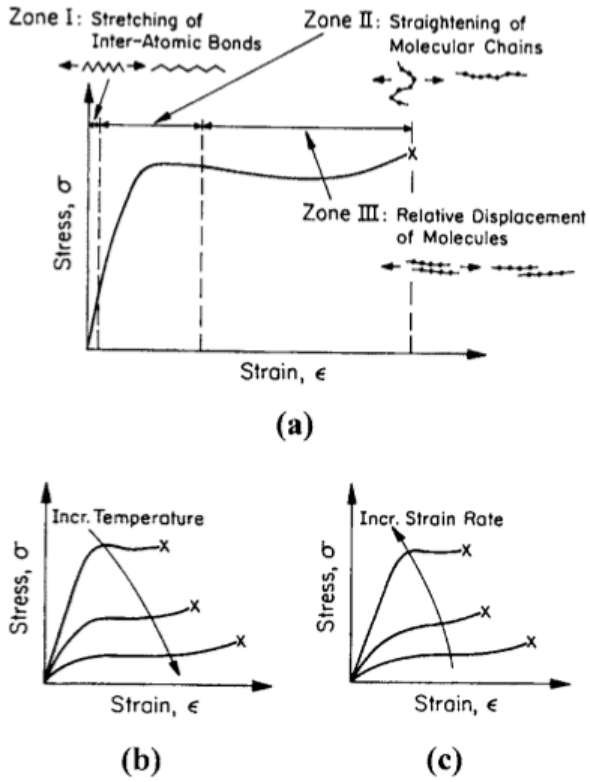

Figure 2.2 Stress-strain behaviour for typical MDPE (Bilgin et al. 2007)

As discussed by Bilgin et al. (2007), the mechanical properties of polyethylene do not remain constant within the range of typical civil engineering applications. The pipes have the ability to soften on heating and reharden on cooling and the temperature-induced changes in the modulus of the pipe are significant. For example, between 0°C and 50°C, the Young's modulus of

polyethylene increases by nearly a factor of two, with higher modulus at lower temperatures. Furthermore, polyethylene exhibits a viscoelastic response to load in the form of material creep and stress relaxation.

Figure 2.2 (b) shows the stress response under a constant strain rate, indicating that with increasing temperature the material deformation modulus would decrease and the material ductility would increase. When the temperature is held constant during testing, the strain rate has a significant effect on material properties with a higher strain rate leading to a stiffer response as illustrated in Figure 2.2 (c).

Weerasekara (2011) provides further discussions detailing some of the analytical models that can be used to represent the viscoelastic behaviour of MDPE. Additionally, Weerasekara (2011) describes the specifics pertaining to the development of the new analytical solution used in this thesis (and described in Section 2.2.3) where a hyperbolic model was used to accurately represent the stress-strain behavior of the viscoelastic MDPE pipes.

2.4 Field monitoring of buried pipelines subjected to ground movement

The most direct option for determining the performance of buried pipelines subjected to ground movement is to directly monitor pipe displacements or strain along the pipe using instrumentation attached to the pipe.

Bruschi et al. (1996) and Bughi et al. (1996) presented such field monitoring of a pipeline located in an Italian mountainous area that was subjected to ground movement. The data obtained from this field project was used in numerical modeling of soil-pipe interaction mechanisms.

It is likely that there are many instances where private pipeline companies have monitored buried pipelines subjected to ground movement. Results from such projects though are seldom published, but it is likely that a significant amount of information exists in various private databases.

Because of the complexity of the soil-pipe interaction problem investigated in the current research, there was a need develop a clear methodology to instrument and monitor stain in the MDPE pipes used throughout this study. This is an important consideration for this research

program and this created an opportunity to explore previous work that has been completed to use strain gauge instrumentation on PE material. Further details relating to this topic are highlighted at the beginning of Chapter 4.

2.5 Research needs identified from the literature review

Based on the above described literature review, it was recognized that only a few full-scale field testing studies have been conducted to investigate the performance of buried pipelines subjected to ground movements. Without the database of information that could be obtained from full-scale field tests, validation of analytical and numerical models are limited to the use of data obtained from relatively smaller-scale laboratory tests conducted under well-controlled conditions.

On this basis, the current research and investigation needs to better understand the behaviour of buried MDPE natural gas pipeline networks subjected to ground movements are summarized as follows:

- Develop a full-scale field testing program to monitor the performance of buried MDPE pipelines subjected to ground movements in the axial and lateral directions, as well as branched pipe systems.
- Create a reliable database of ground movement and associated buried pipe strain that can be used to validate analytical and numerical models.
- Laboratory testing should be conducted to determine the strain gauge stiffening effect on the MDPE pipes and instrumentation in consideration.

CHAPTER 3: FULL-SCALE FIELD TEST INSTALLATION DETAILS

The following chapter provides details pertaining to the experimental aspects of the implementation of the full-scale field test conducted for this research study and includes the details on: (a) field research study location; (b) as-built pipeline installation details; (c) strain gauge instrumentation; (d) on-going data collection; and (e) early stage experimental observations from the field study.

3.1 Research study location details

The selected site for this research study is located within a residential development just east of Chilliwack, BC, on the toe of a landslide mass where ground movements have been observed since the property development in the early 1990's. The site location is depicted in the area map in Figure 3.1 below.

Figure 3.1 Research study location map

Based on the author's review of several engineering reports outlining the preliminary investigation into the cause of the ground movements at the selected research location, it is understood that the site is underlain by an upper colluvium (geo-materials at the foot of a slope brought there by gravity; including landslide material), including surficial fill about 5 m thick and comprising mostly of sand and gravel, with trace to some silt. Underlying the upper colluvium is a distinctively black weathered shale-derived landslide mass comprising mostly of silt and clay mixed with some sand and gravel, and occasional cobbles and boulders. The mass is

generally stiff and moist, but contains discrete softer wet and harder dry zones. The shale-derived mass overlies Fraser River floodplain deposits consisting of organic silts and fine sand. Generally, the ground surface at the site slopes in the Northeastern direction at an angle of about 8° to 12°.

Detailed assessments in the available engineering reports suggest that the ground movements are within the shale-derived landslide mass and that the observed ground movements are promoted by high water pressures in the network of water-filled cracks within this landslide mass. The high groundwater pressures most likely resulted from water infiltration due to land clearing and subdivision development. It should be noted that the mechanisms of ground movement within the shale-derived mass at this location are not fully understood and the cause of the original landslide has not been established.

3.1.1 Historical ground movements at the research site

In addition to the geotechnical reports outlining the preliminary assessment of the cause of the slope movements at the site, the author reviewed several reports summarizing survey field monitoring data for the site dating back to February 2004. The survey monitoring data suggests that throughout a seven year period, from February 2004 to February 2011, as much as 450 mm of ground movement has occurred at the site. This suggests that on average, about 5 mm of ground surface movement is occurring at the site each month. The ground movements are occurring in the North-eastern direction, approximately parallel to the slope of the ground surface.

3.2 Pipeline alignment installation details for the research study

The pipeline alignments selected for this study were installed over the course of three days, from May 21 to May 23, 2013. The as-built pipeline installation details for the installation sequences are presented in this section, and additionally, Appendix A provides a series of photos taken throughout the installation process.

3.2.1 Pipeline instrumentation and transportation logistics

At the onset of this study, the pipeline arrangements were delivered to the civil engineering laboratory at UBC where the strain gauge installations were performed over a six-month period from September 2012 to February 2013. The pipes were delivered to UBC in approximately 6 m long sections allowing for more manageable transport and handling of the segments. Upon completion of the strain gauge installation, the pipes were transported to the site on a flat bed truck using a timber pipe rack fabricated at UBC. At all stages throughout the pipe transportation and handling, extreme caution was used to avoid damaging any of the installed pipe instrumentation.

3.2.2 Pipeline alignment configurations

A total of five pipeline alignments, each approximately 24 m in length, were installed for this study to investigate the performance of straight and branched natural gas pipelines loaded in both the axial, or longitudinal, and lateral, or transverse, directions.

Alignments 1 through 4 were installed such that the axial lengths of the pipelines are parallel to the anticipated direction of the predominant ground movements occurring at the selected research site. The intent is that the soil loads developed from the relative axial soil movement will extend the pipes in the axial direction. In contrast, Alignment 5 was installed with the axial length of the pipeline perpendicular to the ground movement in order to develop tensile forces in the pipe resulting from relative lateral pipe movement.

Two, 3-m long branch pipes, each 26.7 mm outside diameter, were attached to the trunk-line of Alignment 1 using tapping tee connections and butt fusion joining techniques at 2.0 m and 4.0 m from the top, or uphill end, of the alignment. The purpose of the branch connections is to replicate pipe configurations typical of local natural gas pipeline distribution networks.

Figure 3.2 below shows the general pipeline alignment configuration as installed at the site. The angles provided in the figure indicate the orientation of the alignments with respect to North. The pipeline lengths and sizes indicated in Figure 3.2 are described in detail in subsequent sections.

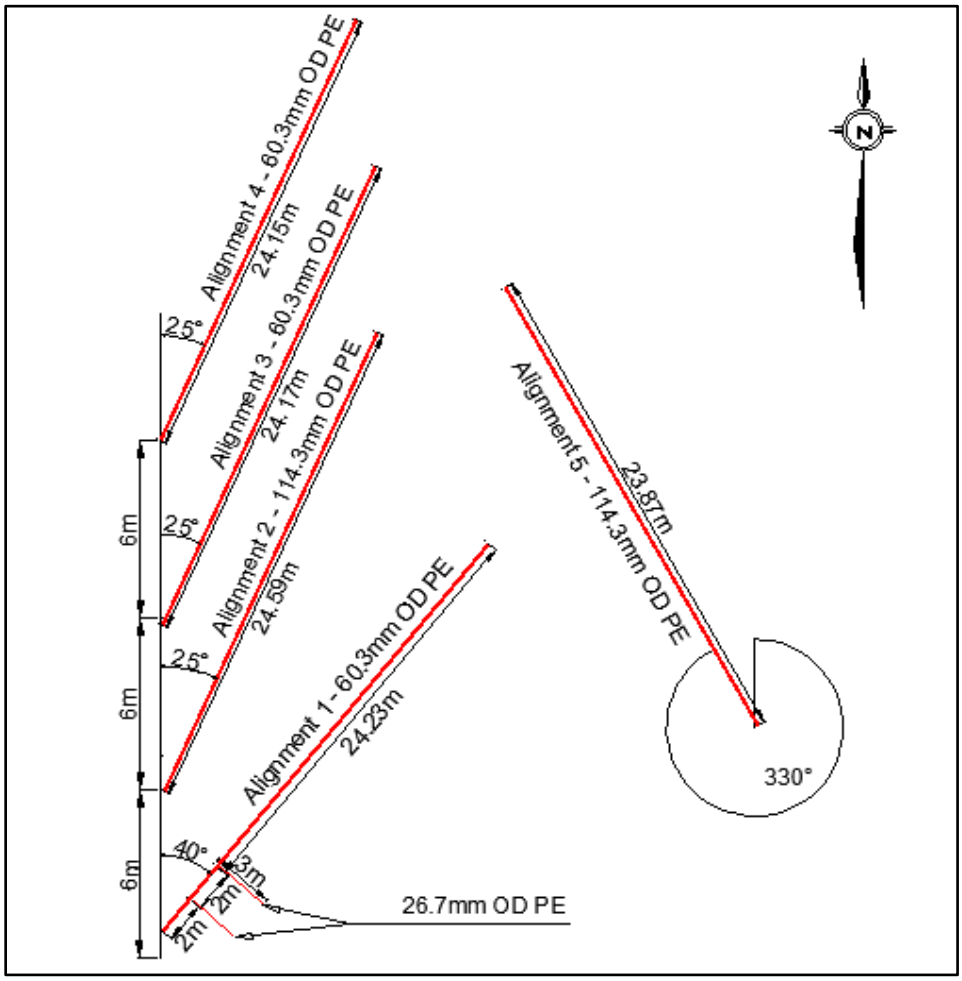

Figure 3.2 Pipeline alignment configurations and layout at the research site

3.2.3 Pipeline alignment lengths

In order to achieve the desired final pipeline lengths of around 24 m, three butt fusions were performed on site for each alignment to join the four segments that made up each alignment. Butt fusions were carried out just prior to placing the pipes into their respective excavated trenches. Table 3.1 below provides a summary of the individual pipe segment lengths (labeled A, B, C and D) installed for each alignment as well at the total length of each pipeline. The segments located at the uphill end of the alignments are labeled 'A,' and the consecutively attached segments, in the downhill direction, referred to as 'B,' 'C' and 'D.'

Pipeline Alignment Number	Pipeline Segment Lengths (m)				Total Trunk Pipe Length (m)
	A	B	C	D	
1	6.02	6.07	6.07	6.07	24.23
2	6.40	6.12	5.97	6.10	24.59
3	6.02	6.03	6.04	6.08	24.17
4	6.02	6.03	6.07	6.03	24.15
5	6.00	6.10	5.89	5.88	23.87

Table 3.1 Pipeline alignment segment lengths and total trunk pipe lengths

The performance of the butt fusion joints depends on the quality of the electro-fusion joint. During the pipe installations, the pipes were heat fusioned by experienced Canadian Utilities Construction Corp. personnel, and it can be assumed that they represent typical field connections.

3.2.4 Pipeline diameters used in this project

Three pipe sizes have been employed in the five pipeline configurations at the site, as indicated above in Figure 3.2. Table 3.2 below provides a detailed summary of the five pipeline properties.

Pipeline Alignment Number	Trunk Pipe OD/WT[1] (mm)	SDR[2]	Branch Pipe OD/WT (mm)	Anticipated Trunk Pipe Loading Direction
1	60.3/5.48	11	26.7/3	Axial
2	114/10.32	11	None	Axial
3	60.3/5.48	11	None	Axial
4	60.3/5.48	11	None	Axial
5	114/10.32	11	None	Lateral

[1]OD/WT: Outer Diameter/Wall Thickness
[2]SDR: Standard Dimension Ratio (Minimum outside diameter/Minimum wall thickness)

Table 3.2 Summary of the installed pipeline alignment sizes

3.2.5 Pipeline trench dimensions and backfill material properties

For all five pipeline installations, Fraser River Sand (FRS) was used as the soil backfill. For typical buried natural gas distribution pipeline installations, it is customary to reuse the excavated trench material as pipe backfill, however FRS was chosen for this project in order to protect the pipe instrumentation throughout installation and compaction as well as for its well-known material properties. Additionally, FRS has been used extensively in previous full-scale natural gas pipeline testing at UBC.

Based on the available literature, the composition of FRS is understood to be 40% quartz, 11% feldspar, 45% unaltered rock fragments, and 4% other minerals (Vaid & Thomas 1995). This fine to medium sand has an angle of internal friction reported in the literature of 32° loose and 38° dense. The average grain size, D_{50}, is 0.23 mm and minimum and maximum void ratios for the material are 0.68 and 1.00, respectively. The grain size distribution curve for the sand used in this research program is shown in Figure 3.3. The coefficient of uniformity (C_u) was found to be 1.5 with a specific gravity (G_s) of 2.70. It is assumed that compaction of the sand on site did not alter the grain size distribution significantly.

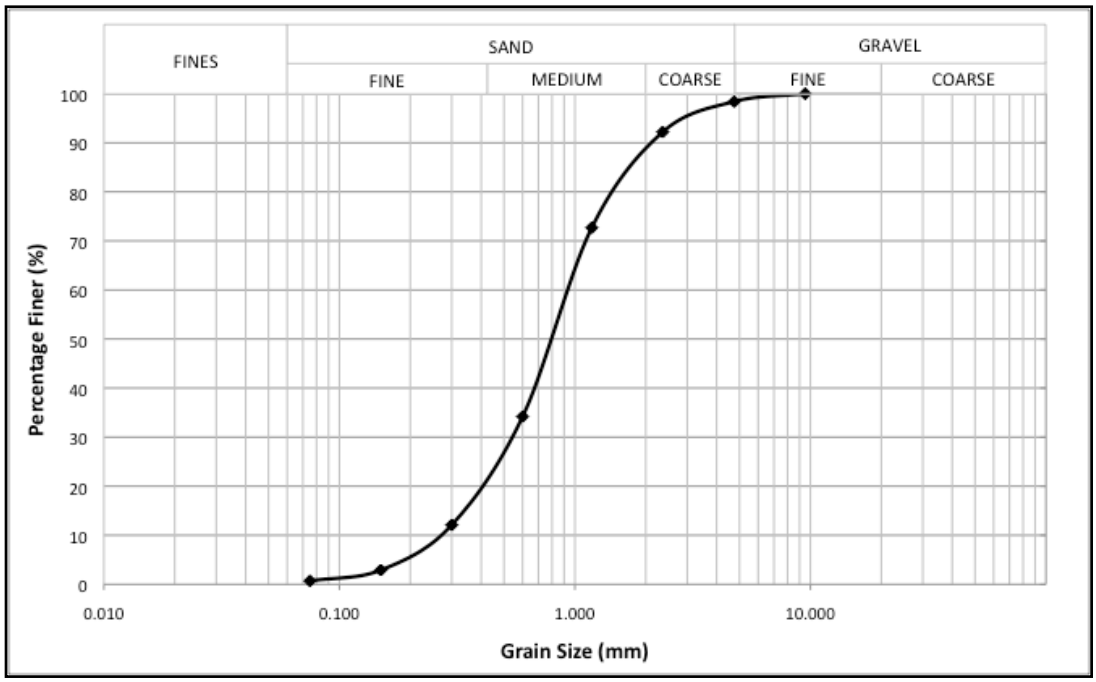

Figure 3.3 Grain size distribution of Fraser River Sand used for this research study

Each of the five alignments were installed with the same general four installation sequences outlined below:

- Trench excavation,
- Placement and compaction of bedding sand,
- Pipe segment fusion and placement of MDPE pipeline, and
- Placement and compaction of structural backfill in two lifts.

The pipe trenches were excavated using a John Deere 310SJ backhoe to lengths of approximately 28 m, allowing for working room on either end of the 24 m long alignments, and room for the anchor installations (anchor installation details are outlined in section 3.2.7 below). Each trench was excavated with a width of about 0.5 m i.e. the width of the backhoe bucket. Pipe trenches for Alignments 1, 3 and 4 were excavated to a depth of approximately 0.90 m and Alignments 2 and 5 to approximately 1.15 m.

Throughout excavation of the trenches, buried surface drainage pipes, electrical and gas conduits, and concrete foundation blocks were encountered that previously serviced two houses that were present at the site. The debris that was encountered throughout excavation was removed from the right away of the installed alignments. Generally, the soil that was encountered through excavation consisted of sands and gravels with a mixture of organics throughout. Some larger boulders were encountered up to about 1.2 m in diameter.

Upon completion of the excavations, minor sloughing of the excavation walls occurred between the times from open excavation to backfilling. When sloughing occurred, the material was removed from the trench prior to completing the backfilling efforts.

The FRS was supplied by Kel-Mor Enterprises of Chilliwack, BC. About 21 tandem truckloads of FRS were hauled to the site for use as backfill. The excavated "native" material was hauled away from the site for disposal. An estimated volume of 1000 m^3 was excavated for the project.

Pipe bedding sand was first placed into the excavated trench using the backhoe and then evenly spread by hand using rakes and shovels. The bedding layer was compacted in four passes using a vibratory tamper to a final average thickness of approximately 0.15 m for each alignment. Once the bedding layer was compacted, the pipes were then carefully placed on to the bedding surface with the axial length of the pipe centered in the trench.

Once the pipes were in position and strain gauge lead wires were arranged to their required ground exit points, the first lift of structural backfill was placed using the backhoe then spread by hand using rakes and shovels, and then compacted in four passes using the vibratory tamper. The first lift of structural backfill was on average 0.20 m to 0.30 m thick. Lastly, the final lift of FRS was placed to fill the remaining depth of the trench and packed using a backhoe-powered packer (commonly referred to as a "hoe-pack"). The strain gauge lead wires were typically positioned so

that the drag forces on the wires would be reduced, and in addition, were located away from the pipe in order to avoid disturbing the soil shear zone around the pipe.

Careful consideration was given to the possibility of damaging the pipe instrumentation throughout the installation process, so all pipe handling and compaction efforts were undertaken with extreme vigilance.

The water table was not encountered at the site throughout the pipeline installations. Additionally, it is expected that the bedding layer of FRS below the pipe depths will allow sufficient drainage for the trenches so additional drainage pipes were not installed.

An average of seven density measurements of the compacted FRS backfill were taken for each alignment using a nuclear densometer (Manufacturer: Troxler Inc., Model: 3440). It was observed that the density readings were approximately 2.0 kN/m^3 higher than the average values reported by Anderson (2004) and Weerasekara (2007) and (2011) for the same sand. In comparison to these previous studies, this installation employed slightly different compaction efforts and the FRS backfill had higher moisture contents. Table 3.3 below provides a summary of the average FRS backfill densities and moisture contents measured during the pipe installations.

Pipeline Alignment Number	Average Backfill Unit Weight (kN/m^3)	Moisture Content (%)
1	18.1	8.6
2	18.1	9.9
3	18.0	10.6
4	18.4	8.3
5	18.9	10.2

Table 3.3 Avg. backfill density and moisture content measured during pipeline installation

3.2.6 Pipeline alignment burial depths

Alignments 1, 3 and 4 (60.3 mm OD pipes) were installed to depths between 0.65 m and 0.75 m below the ground surface and Alignments 2 and 5 (114.3 mm OD pipes) were installed to a depth of 0.90 m (referring to the depth to the centre line, or spring line, of the pipe for each alignment). The installation depths fall within the range of FortisBC Energy Inc.'s standard practice to install

gas distribution pipelines between 0.3 m and 1.5 m, which is designed to prevent exposure to UV radiation and construction damages.

The larger 114.3 mm alignments were buried deeper than the 60.3 mm alignments so that the full mobilized frictional length is reached within the total pipe length. It is anticipated that the full 24 m pipeline length would be mobilized prior to reaching the maximum pullout resistance if buried less than about 0.75 m below the ground surface. For the 60.3 mm alignments, a burial depth of 0.60 m is expected to be sufficient in order to reach the full mobilized frictional length. Table 3.4 below provides a summary of the pipeline alignment burial depths.

Pipeline Alignment Number	Pipe Burial Depth[1] (m)
1	0.75
2	0.90
3	0.65
4	0.75
5	0.90

[1]Depth to springline of the main trunk line

Table 3.4 Summary of the installed pipeline alignment burial depths

3.2.7 Pipeline anchor components

The uphill ends of Alignments 1, 2, 3 and 4 are anchored using buried lock-blocks acting as dead-man anchors. The lock-blocks are attached to the ends of the pipes using steel cable arrangement allowing the ends of the pipes to move freely in the lateral direction, but are fixed in the axial direction. The primary objective of the anchors is to create boundary constraints that can be implemented in subsequent analyses. The downhill ends of these four alignments are left free.

The south end of Alignment 5 has also been attached to a buried lock-block to restrict movement in the lateral and the axial direction at this end. The north end of this pipe has been left free.

Initially, consideration was given to anchoring the pipe ends using either driven piles or drilled and grouted anchors, however these methods were disregarded due to both the cost associated with installation and the concern for unintentionally introducing stabilizing constraints to the moving slope.

It is recognized that there is a possibility that the dead-man anchors are not installed in stable, non-moving ground and that the anchors could move along with the moving ground. For this reason, the anchors are being monitored for displacement using survey monuments installed directly onto the lock-blocks.

The steel cable connections between the lock-block and the top end of Alignments 1, 2, 3 and 4 are tensioned using installed turnbuckles. During the installation, a nominal amount of tension was placed on the anchors to remove the slack in the steel cable connection prior to backfilling. The turnbuckles also allow for the application of tension to the top end of the pipe in the future in the event that the anchors migrate downhill. Figure 3.4 below provides a general schematic of the installed anchor configurations.

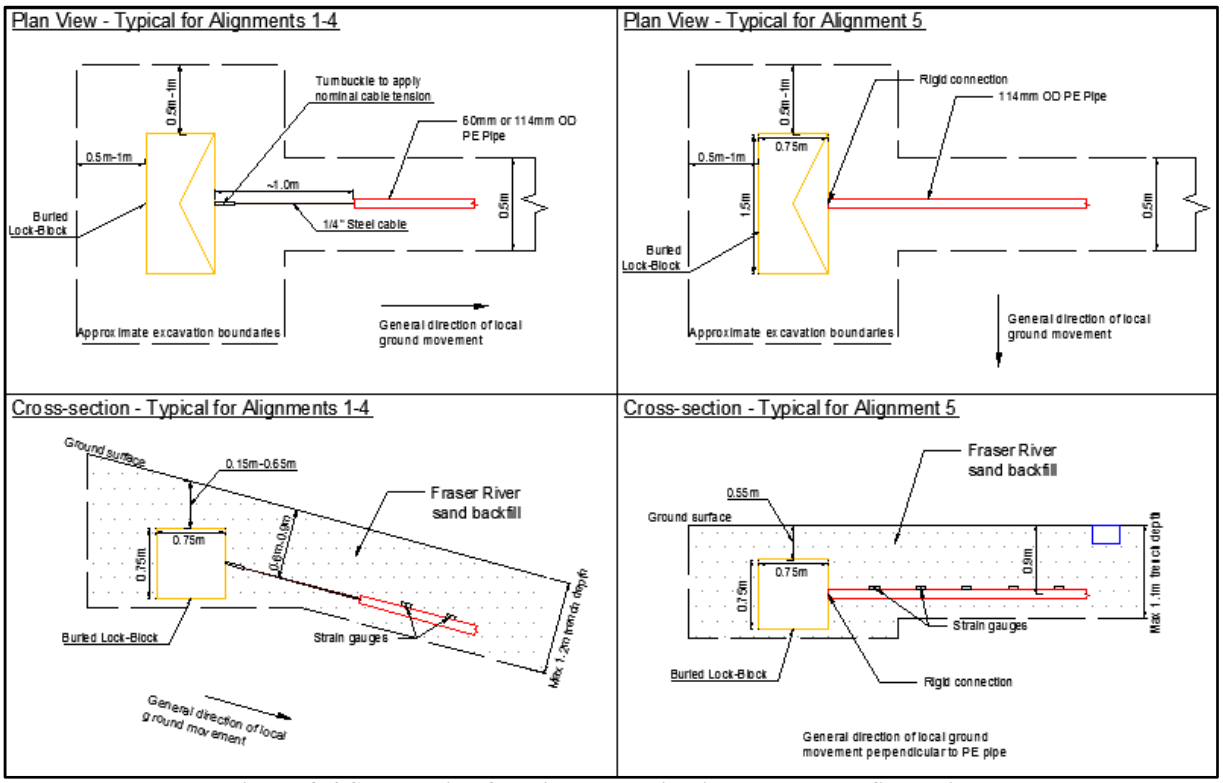

Figure 3.4 Schematic of the installed pipeline anchor configurations

3.2.8 Installed resistive temperature devices and baseline strain gauges

Since the stress-strain response of the buried MDPE pipes depends on the in-situ operating temperature, the temperatures of the pipelines at their respective burial depths are monitored

using six resistance temperature devices (RTDs), which have been installed across the site. Obtaining the temperature measurements at the time of the strain gauge data collection is important in order to be able to normalize the gauge measurements for temperature changes so that any relative strain induced in the pipes caused by relative ground movements can be identified. The RTD calibration curve for temperatures between -15°C and +35°C is provided in Figure 3.5 below.

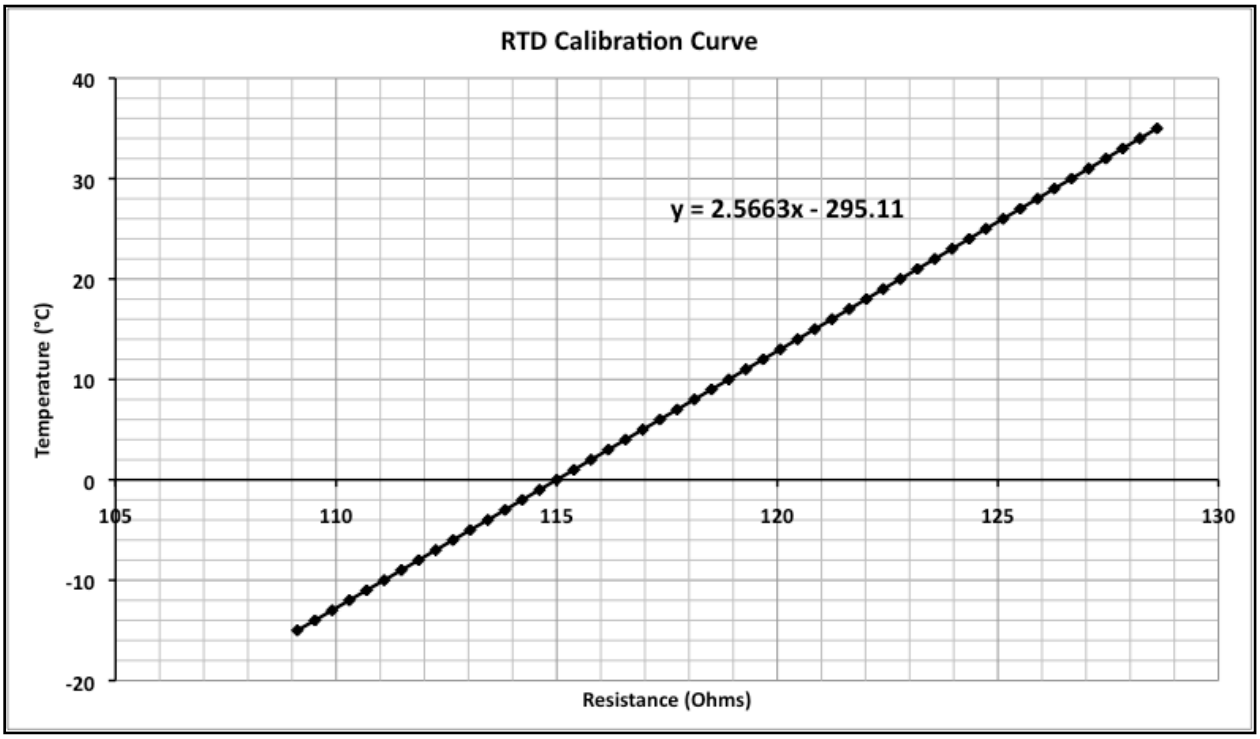

Figure 3.5 RTD calibration curve

Additionally, three separate 0.20 m long sections of 60.3 mm OD pipe, each with two strain gauges attached diametrically opposite from one another, have been installed at the site to provide baseline strain gauge readings for the duration of the project. These three pipe sections were buried adjacent to the pipes at their respective burial depths at three different locations across the site.

Table 3.5 below provides a summary of the locations of the buried RTDs and baseline strain gauges. Additionally, Appendix C includes a plan view schematic drawing of the site indicating the approximate RTD and baseline strain gauge locations.

RTD or Baseline SG No.	General Location at the Site	Depth Below Ground Surface
RTD 1	3.0 m from the uphill end of Alignment 1	0.75 m
RTD 2	20.0 m from the uphill end of Alignment 1	0.75 m
RTD 3	2.0 m from the uphill end of Alignment 3	0.65 m
RTD 4	21.75 m from the uphill end of Alignment 3	0.65 m
RTD 5	3.5 m from the south end of Alignment 5	0.90 m
RTD 6	20.5 m from the south end of Alignment 5	0.90 m
Baseline SG 1A/1B	3.0 m from the uphill end of Alignment 1	0.75 m
Baseline SG 2A/2B	21.75 m from the uphill end of Alignment 3	0.65 m
Baseline SG 3A/3B	3.0 m from the uphill end of Alignment 4	0.75 m

Table 3.5 Locations of the installed RTDs and baseline strain gauges

3.3 Strain gauge instrumentation details

As described above, one of the main objectives of this research work is to obtain a reliable data set of ground surface movement and associated pipe strain data. As such, a considerable amount of effort was put in to installing strain gauges along the lengths of each of the pipeline alignments in order to measure strain within the pipe specimens. The previous experimental pipe research by Anderson (2004) and Weerasekara (2007) and (2011) proved successful with installing strain gauges onto MDPE pipes using specialized procedures developed at UBC. Based on these previous successes, these same procedures for installing strain gauges were adopted for the current research and additionally, a waterproof coating procedure was developed to protect the gauges in the field for the duration of the research, which is expected to be several years.

3.3.1 Strain gauge manufacturer details

Kyowa KFEL-5-120-C1 type strain gauges were selected based on the previous success with strain gauge installations on MDPE pipes. The strain gauge manufacturer information is provided in Table 3.6 below. These gauges are high-elongation foil strain gauges capable of measuring strains of 10% to 15% and are therefore applicable for large strain measurements of plastics like MDPE (although strain measurements are limited to the adhesive bond between the gauge and the MDPE).

Manufacturer	Kyowa
Type	KFEL-5-120-C1
Gauge Length	5 mm
Strain Range	±15%
Gauge Resistance	119.8±0.2
Gauge Factor (24°C, 50% RH)	2.13±1.0%
Temperature coefficient of gauge factor	+0.015%/°C

Table 3.6 Strain gauge manufacturer details

3.3.2 Strain gauge installation details

Generally, the strain gauge installation procedure began with cleaning the MDPE pipe surface at the selected gauge location with an isopropanol degreaser, then etching the location with 220 grit sand paper and coating it with Loctite 770 primer. The gauges were then positioned using cellophane tape and bonded using Loctite 414 adhesive. The lead wires were then soldered to a soldering pad that was also bonded to the pipe just behind the strain gauge. The connecting three-strand lead wires were housed in a 2 mm thick, black polyurethane jacket providing adequate waterproof protection for field installations. At the connection points between the lead wires and the strain gauges, stress relief loops were applied in order to prevent the wires from pulling away from the gauges as the pipes are stretched over time. The lead wires are each long enough to run from the installed pipe burial depth to the ground surface at various exit points along the alignments where the strain data can easily be collected.

As indicated above, it was considered paramount to provide adequate strain gauge waterproofing protection and therefore, a three layer waterproof coating was applied to each gauge and consisted of:

1. Two coats of M-Coat D (air-drying acrylic coating produced by Intertechnology Inc.),
2. One layer of 2 mm thick butyl rubber tape extending beyond the outer limits of layer one,
3. Two layers of 3M 130C linerless rubber splicing tape wrapped around the diameter of the pip extending a minimum of 15 mm beyond the boundary of layer two.

At each gauge location, the waterproof coating extended axially along the pipe for a length of approximately 120 mm and protruded from the outside surface of the pipe by

approximately 5 mm (for example, the final outside diameter of the 60.3 mm pipe with two gauges installed 180° from one another with waterproof coating would be about 70.3 mm). When the area influenced by the strain gauge application and waterproof coating is considered in relation to the overall length of the pipeline alignments, the long length of the alignments are beneficial for reducing the relative contribution of the strain gauges and waterproof coating to the total pullout force. Across the five alignments, the strain gauge applications cover between 5% and 15% of the outside surface of the alignments.

The reliability of the waterproofing application was verified, where two specimens were submerged under 0.60 m of water. The stain gauges continued to produce truthful strain measurements with this waterproof coating applied after one year of submersion, therefore proving to be adequate for the field application.

Further details outlining more specific strain gauge installation procedures are included in Appendix B at the end of this report. Photos taken throughout the strain gauge installations are also provided in Appendix A.

3.3.3 Strain gauge positioning and labeling along pipeline alignments

In total, 227 strain gauges were installed along the lengths of the five alignments. Table 3.7 below provides a summary of the number of gauges installed on each of the alignments, the typical gauge spacing along the lengths of the alignments and the gauge position in cross-sectional area of the pipe.

Pipeline Alignment Number	Total No. of SG's[1]	SG Spacing[2]	SG Positions[3]
1	65	0.5 to 1.0 m	0°/90°/270°
2	50	1.0 m	90°/270°
3	46	1.0 to 2.0 m	0°/90°/270°
4	27	3.0 m	0°/90°/270°
5	39	2.0 m	0°/90°/270°

[1]SG: Strain Gauge
[2]SG Spacing refers to the spacing along the axial lengths of the alignments
[3]SG positions refers to the location of the strain gauge around the circumference of the pipe, with 0° referring to the crown of the pipe and subsequent locations measured in the clockwise direction while looking in the downhill direction

Table 3.7 Summary of the strain gauge positioning along the pipe alignments

A detailed strain gauge labeling procedure was created for the research study in order to associate the strain gauge readings from the lead wires at the ground surface to the strain gauges

attached to the buried alignments. Each of the strain gauge lead wires exiting at the ground surface is labeled with its respective gauge identification.

Each gauge is labeled with reference to their respective pipeline alignment, pipe segment, gauge number per segment, and finally gauge position in respect to the cross sectional pipe location. For example, a strain gauge labeled AL1-A-1A therefore refers to Alignment 1 – Segment A – the first gauge along that segment and at position A (1A in this case is located 0.10 m from the uphill end of the alignment and at the 90° location when looking in the downhill direction of the alignment). Detailed tables and drawings of the strain gauge positioning and labeling along each of the five alignments are included in Appendix C.

Anderson (2004) showed in preliminary tests that, with predominantly axial soil loading, multiple strain gauges mounted at 0°, 90°, 180° and 270° around the outside diameter of the pipe gave essentially identical results indicating that the distribution of tensile strain throughout the cross section of the pipe can be considered relatively uniform; based on this, the number of strain gauges at a given location was reduced as observed in the drawings in Appendix C.

3.4 Data collection for the research study

As part of the ongoing research study, the test data that is regularly collected includes the following: strain gauge measurements, ground surface movements, pipe displacements, ground temperatures at the pipe burial depths, air temperatures and the precipitation levels.

3.4.1 Monitoring pipeline alignment strain

The strain gauge measurements are manually recorded using a Model P3 Strain Indicator obtained form Vishay Micro Measurements, Wendell, NC, USA. This strain indicator uses an excitation voltage for the strain gauges of 1.5 VDC. The measurements from the strain gauges are collected on site at a minimum frequency of once per week (a higher frequency was adopted at the onset of the project).

As mentioned above, the strain gauge lead wires attached to each gauge extend from the pipe burial positions to the ground surface where the data can be collected. Clusters of strain gauge lead wires were formed for the set of gauges located on each of the four pipe segments for each alignment. These clusters exit the ground surface at four points located along the lengths of each

of the pipes. Each exit point consists of a 30 cm tall by 38 cm wide by 45 cm long plastic box, where the wire clusters can be accessed. The plastic boxes provide good weather protection to the ends of the lead wires and are buried flush with the ground surface.

3.4.2 Monitoring ground surface movements

Following the pipe installations, a series of survey monuments were installed at the site in order to monitor the ongoing ground surface movements in detail. On May 27, 2013, a total of 12 ground surface survey monuments were installed across the site. The survey monuments are comprised of a two-inch diameter circular brass survey hub attached to the top end of a 2.5-foot long rebar pin pounded into the ground. Survey measurements at the site are taken at a frequency of about once every three months, with a higher frequency rate adopted at the beginning of the project to establish reliable baseline readings. Topographic surveys of the site are also taken annually at the site. Survey monument locations, as well as the initial topographic survey, are included in Appendix D .

3.4.3 Monitoring anchor and pipe movements

At three locations along each of the pipe alignments, 100-mm (4") diameter "Big-O" corrugated tubes were installed vertically above the buried pipes allowing access from the ground surface to the crown of the pipes. These access points allow the surveyors to monitor the displacement of the pipe at these three points which are marked with 1/8" drilled holes in the crown of the pipe. Each of the alignments has three of these monitoring points along their lengths, one at each end and at the mid point.

In addition to the three access points along each of the alignments, two monitoring points have also been installed on each of the buried lock-block anchors. Again, vertical Big-O tubes were installed above each of the monitoring points allowing access to the survey points.

Locations for these monitoring points are shown in the drawings in Appendix D .

3.4.4 Monitoring temperature and precipitation at the site

Daily temperature and precipitation levels during the testing period are obtained and recorded from http://chilliwack.weatherstats.ca.

3.5 Early stage experiment observations from the field test

In order to provide an illustration of the data collected from the field test to date, experimental observations for the time period between May 23, 2013 (study implementation), and December 31, 2013, are shown in Appendix E. Appendix E presents the following data:

- Measured strain gauge data for Alignment No. 4, for strain gauges located along the crown of the pipe only,
- Measured data from the six baseline strain gauges,
- Measured data from the RTDs buried across the site, and
- Daily maximum, minimum and mean air temperatures as well as precipitation levels at the site.

In light of the early stage of this research study, these results presented are only meant to provide an indication of the data obtained to date. At this point in time, attempts were not made to deduce any conclusions from the current data set. It is considered that a longer time period of data collection is required for proper interpretation of results.

More detailed and up to date results can be obtained by contacting Professor Dharma Wijewickreme at the Department of Civil Engineering at the University of British Columbia, Vancouver, BC.

CHAPTER 4: ESTIMATING THE STRAIN GAUGE STIFFENING EFFECT ON LOCAL STRAIN READINGS ON MDPE PIPES

The strain gauges installed on the MDPE pipes used for this study play a vital role in assessing the field performance of the buried pipelines. As such, ensuring their accuracy and precision is an important consideration before deducing any conclusions from the raw strain gauge data that is collected from the research site. It was recognized that the strain gauge readings can potentially be affected by the presence of the gauge itself, which arises as the stiffness of the gauge (metal foil, polymer backing, and glue) is similar in order-of-magnitude to that of the polyethylene (Brachman 1999).

As part of the current study, experimental investigations were undertaken to assess the local stiffening effects at the strain gauge location and, in turn, quantify the associated errors on the local strain readings made on MDPE pipes, and the details related to this are presented in this chapter. In this regard, specific comparisons between measured strains using strain gauges mounted on MDPE pipe segments and calculated strains based on independently measured deflections on the same piping are made to estimate these stiffening effects.

Through experimental tests conducted on low-density polyethylene (LDPE) films to investigate the elastic mechanical behavior of the material, Briassoulis (2002) showed that strain gauge arrangements installed on LDPE film to measure strain at selected points on the film gave consistently lower results compared to those predicted manually by optical, numerical or theoretical means. It was further suggested that the use of strain gauges to measure strain of thin films is a delicate procedure in general, and since the effect of the geometric change (i.e. thickness change) at the point where the strain gauge is bonded to a thin film probably results in a local stress redistribution, introducing additional errors in the strain gauge measurements (Briassoulis 2002).

Brachman (1999) performed tests on 320 mm outer diameter (SDR of 11) high-density polyethylene (HDPE) pipes mounted with strain gauges as part of a research program on the mechanical performance of landfill leachate collection pipes. It was reported that the effect of the strain gauge stiffness on the local strain readings could be observed by comparing circumferential strain values measured using the strain gauges with values of strain calculated

from measured deflections. For axisymmetric conditions, where there is no variation of circumferential deflection in the circumferential direction, the strains on the inside surface of the pipe were expressed as $\varepsilon_\theta=\Delta D/D_i$, where D_i is the inside diameter of the pipe. The experiments reported that the average strains measured with the strain gauges were consistently smaller in magnitude than the strains computed from the average diameter changes ($\Delta D_{avg}/D_i$). In some instances, it was shown that the strain gauges measured only 73% of the circumferential strain calculated based on the deflections. It was further suggested that the strain gauge readings were consistently smaller because of a reinforcing effect presented by the gauge itself and that the surface strain readings on polyethylene obtained from conventional strain gauges should be corrected for this stiffening effect. Throughout the tests conducted on HDPE pipes as part of Brachman's (1999) research, a stiffening effect from strain readings using electrical foil strain gauges was observed and a simple correction factor of 1.4 was applied based on measured deformations.

Mwanang'onze, H. et al. (2003) performed experimental work on HDPE pipes to characterize the coefficients of thermal expansion in the longitudinal and circumferential directions, and to investigate the dependence of thermal strain on thermal loading history. In this testing work, two 1100 mm long HDPE pipe specimens with outer diameters of 323 mm and 206 mm, with SDR values of 26 and 9 respectively, were subjected to thermally induced strains by decreasing the air temperature of the testing room. Linear potentiometers (LPs) were used to measure the longitudinal and diametric contraction of the specimens and strain gauge rosettes were attached to perform local strain measurements. Throughout testing, it was observed that the strains recorded by the strain gauges were significantly smaller than those calculated from the LP measurements. The results were attributed to the local stiffening effects created by the glue with which the strain gauges were fixed to the pipes. Based on this work,
Mwanang'onze, H. et al. (2003) suggested that in order to accurately use strain gauges to measure thermal strains in polyethylene, some stiffening factor must be calculated and applied to the collected strain gauge data.

4.1 Investigation using thermal contraction of MDPE pipe sections

In recognition of the effects of strain gauge stiffening on local strain readings on polyethylene material as per above, an experimental program was undertaken to determine the effect of strain gauge stiffening on the MDPE pipes used for this research project. The details from this experimental work are highlighted below.

4.1.1 Test methodology

Element level experimental work was conducted on four MDPE pipe specimens representative of the main natural gas trunk lines used in the project described in the preceding chapter. Two of the specimens were 150 mm long with an outer diameter of 60.3 mm and an SDR of 11. The other two specimens were 285 mm long with an outer diameter of 114.3 mm and an SDR of 11. In this chapter, the four specimens are referred to as SA60-1, SA60-2, SA114-1 and SA114-2, respectively.

The pipe specimens were subjected to thermally induced strains by placing them inside of a refrigerator for a period of three hours for specimens SA60-1 and SA60-2 and six hours for specimens SA114-1 and SA114-2. In all tests, the temperatures of the specimens were reduced from room temperature to refrigerator temperature for a total temperature difference of approximately 20°C. The specimens experienced unrestrained contraction due to the temperature reduction. Throughout the tests the temperature was measured on the surface of each of the MDPE pipes using attached RTDs.

Throughout testing, two linear variable displacement transducers (LVDTs), installed diametrically opposite from one another on the pipes, were used to measure the axial deflections of the specimens. For specimens SA60-1 and SA60-2, the LVDTs spanned 140 mm vertically across the height of the specimens and for specimens SA114-1 and SA114-2, the LVDTs spanned 200 mm vertically across the height of the specimens. The axial strain, ε_{axial}, was derived by computing $\varepsilon_{axial}=\Delta_{length}/(\text{length across LVDT})$, where Δ_{length} is the change in length of the specimen measured from the axial orientated LVDTs.

Novotechnik type TR50 LVDTs were used for the described tests. Prior to testing the MDPE pipe specimens, the LVDTs were independently checked to assess the effect of thermal changes

on the measured displacements. The checks showed that the LVDT readings were not effected by the changes in temperature and that no thermal corrections to the raw LVDT readings were required.

Two strain gauges were also installed to the outside surface of each specimen to obtain local strain measurements throughout thermal contraction. Again, the strain gauges were positioned diametrically opposite from one another at the axial midpoint of the pipes. The instrument configurations for specimens SA60-1 and SA114-1 are shown in Figure 4.1 below. Additionally, the concept of testing is shown schematically in Figure 4.2.

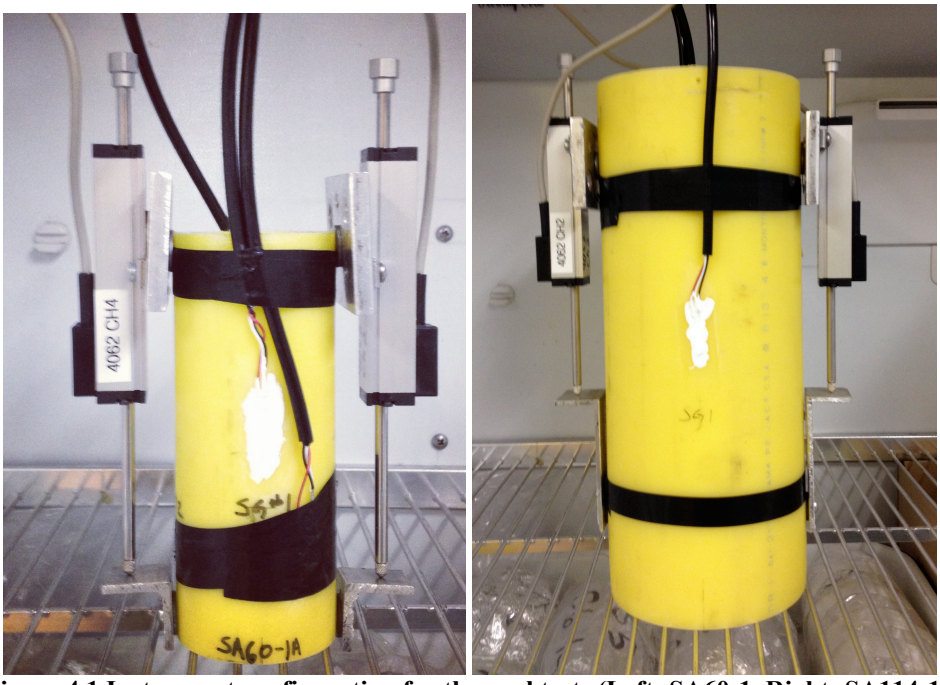

Figure 4.1 Instrument configuration for thermal tests (Left: SA60-1, Right: SA114-1)

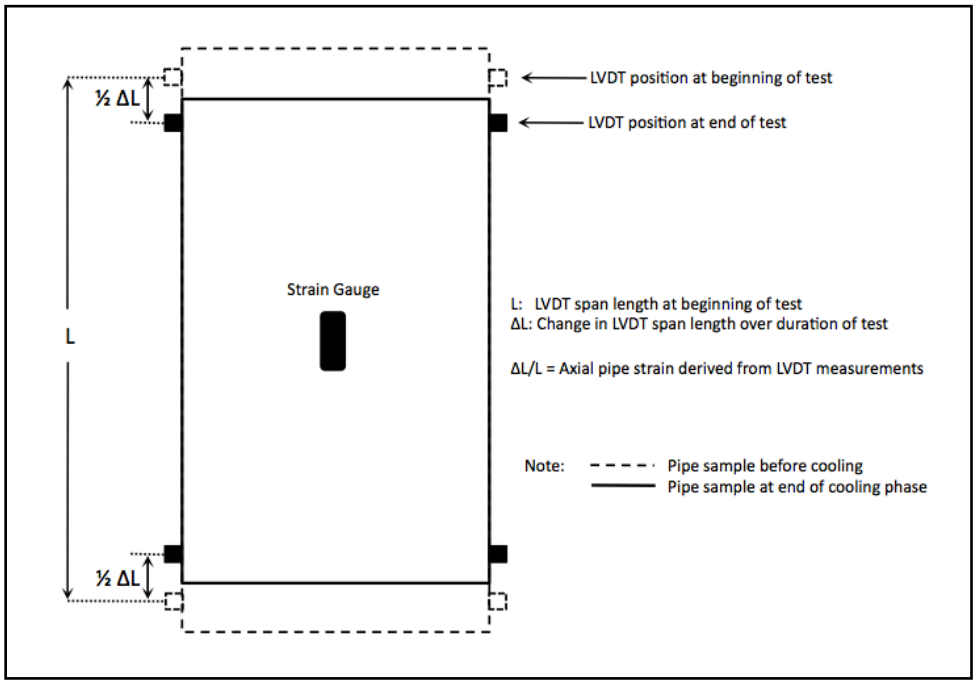

Figure 4.2 Conceptual schematic of thermal contraction testing of pipe specimen

4.1.2 Results from thermally induced axial contraction tests on MDPE pipes

For each of the four specimens, two thermal contraction tests were carried out and are referred to as tests A and B for each specimen. Thus, for example, the two tests carried out on specimen SA60-1 are SA60-1A and SA60-1B. This same test identification was adopted for the remaining three specimens.

For each of the eight tests, the specimens were taken from a condition of thermal steady state at room temperature and placed in the refrigerator. Contraction of the specimens in the axial direction was recorded by the two LVDTs and the two strain gauges at 15-second intervals. The test durations were selected so that they are sufficiently long enough to allow the specimens to achieve an acceptable thermal steady state in the refrigerator temperature of around 1°C. Following completion of the tests, the strains derived from the LVDT measurements were compared with those from strain gauge measurements.

The results obtained from the two tests on specimen SA60-1 are shown in Figure 4.3 where the strain values obtained from the strain gauges are directly compared with the strains derived from the LVDTs. Figure 4.3 also shows a comparison of the average strain gauge reading to the

average LVDT reading for each test, as well as the temperature change throughout the tests. The results observed by specimen SA60-1 are representative of the test results from the other specimens and subsequent test results are found in Appendix F.

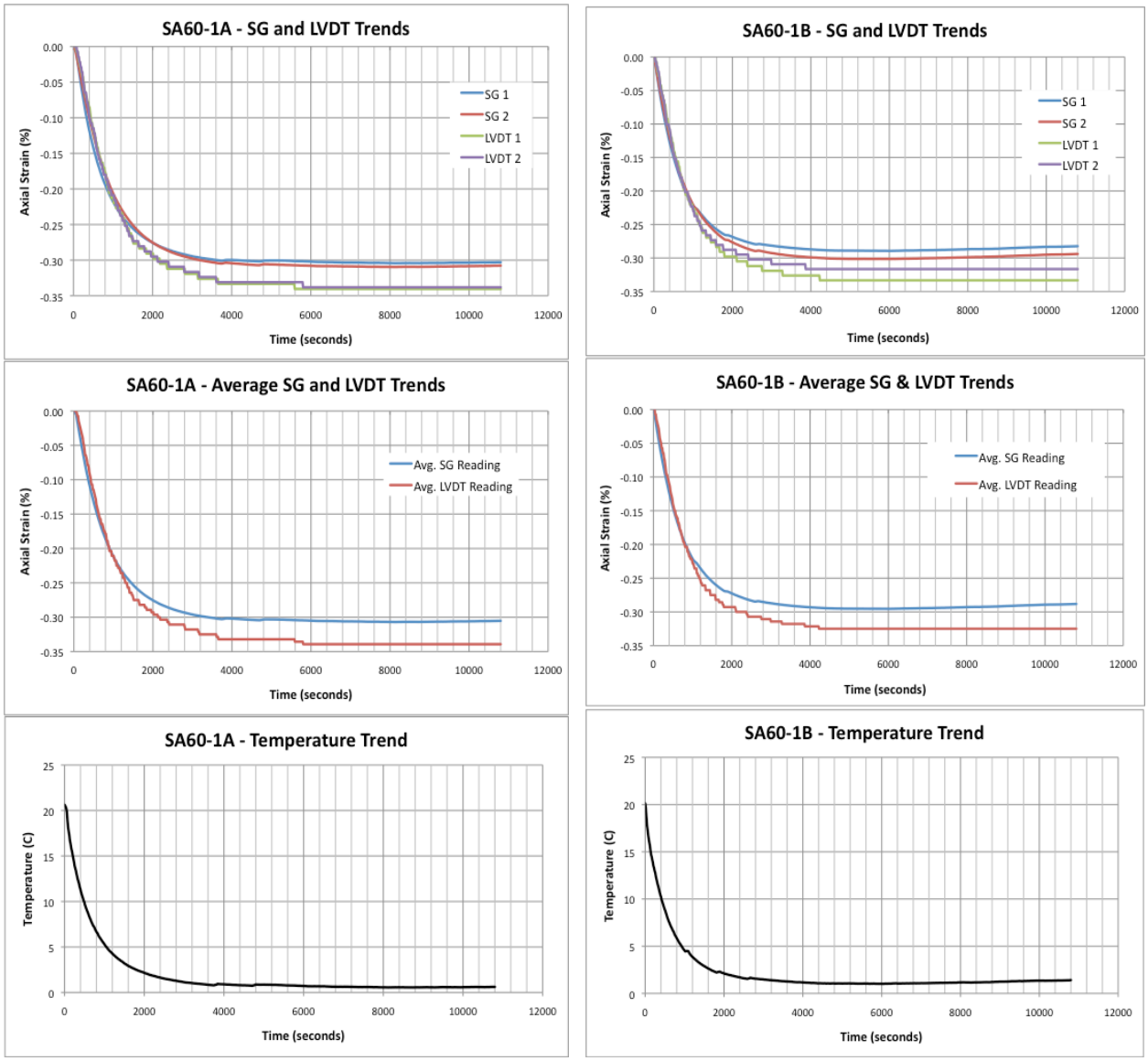

Figure 4.3 Comparison of strain measured from strain gauges and strain derived from LVDTs

Table 4.1 below provides a summary of the results from the experimental work conducted to estimate the strain gauge stiffening effect on local strain readings. In Table 4.1, the average strain values obtained from the two strain gauges and the two LVDTs are provided and the ratio of

these two values provides an indication of the closeness between the strain gauge readings to the LVDT readings, where a ratio of 100% indicates a perfect match between the two.

Pipe Specimen No.	Avg. SG Strain at Steady State[1] (%)	Avg. LVDT Strain at Steady State[2] (%)	Induced Temperature Change (°C)	Ratio of Avg. SG to Avg. LVDT Strain
SA60-1A	-0.31	-0.34	-20.0	91%
SA60-1B	-0.29	-0.32	-19.0	91%
SA60-2A	-0.28	-0.30	-18.9	93%
SA60-2B	-0.30	-0.34	-19.8	88%
SA114-1A	-0.28	-0.28	-19.2	100%
SA114-1B	-0.25	-0.25	-16.6	100%
SA114-2A	-0.22	-0.22	-14.9	100%
SA114-2B	-0.27	-0.27	-18.6	100%

[1]Average strain of the two strain gauges at steady state inside the refrigerator
[2]Average strain of the LVDTs at steady state inside the refrigerator
Note: Sign convention for strains: Extension – positive; Compression – negative

Table 4.1 Summary of results from thermal contraction tests on MDPE pipe samples

4.2 Discussion of test results from thermally induced axial contraction tests on MDPE

From the typical test results shown in the plots in Figure 4.3 above and the summary data in Table 4.1, it is consistently observed that in each of the tests conducted on 60.3 mm outer diameter pipes with an SDR of 11, the average strains recorded by the strain gauges were slightly less than the average strains derived from the LVDTs. This is in accord with the expectations since the strains within the MDPE pipe are expected to be locally constrained at the strain gauge locations.

However for pipes with an outer diameter of 114.3 mm and an SDR of 11, the average strains recorded by the strain gauges are almost equal to the average strains derived from the LVDTs.

It appears that the effect of the presence of the strain gauge is dependent on the overall stiffness of the MDPE member (governed by the thickness of the pipe) in addition to the intrinsic properties of the MDPE material.

In terms of practical usage for the present research project, the data presented herein suggests that only a small correction factor would be required to accurately consider the use of strain

gauges to measure point strains on the 60.3-mm diameter MDPE pipes used in this research project; on the same basis, no correction would be required for the 114.3-mm diameter pipes.

4.3 Coefficient of thermal expansion of MDPE pipes

In addition to providing an estimate of the strain gauge stiffening effect on local strain readings on MDPE pipes, the thermal contraction tests on MDPE pipes provide an opportunity to characterize the coefficient of thermal expansion (CTE) of this material. The described test configuration allows for characterization of the CTE in the axial direction. In consideration to future research work related to the study of MDPE pipes, the CTE provides part of the parameter data necessary to model the behavior of MDPE under thermal loading using numerical models. Table 4.2 below provides a summary of the measured changes of axial strain for the average strain gauge readings and the average LVDT readings, the measured change in temperatures, as well as the calculated CTE for the strain gauge and the LVDT readings for each of the eight tests conducted. The CTE is taken as the ratio between the change in axial strain of the pipe specimen and the change in temperature over the duration of the test.

Throughout tests conducted by Bilgin et al. (2007) to investigate the thermal and mechanical properties of polyethylene pipes, average CTE values for MDPE pipes in the axial direction were reported as 1.65×10^{-4}/°C. The CTE values for the MDPE pipes tested herein therefore are in accord with the expected range. Any differences between the axial CTE's can be attributed to material anisotropy caused by the manufacturing process (Bilgin et al. 2007).

Pipe Specimen No.	$\Delta\varepsilon_{Axial}$ from the Avg. SG (%)	$\Delta\varepsilon_{Axial}$ from the Avg. LVDT (%)	ΔTemp. (°C)	Axial CTE Derived from SG Readings (mm/mm/°C)	Axial CTE Derived from LVDT Readings (mm/mm/°C)
SA60-1A	-0.31	-0.34	-20	1.70×10^{-4}	1.55×10^{-4}
SA60-1B	-0.29	-0.32	-19	1.68×10^{-4}	1.52×10^{-4}
SA60-2A	-0.28	-0.30	-18.9	1.59×10^{-4}	1.48×10^{-4}
SA60-2B	-0.30	-0.34	-19.8	1.72×10^{-4}	1.52×10^{-4}
SA114-1A	-0.28	-0.28	-19.2	1.46×10^{-4}	1.46×10^{-4}
SA114-1B	-0.25	-0.25	-16.6	1.51×10^{-4}	1.51×10^{-4}
SA114-2A	-0.22	-0.22	-14.9	1.47×10^{-4}	1.47×10^{-4}
SA114-2B	-0.27	-0.27	-18.6	1.45×10^{-4}	1.45×10^{-4}

Table 4.2 Calculated coefficient of thermal expansion of MDPE pipes

CHAPTER 5: FRAMEWORK FOR USING FIELD DATA FOR PREDICTING AXIAL PIPE STRAIN USING UBC MODEL

The following chapter provides a general framework for using the field data from this study to calculate the pipeline axial strain for the buried pipes installed for this research using the new analytical model developed at UBC (Weerasekara 2011; Weerasekara and Wijewickreme 2008; Wijewickreme and Weerasekara 2014). The objective is to demonstrate the outline for the computation of soil loads and pipeline strains on the four of the five pipe alignments in this study that are subjected to relative axial movements, namely Alignments 1, 2, 3 and 4. The analytical solution to assess the performance of Alignment 5 (the pipe alignment in this study subject to relative transverse soil movements) is still in progress and is therefore is not currently considered.

The main purpose is to provide a set of model input parameters that will allow for the proposed analytical work to be validated and used with a higher level of confidence. Results from the analytical predictions can be compared with the field experimental data set as more data becomes available over the duration of the research study. However, before discussing the implementation of the field research program conducted under this study to the analytical model, it is important to provide a brief summary of the model with the associated laboratory work conducted previously at UBC to validate such model.

5.1 Overview of the UBC analytical model

As previously discussed in Chapter 2, the overall buried pipe response depends on the pipe properties (e.g. pipe cross-sectional area, stress-strain behaviour of pipe material) and the soil characteristics (e.g. pipe burial depth, soil density, internal friction angle of the soil, interface friction angle between pipe and soil, stiffness of the soil, coefficient of lateral earth pressure), The analytical framework derived by Weerasekara (2011) incorporates all of these aspects into the model.

Generally, the model is a closed-form solution that incorporates a new interface friction model to idealize more realistically the effect of the soil loads developed from relative axial soil movement. The model was mainly developed to overcome the shortcomings of the soil-pipe

bilinear frictional models that are commonly adopted in pipeline guidelines. Additionally, the nonlinear viscoelastic properties of the polyethylene pipes are accounted for in the formulation as opposed to the typical linear-elastic or bilinear stress-strain response adopted in practice. The analytical solution was derived to determine the pipe response arising from axial soil loading by combining the new interface friction model and the nonlinear stress-strain behaviour of the pipe material (Weerasekara 2011).

Further details pertaining to the derivation of the new analytical model can be obtained form Weerasekara (2011), Weerasekara and Wijewickreme (2008), and Wijewickreme and Weerasekara (2014).

5.1.1 Previous validation of the new analytical model

The validity of the closed-form solution was previously assessed by comparing the calculated response of 60 mm and 114 mm diameter pipes in axial pullout with experimental results from pullout tests performed on the same diameter pipes using the soil chamber at UBC. The predictions were made using parameters determined from element testing of pipe and soil combined with experience-based judgment from axial tests conducted on steel pipes.

The experimental pullout resistance and strain characteristics were obtained from load cell and strain gauge readings directly from the axial pullout tests performed on the pipes. A comparison of the predicted values from the closed-form solution and the experimental results obtained from Weerasekara (2011) are shown in Figure 5.1 and 5.2 below. A close match between the predicted and experimental results for the tests validated the parameter selection for the formulation of the closed-form solution (Wijewickreme and Weerasekara 2014). In each figure, the ‘leading end’ and the ‘trailing end’ of the pipes refer to the pulling end and the free end of the pipes, respectively, in the soil-testing chamber.

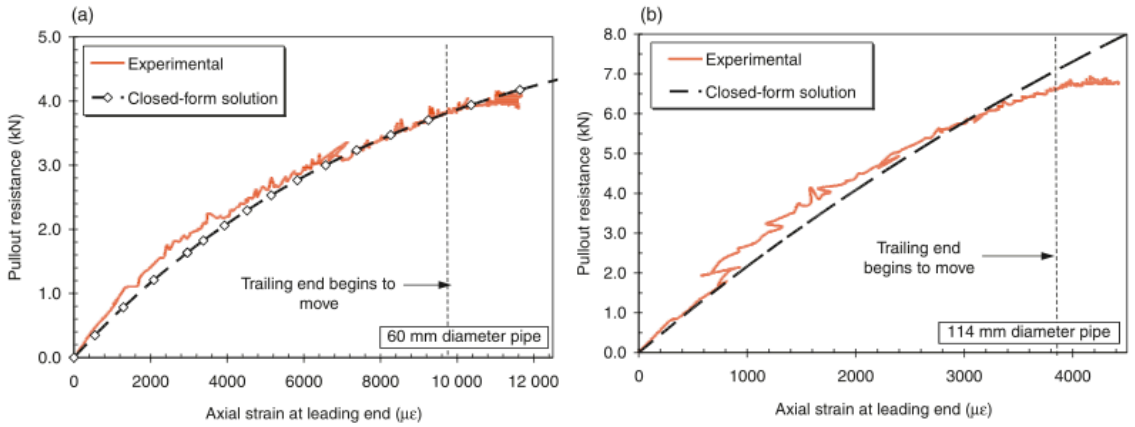

Figure 5.1 Predicted and measured force-strain relationship under axial loading in (a) 60 mm pipe, and (b) 114 mm pipe (Weerasekara 2011)

Figure 5.2 provides further comparison of the predicted versus measured response of the pipes and shows the strain versus displacement predictions for 60 mm and 114 mm pipes. In all these cases, very good agreement between the measured and the predicted value were observed, confirming the ability of the closed-form solution to represent the mobilization of friction along the pipe length at low to moderate strains in general.

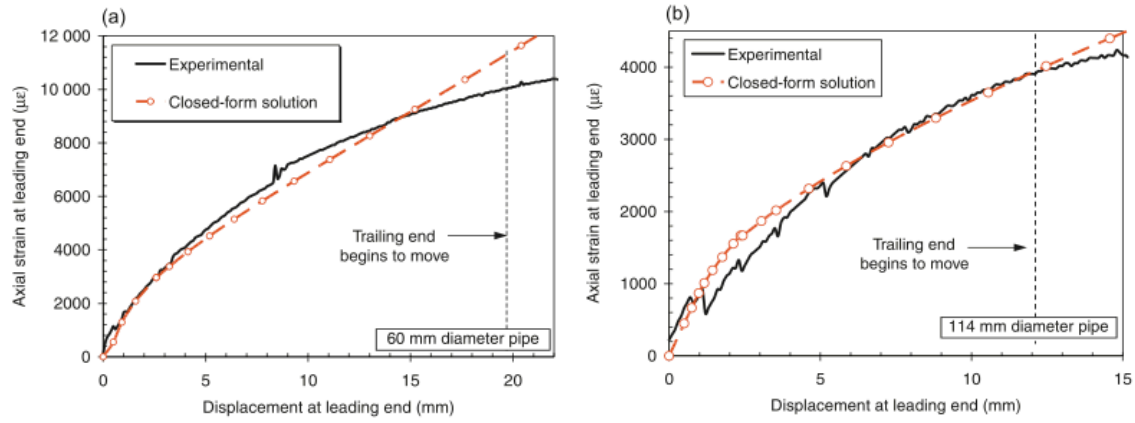

Figure 5.2 Predicted and measured strain-displacement relationship under axial loading in (a) 60 mm pipe, and (b) 114 mm pipe (Weerasekara 2011)

5.2 Summary of field data for model input parameters

The following sections provide a summary of the field data for the model input parameters to calculate the pipeline axial strain for the current field study and includes discussions to identify the landslide geometry at the research site, selection of input parameters, and a brief summary of

the underlying assumptions made to enable such predictions at this early stage of the research program.

5.2.1 Identifying slide geometry at the subject research site

In order to apply any soil-pipe interaction model to a real-life scenario, identifying the geometry of the sliding soil mass is of significant importance. The developed sets of equations are valid for a slide geometry in which the ground moves as a block in the vicinity of the pipe as opposed to flowing around the pipe.

Generally, under a landslide, tensile stresses can develop in the pipe section at the ground separation zone when the sliding block is separated from the stable ground. The slide geometry shown in Figure 5.3 below provides a schematic example of the block type slide movement that has been assumed for the current framework. For experimental studies on pipeline components, a block-displacement type ground deformation is a reasonable simplification for reproducing the soil displacement conditions occurring around a relatively localized section of pipeline (Anderson, 2004), and has also been adopted for previous research work carried out at UBC.

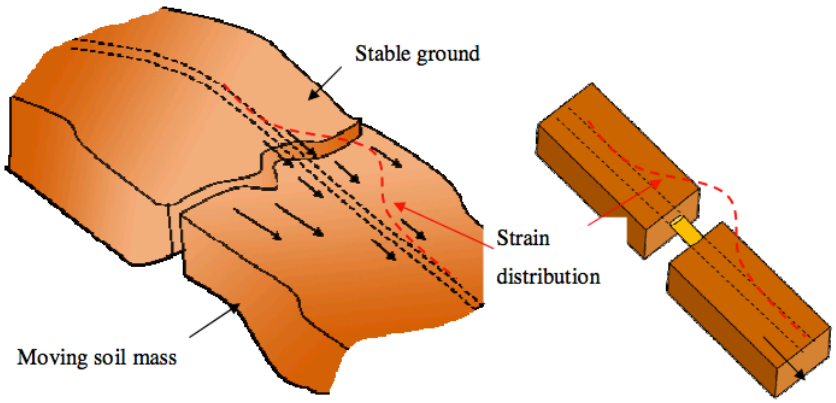

Figure 5.3 Schematic of the slide geometry assumed for the current framework (Weerasekara 2011)

For the present study, ground surface survey hubs that were installed at the research site following the pipeline installations are used to monitor the relative ground displacements occurring. At this point in time, however, it is considered that the ground movements that have occurred at this early stage of the project are too small to be accurately identified by survey methods. In consideration of this, for the framework presented, a hypothetical scenario of

landslide-induced movement has been assumed. Under this scenario, a block type slide movement with the weak soil layer situated below the pipe burial depth is considered to be the mobilized field ground movement. Furthermore, it is assumed that the relative ground movements at the site are acting parallel to the axial lengths of Alignments 1, 2, 3 and 4 depicted in Figure 3.2, and that the ground separation point is located at the axial midpoint of each of the alignments i.e. at the 12 m point from the uphill ends of the alignments.

As the ground continues to move at the research site and more ground surface survey data is collected, further refinements of the slide geometry and relative ground movements can be made allowing for more detailed analysis of the buried alignments. At this time however, the above listed assumptions are adopted in order to complete the framework proposed herein.

5.2.2 Selection of input parameters for analytical calculations

When using the derived equations from the closed-form solution, the geometric parameters of pipe burial depth to springline (H), outside pipe diameter (D), pipe cross-sectional area (A_p) and average soil density (γ) are constants that are measured directly and were accounted for relative easily prior to and during the pipeline installations. Determining appropriate input parameters for the remainder of the closed-form solution however is not quite a straightforward task. For the current study the selection of these parameters generally follows those from the analysis conducted by Weerasekara (2011), and therefore only limited discussion on these are included herein. Adopting model parameters from previous analysis is considered reasonable for the purpose herein, which is to provide a framework for strain calculations of the axially loaded pipelines.

Table 5.1 below provides a summary of the input parameters for the study to be used for modeling the pipeline performance. In Table 5.1, the ground-movement rates have note been identified at this point in time. However, the model user can choose a ground displacement rate of approximately 5 mm/month for the time being until appreciable ground surface movements have been observed in the field.

Model Input Parameter	Align. No. 1	Align. No. 2	Align. No. 3	Align. No. 4	Align. No. 5
Interface friction on pipe					
Δt_d (mm)	3	3	3	3	3
$G_{(\gamma=2.5\%)}$(kN/m^2)	600	600	600	600	600
γ (kN/m^3)	18.1	18.1	18.0	18.4	18.9
H (m)	0.75	0.90	0.65	0.75	0.90
K_0	0.5	0.5	0.5	0.5	0.5
δ (degrees)	16	16	16	16	16
Displacement at zero dilation (mm)	50	50	50	50	50
Pipe Properties					
Pipe outside diameter (mm)	60.3	114.3	60.3	60.3	114.3
Pipe wall thickness (mm)	5.48	10.32	5.48	5.48	10.32
Rate dep. hyperbolic constants					
a	2020	2020	2020	2020	2020
b	0.109	0.109	0.109	0.109	0.109
c	43.35	43.35	43.35	43.35	43.35
d	1.37	1.37	1.37	1.37	1.37
Ground movement conditions					
Ground movement rate (mm/mo.)	-	-	-	-	-
Parameters that are not part of the analytical solution					
Alignment Burial length (m)	24.23	24.59	24.17	24.15	23.87

Table 5.1 Summary of model input parameters for the analytical solution

5.3 Projected model results

As noted by Weerasekara and Wijewickreme (2008), when comparing the full-scale test results with the predictions form the closed-form solution, the comparison can only be made until the displacement at which the full pipe frictional length is mobilized. Beyond this point the boundary conditions of the pipe end will affect the results.

For the current framework under consideration, it is assumed that the relative displacement occurring for the sliding block failure is located at the midpoint of the axially loaded pipes. With this assumption, Figure 5.4 provides a generalized schematic plot of one potential scenario of the projected mobilized friction length over time as the ground continues to move at the subject research site.

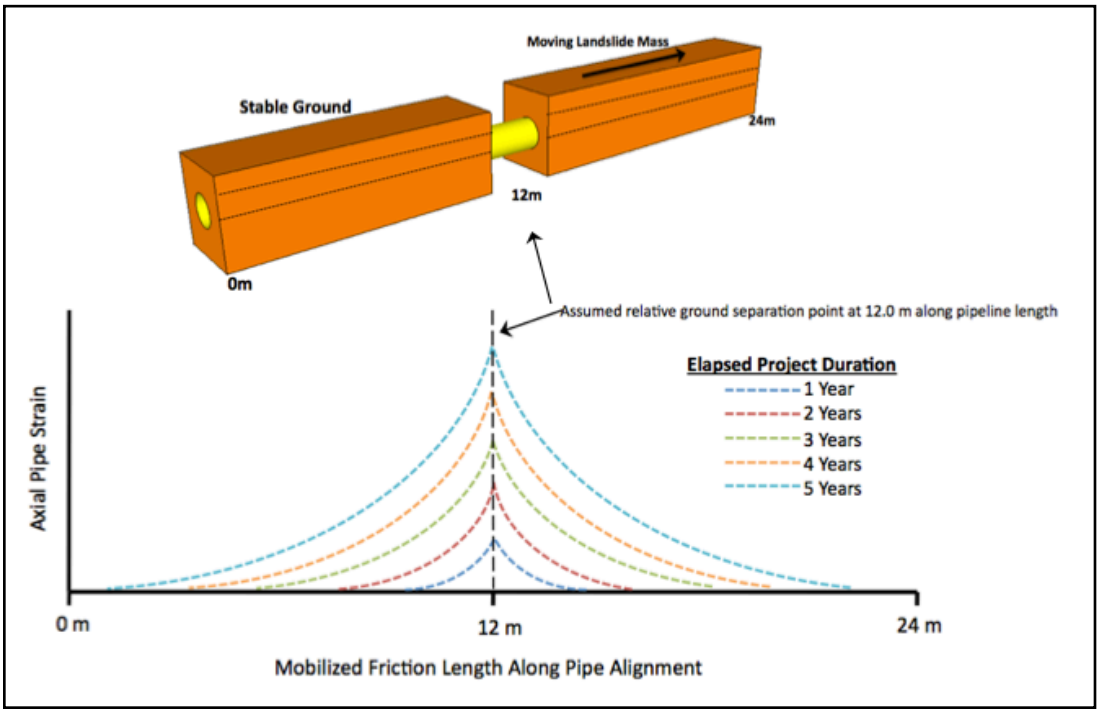

Figure 5.4 Schematic of the projected axial pipe strain over the duration of the research study

CHAPTER 6: SUMMARY AND CONCLUSIONS

Soil-pipe interaction models for modern day PE pipelines are not as well established compared to steel pipes mainly due to the more recent adoption of PE pipes to the industry. The capabilities and characteristics of PE, however, have greatly improved since their initial implementation more than 40 years ago, and PE pipeline networks have established an impressive safety record over the past few decades. Today's natural gas distribution companies install PE services confidently as a result of continued industry attention and education involving better materials and a better understanding of the performance of these materials for both immediate and long term system integrity.

The performance of buried natural gas pipelines located in areas prone to ground movement is a major concern for utility owners since the failures of such pipeline systems during service is extremely serious due to the potential for loss of life, as well as the associated environmental and economical impacts. With plastic pipes now the industry standard for most utility distribution systems, understanding the response of these extensible pipes when subjected to ground movements is an important consideration and critical for their integrity.

A research program was initiated at UBC to investigate the performance of buried MDPE pipelines subjected to ground movements. During the earlier stages of this research, a full-scale pipe-soil testing facility was developed and several full-scale pipe pullout tests on selected diameters and configurations of MDPE pipes were performed. During more recent stages of this research, a field testing program was conducted on five axial pipe pullout tests with different burial depths, pullout rates and loading regimes. The laboratory and field pullout tests led to the development of a new analytical model to determine the response of pipes subjected to axial and lateral soil loading. The model was derived using an advanced interface friction model to account for the soil dilation and interface friction aspects, and combined with the MDPE pipe nonlinear stress-strain pullout resistance, displacement and mobilized frictional lengths obtained from the experimental data.

The main objective of the current research was to further validate the new analytical model that was developed at UBC using a full-scale field test established to monitor the performance of MDPE pipes subjected to ground movement. The ultimate goal of this research is to provide

further contributions to the previous research work on this subject to help develop guidelines and criteria to determine the amount of ground displacement associated with the safe operational limits of buried natural gas distribution pipelines.

6.1 Summary of research contributions for the current study

The following sections provide a brief summary of the work that was carried out throughout the current study subsequent to the previous research work at UBC on this subject.

6.1.1 Full-scale field test of buried MDPE natural gas distribution pipelines

A full-scale field testing program was designed and implemented at a selected research site located in Chilliwack, BC, which consisted of burying five MDPE pipeline alignments in a slow moving landslide. Historical survey field monitoring data from the selected site suggests that throughout a seven year period, from February 2004 to February 2011, as much as 450 mm of ground movement had occurred at the site. This suggests that on average, about 5 mm of ground surface movement is occurring at the site each month.

A total of five pipeline alignments, each approximately 24 m in length, were installed for this research to investigate the performance of straight and branched natural gas pipelines loaded in both the axial and lateral directions.

Alignments 1 through 4 were installed such that the axial lengths of the pipelines are parallel to the anticipated direction of the predominant ground movements occurring at the site. The intent is that the soil loads developed from the relative axial soil movement will extend the pipes in the axial direction. In contrast, Alignment 5 was installed with the axial length of the pipeline perpendicular to the ground movement in order to develop tensile forces in the pipe resulting from relative lateral pipe movement.

One of the main objectives of this research is to obtain a reliable data set of ground movement and associated pipe strain data. As such, a considerable amount of effort was put in to installing strain gauges along the lengths of each pipe alignment in order to measure strain within the pipe specimens. Previous experimental pipe research at UBC proved successful with installing strain gauges onto MDPE pipes using specialized procedures developed at UBC. Based on the previous success, these same procedures for installing strain gauges were adopted for the current research

and additionally, a three layer waterproof coating procedure was developed and applied to protect the gauges in the field for the duration of the research, which is expected to be several years. Prior to the installation, the pipes were instrumented with over 200 strain gauges to provide pipe strain data as they are induced to deformations caused by the continuing ground movement at the site.

Additionally, a data collection program was established for the program, which includes regular acquisition of the buried pipe stain, pipe deformation and ground surface movement data from the site.

6.1.2 Strain gauge stiffening effect on local strain readings on MDPE pipe

In addition to the field program established for this research and in recognition of the effects of strain gauge stiffening on local strain readings on PE material, an experimental program was undertaken to determine the effect of strain gauge stiffening on the MDPE pipes used for this sttudy. Thermally induced contraction tests were carried out on four MDPE pipe specimens to determine the effects of strain gauge stiffening on local strain readings on these pipes. In terms of practical usage for the present research project, the data from these tests suggests that only a small correction factor would be required to accurately consider the use of strain gauges to measure point strains on the 60.3-mm diameter MDPE pipes used in this research project; on the same basis, no correction would be required for the 114.3-mm diameter pipes.

6.1.3 Framework for using field data for predicting axial pipe strain using UBC model

A general framework for using the field data from this study to calculate the pipeline axial strain for the buried pipes installed for this research using the new analytical model developed at UBC was presented. The objective is to demonstrate the outline for the computation of soil loads and pipeline strains on the four of the five pipe alignments in this study that are subjected to relative axial movements. The main purpose is to provide a set of model input parameters that will allow for the proposed analytical work to be validated and used with a higher level of confidence. Results from the analytical predictions can be compared with the field experimental data set as more data becomes available over the duration of the project.

A generalized plot of one potential scenario of the projected mobilized friction length over time as the ground continues to move at the subject research site was presented assuming a hypothetical scenario of landslide-induced movement.

6.2 Future research considerations

Previous studies performed at UBC over the past 13 years have clearly demonstrated that the performance of buried MDPE pipes subjected to ground movements is a complex-soil-pipe interaction problem. Continued research on this subject will help to compliment the current findings and help develop guidelines and criteria to determine the amount of ground displacement associated with the safe operational limits of buried natural gas distribution pipelines.

1. This project takes advantage of the rare opportunity to instrument, install and monitor gas pipeline sections subject to ground movement. Continued collection of the field data from the subject research site is critical in order to develop a reliable database of ground movement and associated pipe strain to use for future validation of analytical and numerical models.

2. Perform detailed analytical model predictions for the pipelines in this study using the framework included herein to further validate the new UBC model.

3. The critical information gathered from this study provides soil and pipe data measured directly at this high-risk site, which will also enable gas distribution network owners to assess the risk of ground movements on their pipeline networks in other locations.

Research leads to better designs, optimized overall cost and safer more predictable pipeline infrastructure. Continued studies and evaluation to better understand MDPE pipe performance behaviour leads to an overall industry benefit. The active research carried out at UBC and the associated results of this research will bring a better understanding of and improved MDPE pipe design and applications. While the primary objective is to maintain public safety and uphold the reliability of supply delivery, an important secondary objective

is to manage the level of costs incurred, particularly for natural gas distributors that have significant replacement challenges.

REFERENCES

ALA (2001) "Guidelines for the design of buried steel pipe," American Lifeline Alliance, available from www.americanlifelinesalliance.org/Products_new3.htm (cited December 6, 2013).

American Standards for Testing and Materials (ASTM) International (1999) "Standard guide for use of maxi-horizontal directional drilling for placement of polyethylene pipe or conduit under obstacles, including river crossings." ASTM F 1962-99, 1-17.

Anderson, C. (2004) "Response of buried polyethylene natural gas pipelines subjected to lateral ground displacement," M.A.Sc. thesis, Department of Civil Engineering, University of British Columbia, Vancouver, B.C., Canada.

ASCE (1984) "Guidelines for the seismic design of oil and gas pipeline systems," Committee on Gas and Liquid Fuel Lifelines, Technical Council on Lifeline Earthquake Engineering, American Society of Civil Engineers (ASCE), New York, USA.

Bilgin, O. and Steward, H.E. (2009) "Design guidelines for polyethylene pipe interface shear resistance," Journal of Geotechnical and Geoenvironmental Engineering, 135 (6): 809-818.

Bilgin, O., Stewart, H. E. and O'Rourke, T. D. (2007) "Thermal and mechanical properties of polyethylene pipes," Journal of Materials in Civil Engineering, 19 (12): 1043-1052.

Brachman, R.W.I. (1999) "Mechanical performance of landfill leachate collection pipes," Ph.D. thesis, Department of Civil and Environmental Engineering, The University of Western Ontario, London, Ontario, Canada.

Brachman, R.W.I, Moore, I.D. and Rowe, R.K. (2000) "The design of a laboratory facility for evaluating the structural response of small-diameter buried pipes," Canadian Geotechnical Journal, 37: 281-295.

Brachman, R.W.I, Moore, I.D. and Rowe, R.K (2001) "The performance of a laboratory facility for evaluating the structural response of small-diameter buried pipes," Canadian Geotechnical Journal, 38: 260-275.

Briassoulis, D., and Schettini, E. (2002) "Measuring strains of LDPE films: the strain gauge problems." Polymer Testing, 21(5), 507-512.

Bruschi, R., Glavina, S., Spinazze, M., Tomassini, D., Bonanni, S., and Cuscuna, S. (1996) "Pipelines subjected to slow moving landslide movements: Structural modeling vs. field measurement," Proceedings of the 15th International Conference on Offshore Mechanics and Arctic Engineering, ASME, pp. 343-354.

Bughi, S., Aleotti, P., Bruschi, R., Andrei, G., Milani, Gl, Scarpelli, G., and Sakellardiadi, E. (1996) "Slow movements of slopes interfering with pipelines: Modelling and monitoring," Proceedings of the 15th International Conference on Offshore Mechanics and Arctic Engineering, ASME, pp. 363-372.

Chehab, A.G. (2008) "Time dependent response of pulled-in-place HDPE pipes," Ph.D. thesis, Department of Civil Engineering, Queen's University, Kingston, Ontario, Canada.

Chehab, A.G. and Moore, I.D. (2004) "A uniaxial linear viscoelastic-viscoplastic model for high density polyethylene," Proceedings of 57th Canadian Geotechnical Conference, Quebec, October, 6D1-6D6.

Chehab, A., and Moore, I.D. (2006) "Constitutive model for high density polyethylene to capture strain reversal," ASCE 2006 Pipeline conference, ASCE, Reston, VA.

Chehab, A.G. and Moore, I.D. (2010) "Parametric study examining the short and long term response of HDPE pipes when installed by horizontal directional drilling," Tunnelling and Underground Space Technology, 25: 782-794.

Chehab, A.G. and Moore, I.D. (2010) "Pipe-soil interaction stiffness in horizontal directional drilling and pipe bursting," Geomechanics and Geoengineering: An International Journal, 5(2): 69-77.

Chehab, A.G. and Moore, I.D. (2012) "Analysis for long-term response of pipes installed using horizontal directional drilling," Journal of Geotechnical and Geoenvironmental Engineering, 138 4: 432-440.

Hansen, B.J. (1961) "The ultimate resistance of rigid piles against transversal forces," Bulletin 12, Danish Geotechnical Institute, Copenhagen, Denmark.

Karimian, A.H. (2006) "Response of buried steel pipelines subjected to longitudinal and transverse ground movement," Ph.D. Thesis, Department of Civil Engineering, The University of British Columbia.

Kennedy, R.P, Chow, A.W. and Williamson, R.A. (1977) "Fault movement effects on buried oil pipeline," Transportation Engineering Journal, ASCE, 103:617-633.

Moore, I.D., and Hu., F. (1996) "Linear viscoelastic modeling of profiled high density polyethylene pipe," Canadian Journal of Civil Engineering, 23(2), 395-407.

Mwanang'onze, H., Moore, I., and Green, M. (2003) "Coefficient of thermal expansion characterization for plain polyethylene pipe," New Pipeline Technologies, Security and Safety: pp. 1302-1311.

Newmark, N.M and Hall, W.J. (1975) "Pipeline design to resist large fault displacement," Proceedings of US National Conference on Earthquake Engineering, Ann Arbor, Michigan, pp. 416-425.

Nishio, N. (1995) "Mechanisms of gas pipeline failures on Balboa Boulevard during the 1994 Northridge Earthquake," Proceedings of the 4th US Conference of Lifeline Earthquake Engineering, San Francisco, August 22-23, pp. 216-223.

O'Connor, C. and Noble Denton (2012) "The nature of polyethylene pipe failure," Pipeline and Gas Journal, 239 (12): 76:77.

O'Rourke, M.J. (1989) "Approximate analysis procedures for permanent ground deformation effects on buried pipelines," Proceedings of the Second Japan-US Workshop on Liquefaction, Large Ground Deformation and Their Effects on Lifelines, Technical Report NCEER-89-0032, National Center for Earthquake Engineering Research, Buffalo, NY, pp. 336-347.

O'Rourke, T.D., Druschel, S.J. and Netravali, A.N. (1990) "Shear strength characteristics of sand-polymer interfaces," Journal of Geotechnical Engineering, ASCE, 116 (3): 451-469.

O'Rourke, M.J. and Nordberg, C. (1990) "Analysis procedures for buried pipelines subject to longitudinal and transverse permanent ground deformation," Proceedings of the Third Japan-US Workshop on Earthquake Resistant Design of Lifeline Facilities and Countermeasures for Soil Liquefaction, Technical Report NCEER-91-0001, National Centre for Earthquake Engineering Research, Buffalo, NY.

O'Rourke, T.D., and O'Rourke, M.J. (1995) "Pipeline response to permanent ground deformation: A benchmark case," Proceedings of the fourth US Conference on Lifeline Earthquake Engineering, TCLEE, ASCE, San Francisco, California, August 1995, pp. 288-295.

O'Rourke, T., and Tawfik, M. (1983) "Effects of lateral spreading on buried pipelines during the 1971 San Fernando Earthquake," Earthquake Behaviour and Safety of Oil and Gas Storage Facilities, Buried Pipelines and Equipment, PVP Vol. 77, ASME, New York, NY, pp. 124-132.

Paulin, M.J., Phillips, R., Clark, J.I., Hurley, S. and Trigg, A. (1997) "Establishment of a full-scale pipeline/soil interaction test facility and results from lateral and axial investigations in sand," Vol. V, 16th International Conference Offshore Mechanical and Arctic Engineering '97, Yokohama, pp. 139-146.

Paulin, M.J., Phillips, R., Clark, J.I., Trigg, A. and Konuk, I. (1998) "A full-scale investigation into pipeline/soil interaction," Proceedings of International Pipeline Conference, ASME, Calgary, AB., pp 779-788.

Petroff, L.J. (1990) "Stress relaxation characteristics of HDPE pipe-soil systems," Proceedings of the International Conference on Pipeline Design and Installation, ASC Pipeline Division, Las Vegas, pp. 280-294.

Petroff, L.J. (1990) "Review of the relationship between internal shear resistance and arching in plastic pipe installations," Symposium on Buried Plastic Pipe Technology, ASTM STP 1093, George S. Buczala and Michael J. Cassady, Eds., ASTM, Philadelphia, pp. 226-280.

PHMSA (2010) Distribution, transmission, and liquid annual data, Pipeline Hazardous Material Safety Administration. Available from www.phsma.dot.gov

PPI (2007) Handbook of PE Pipe, 2nd ed. Plastic Pipe Institute, Irving, TX.

PRCI (2009) "Guidelines for constructing natural gas and liquid hydrocarbon pipelines in areas subject to landslide and subsidence hazard," Report prepared by D.G. Honegger Consulting, C-Core and SSD Inc. for the Design, Construction & Operations. Technical Committee of Pipeline Research Council International Inc. Catalog No. L52292(V).

Ranji, B.B., Robertson, P.K. and Morgenstern, N.R. (1995) "Simplified design methods for pipelines subject to transverse and longitudinal soil movements," Canadian Geotechnical Journal, 32: 309-323.

Stewart, H.E., Bilgin, O., O'Rourke, T.D. and Keeney, T.M (1999) "Technical reference for improved design and construction to account for the thermal loads in plastic gas pipelines," Technical report, Cornell University, Ithaca, N.Y.

Trautmann, C.H., and O'Rourke, T.D. (1983) "Behaviour of pipe in dry sand under lateral and uplift loading," Geotechnical Engineering Report 83-7, Cornell University, Ithaca, N.Y.

Vaid, Y.P. and Thomas, J. (1995) "Liquefaction and postliquefaction behaviour of sand," Journal of Geotechnical Engineering, 121(2), pp. 163-173.

Weerasekara, L. (2007) "Response of buried natural gas pipelines subjected to ground movements," M.A.Sc. thesis, Department of Civil Engineering, University of British Columbia, Vancouver, B.C., Canada

Weerasekara, L. (2011) "Pipe-soil interaction aspects in buried extensible pipes," Ph.D. thesis, Department of Civil Engineering, University of British Columbia, Vancouver, B.C., Canada.

Weerasekara, L. and Wijewickreme, D. (2008) "Mobilization of soil loads on buried, polyethylene natural gas pipelines subject to relative axial displacements," Canadian Geotechnical Journal, 45: 1237-1249 (2008).

Wijewickreme, D., Honegger, D.G., Mitchell, A., and T.P. Fitzell (2005) "Seismic vulnerability assessment and retrofit of a major natural gas transmission system: A case history," Earthquake Spectra, Journal of Earthquake Engineering Research Institute (EERI), Vol. 21, No. 2, pp. 539-567.

Wijewickreme, D., Karimian, H. and Honegger, D. (2009) "Response of buried steel pipelines subject to relative axial soil movement," Canadian Geotechnical Journal, 46(7): 735-752.

Wijewickreme, D. and Weerasekara, L., (2014) "Analytical modeling of field axial pullout tests performed on buried extensible pipes," International Journal of Geomechanics, Accepted for publication December 23, 2013.

Yimsiri S, Soga K, Yoshizaki K, Dasari GR, and O'Rourke TD. (2004) "Lateral and upward soil-pipeline interactions in sand for deep embedment conditions," ASCE Journal of Geotechnical and Geoenvironmental Engineering 2004; 130 (8).

Zhang, C., and Moore, I.D. (1997) "Nonlinear mechanical response of high density polyethylene. Part II: Uniaxial constitutive modeling," Polymer Engineering and Science, 37(2), 414:420.

APPENDIX A

Field program installation photos

MDPE pipe delivery to UBC on September 14, 2012

MDPE pipe delivery to UBC on September 14, 2012

Strain gauge installation at UBC
(Sept. 2012 to Feb. 2013)

Strain gauge installation
(Note stress relief loop in lead wire)

Strain gauge installation with first layer of waterproof coating applied

Strain gauge installation with second layer of waterproof coating applied

Strain gauge installation with third and final layer of waterproof coating applied

Timber frame used for transporting pipes to research location

Loading pipes onto flat bed truck for transport to research location

General view of the research location (photo taken facing south)

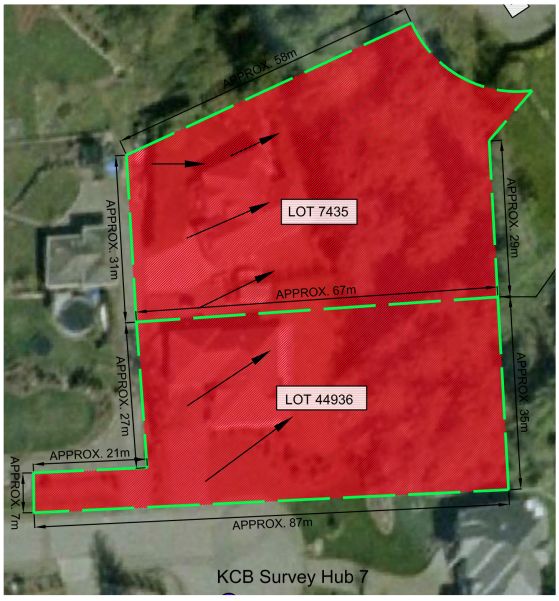

Plan view of the site location with the black arrows indicating direction of ground movement (approx. NE)

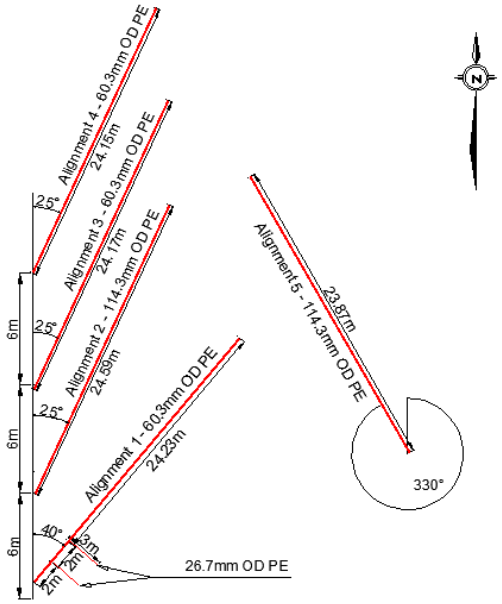

Installed pipeline configurations

View of the site from Ridgeview Drive, Chilliwack, BC. Photo taken facing North.

Pipe installation (May 21 to May 23, 2013) showing excavated trench for Alignment 4

Excavated trench for Alignment 5, and buried lock-block anchor

Compaction of bedding layer prior to pipe placement for Alignment 4

Preparing MDPE pipes for placement in excavated trench

Pipe segment butt fusion (114.3 mm pipe)

Pipe segment butt fusion (114.3 mm pipe)

Pipe placement (Alignment 2)

Pipe placement (Alignment 1)

Left: Baseline strain gauge arrangement Centre: RTD
Right: Alignment 4 trunk line

Typical dead-man anchor installation

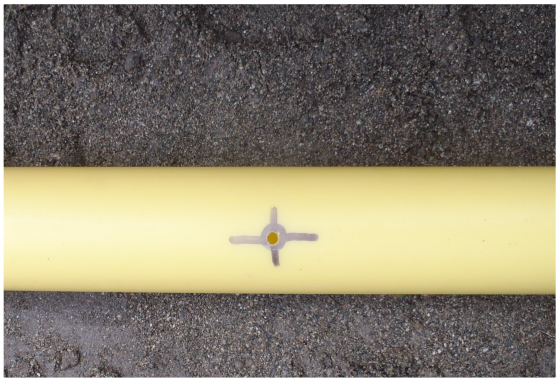

Drilled hole in MDPE to monitor pipe displacement using survey techniques

4” Big-O tube installed vertically above drilled hole to provide access for survey measurements

Compacting first lift of FRS above buried pipe

Plastic irrigation box used for strain gauge lead wire exit points for easy data collection

Establishing survey monument to monitor ground surface movements

Establishing survey monument to monitor ground surface movements

Site conditions four months after installation (September 2013)

Site conditions four months after installation (September 2013)

APPENDIX B

Detailed strain gauge installation procedures used for the current research study

THE INFOMRATION HEREIN PROVIDES DETAILED STRAIN GAUGE INSTALLATION PROCEDURES FOR THIS RESEARCH. THE INFORMATION WAS OBTAINED FROM: ANDERSON (2004), WEERASEKARA (2007), WEERASEKARA (2011) AND VISHAY MICRO-MEASUREMENTS AT WWW.VISHAYPG.COM/MICRO-MEASUREMENTS, AS WELL AS CONSULATIONS WITH SCOTT JACKSON IN THE DEPARTMENT OF CIVIL ENGINEERING AT UBC	
Note: Hands, work surfaces and tools should be cleaned prior to beginning. Use clean clothes and MG Chemicals Cleaner Degreaser (or equivalent) to clean all surfaces.	
1) Polyethylene surface preparation for strain gauge installation	
Properly prepared surfaces are required for the strong stable bonds necessary for the transmission of surface strains to the gauge.	
1.	Thoroughly wipe PE surface with clean rag to remove any residual dirt or contaminants.
2.	Clean PE surface with degreaser (isopropanol) to remove any residual chemicals and/or contaminants (spray degreaser into a clean cloth and then wipe the specimen surface thoroughly). The entire diameter of the PE pipe should be wipe clean where the waterproofing protection will be applied. Discard soiled cloth to prevent any recontamination. Continue wiping the specimen surface until the sponge comes up clean. Be careful not to wipe contaminated areas into the cleaned areas. Allow surface to dry for 15 minutes.
3.	Lightly etch PE surface in the area where the strain gauge is to be installed with 220 grit sand paper (do not excessively roughen PE surface as large gouges in the surface may effect gauge bonding and create local strain concentrations).
4.	Clean PE surface in the etched region with degreaser to remove residual chemicals and/or PE etchings form the application surface. Allow surface to dry for 15 minutes.
5.	Apply a coat of Loctite 770 Primer using a clean cloth and allow surface to dry for 15 minutes. An area of about 30mm by 60 mm should be primed in the region where the strain gauge will be applied. Apply the gauge within 30 minutes of step 4 to prevent recontamination of primed surface.
2) Gauge and soldering pad application	
1.	Carefully remove the gauge and soldering pad from the Mylar package with tweezers by pinching at one corner of the gauge without touching the grid area. Place the gauge and the pad on the clean work surface with the bonding sides facing downwards.
2.	Align the gauge and pad on the work surface with ~6mm separation between the two. Ensure that the gauge lead wires are aligned approximately straight and are showing on top of the soldering pad so that they do not end up bonded below the pad. Use a ~75mm long piece of Mylar tape to cover the entire gauge and pad assembly.
3.	Wipe through the tape with the side of your thumb to ensure good contact with the gauge and pad. Lift the tape at a shallow angle to prevent damage to the un-bonded gauge. Remove it from the work surface.
4.	Align the tape/gauge assembly with the axis of the PE pipe specimen and secure it in place on the pipe surface. Reposition if necessary.

5.	Peal back the tape at a shallow angle starting at the end of the gauge to expose the bonding side of the gauge and the pad. Pull the tape back until the pad is exposed.
Note: The following three steps should be undertaken in a timely fashion to ensure proper adhesion of the strain gauge to the pipe surface.	
6.	Apply a small amount (a drop) of **Loctite 414 cyanoacrylate adhesive** on the PE pipe surface right beside the tape, and directly on the bonding side of the end of the strain gauge nearest to the soldering pad.
7.	Align the gauge/tape assembly over the bonding area. In one motion, wipe the gauge/tape assembly down onto the PE surface using thumb, expelling any excess adhesive with thumb pressure.
8.	Apply and maintain immediate thumb pressure for one minute over the gauge and pad. The warmth of the thumb help with the adhesion process. Apply a twisting action to the thumb when removing from the surface.
9.	Leave tape in place and apply a piece of foam tape overtop of the gauge and pad, wrap assembly with electrical tape to apply a nominal pressure to the gauge. Allow adhesive to set for 24 hours.
10.	After 24 hours, carefully remove tape from the surface by pulling at a sharp angle away from the gauge. Inspect gauge installation. Ensure good adhesive flow around the gauge and that no voids are present under the grid area.
11.	If adhesive has spread and tape remains stuck to the pipe, carefully pick away at the adhesive using an exacto knife, being careful not to damage the PE pipe of the gauge.
3) Soldering lead wires to soldering pads	
1.	Lightly place a piece of electric tape (or similar) overtop of the strain gage in order to protect it throughout the soldering application. The tape should not touch the gauge, rather arch it overtop of the grid and apply it on either side of the gauge onto the pipe.
2.	Carefully pull the lead wires up off the PE pipe using tweezers. The lead wires may be lightly adhered to the pipe after the gauge application procedure. Pull them back to the edge of the strain gauge.
3.	Strip ~40mm of the black polyurethane jacket from the lead wires to expose the four wires (red, white, black and un-insulated). Strip by scoring ~1mm deep into the jacket with an exacto knife, and exercise the jacket until the foil protective coating is exposed. Pull away the jacket once it's free.
4.	Cut off the drain wire (un-insulated wire) off where it meets the black polyurethane jacket.
5.	Strip ~10mm of the insulation from each of the red, white and black wires.
6.	Twist the red bundle tightly back to the end of the insulation.
7.	Twist the black and the white bundles together back to the end of the insulation.
8.	Tin the two bundles: Create a small puddle of solder at the tip of the soldering iron. Individually, place each bundle in the puddle starting at the end closest to the insulation. Add more solder while drawing the wire through the puddle if needed. Tin the entire ~10mm section of the exposed wire.
9.	Clean the iron tip on a clean cloth and apply more solder to the tip.

10.	Tin the soldering tabs: Set the solder on the tab, apply firm pressure with the tin soldering iron tip and add more solder for about one second. Be sure not to apply heat to the tab for a prolonged period or the pad may de-bond from the pipe.
11.	Create a stress relief loop in the gauge lead wires and set the gauge lead wires in place overtop of the soldering pads. Cut off excess (about half) of the tinned lead wires. Apply heat with the soldering iron momentarily to secure the lead wires. Its helpful to tape the jacketed lead wires temporarily onto the pipe to hold the lead wires in position through this step.
12.	Use two plastic zip ties to attach the lead wire to the PE pipe. The end of the jacket should be 10mm to 20mm away from the back of the solder pad allowing strain relief loops in the conducting wires.
13.	Solder the wires to the soldering pad. Additional solder should not be required at this stage as the pads and wires are already tinned.
14.	Clean the gauge and wire assemble using a M-Line Rosin Solvent to remove rosin flux. Soak up any excess solvent with a clean cloth. Repeat two or three times until all flux residue is removed. The key area is between the lead wires soldered to the pad.
4) Apply waterproof/weather protective coatings	
1.	Applying M-Coat D acrylic coating: Tape down the stress relief loops in the lead wires so that they are resting directly on the PE pipe surface and generously apply M-Coat D to cover the strain gauge, soldering pad and exposed insulated wires. Allow the coating to dry for about an hour and apply a second coat. The second coat should exceed the boundaries of the first coat to seal in the first coat. Make sure all exposed wires are covered. Allow coating to dry for 24 hours.
2.	Cut out a 15mm by 25mm rectangular piece of butyl rubber tape and place it just behind the lead wire stress relief loops underneath of the polyurethane lead wire jacket. Using thumbs, kneed the butyl tape thoroughly against the PE pipe until a good bond is achieved. Press the lead wire jacket into the butyl tape. Be sure to kneed out all air bubbles that are present below the butyl tape.
3.	Cut out a 30mm by 70mm rectangular piece of butyl rubber tape and apply it over top of the strain gauge and lead wire arrangement. The sides of the butyl tape should cover the boundaries of the applied M-Coat D as well as the small piece of butyl tape already applied.
4.	Using thumbs, carefully press the butyl tape edges down onto the PE surface to secure the bond. It is imperative to prevent moisture from travelling along the lead wire jacket, so thoroughly press the tape around the polyurethane jacket to seal it off.
5.	Apply two layers of 3M Scotch 130C Linerless Rubber Splicing Tape around the entire diameter of the pipe. The tape should be stretched to half of its initial width before applying as the more stretch, the less chance of voids. Check that the pipe diameter is clean before application. The limits of the 130C tape should extend beyond the butyl rubber coating on either end of the strain gauge arrangement.
5) Preparing data acquisition instrumentation end of the lead wires	
1.	Strip ~50mm of the black polyurethane jacket from the lead wires to expose the four

1.	Strip ~50mm of the black polyurethane jacket from the lead wires to expose the four wires (red, white, black and un-insulated).
2.	Cut off the drain wire (un-insulated wire) off where it meets the black polyurethane jacket.
3.	Strip ~10mm of the insulation from each of the red, black and white wires.
4.	Individually twist the red, black and white bundle tightly back to the end of the insulation.
5.	Individually tin each of the bundles.

APPENDIX C

Detailed strain gauge positioning and labeling along buried MDPE pipeline alignments

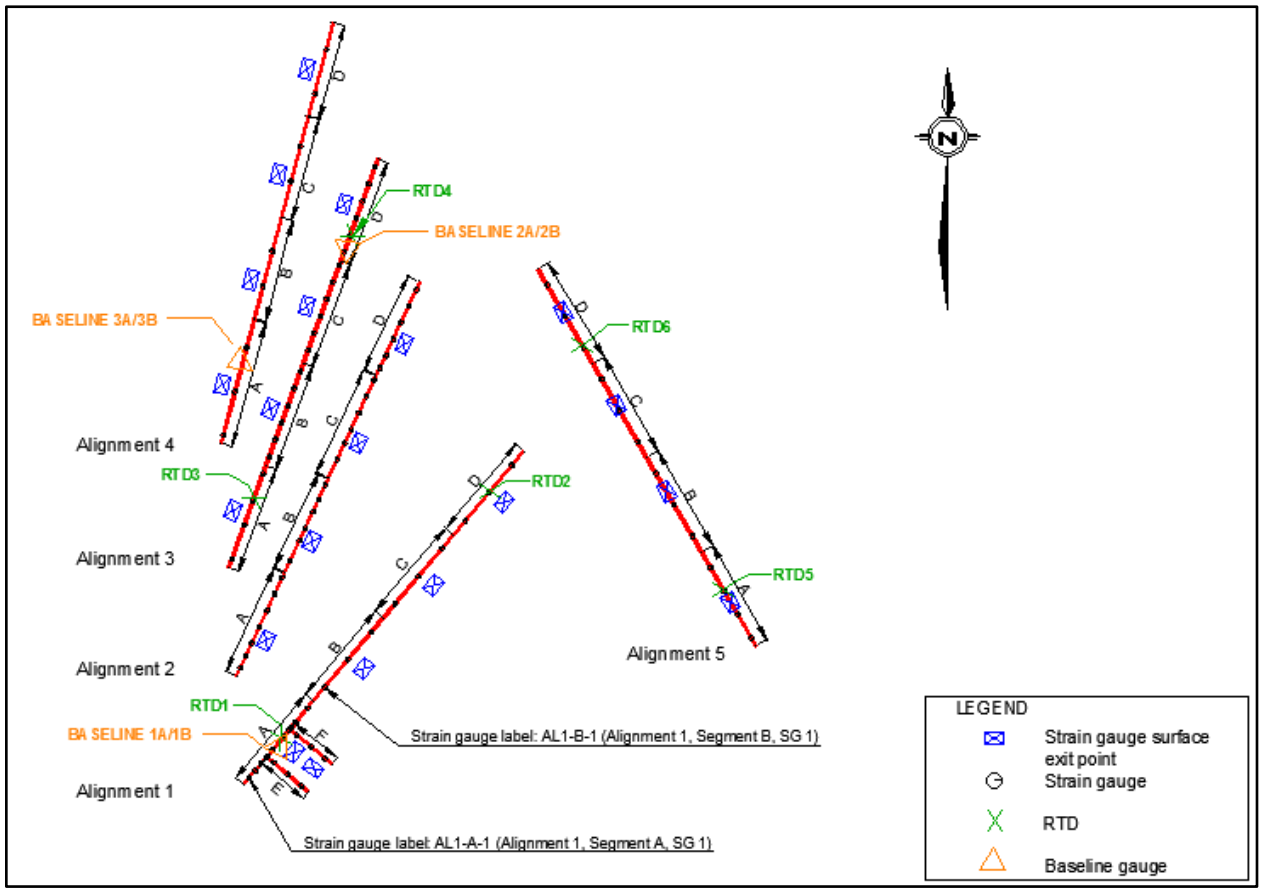

As-built pipeline alignment layouts, including RTD, baseline gauge, and strain gauge surface exit point locations across the site.

Alignment No. 1			
Strain Gauge Label and Location Along Alignment			
Strain Gauge No.		Strain Gauge Position[1] (°)	Distance From Top[2] (m)
Pipe Segment A (60.3 mm OD)			
1	AL1-A-1A	90	0.10
2	AL1-A-1B	270	0.10
3	AL1-A-2A	90	0.50
4	AL1-A-2B	270	0.50
5	AL1-A-3A	90	1.50
6	AL1-A-3B	270	1.50
7	AL1-A-4A	0	1.95
8	AL1-A-4B	90	1.95
9	AL1-A-4C	180	1.95
10	AL1-A-4D	270	1.95
11	AL1-A-5A	0	2.08
12	AL1-A-5B	90	2.08
13	AL1-A-5C	180	2.08
14	AL1-A-5D	270	2.08
15	AL1-A-6A	90	2.50
16	AL1-A-6B	270	2.50
17	AL1-A-7A	90	3.50
18	AL1-A-7B	270	3.50
19	AL1-A-8A	0	3.95
20	AL1-A-8B	90	3.95
21	AL1-A-8C	180	3.95
22	AL1-A-8D	270	3.95
23	AL1-A-9A	0	4.08
24	AL1-A-9B	90	4.08
25	AL1-A-9C	180	4.08
26	AL1-A-9D	270	4.08
27	AL1-A-10A	90	4.50
28	AL1-A-10B	270	4.50
29	AL1-A-11A	90	5.50
30	AL1-A-11B	270	5.50
Pipe Segment B (60.3 mm OD)			
31	AL1-B-1A	270	7.01
32	AL1-B-1B	0	7.01
33	AL1-B-1C	90	7.01
34	AL1-B-2A	270	9.01
35	AL1-B-2B	90	9.01
36	AL1-B-3A	270	11.01
37	AL1-B-3B	0	11.01
38	AL1-B-3C	90	11.01
Pipe Segment C (60.3 mm OD)			
39	AL1-C-1A	270	13.00
40	AL1-C-1B	90	13.00
41	AL1-C-2A	270	15.00
42	AL1-C-2B	0	15.00
43	AL1-C-2C	90	15.00
44	AL1-C-3A	270	17.00
45	AL1-C-3B	90	17.00
Pipe Segment D (60.3 mm OD)			
46	AL1-D-1A	270	19.00
47	AL1-D-1B	0	19.00
48	AL1-D-1C	90	19.00
49	AL1-D-2A	270	21.00
50	AL1-D-2B	90	21.00
51	AL1-D-3A	270	23.00
52	AL1-D-3B	0	23.00
53	AL1-D-3C	90	23.00
Pipe Segment E (Branch Pipe - 26.7 mm OD)			
54	AL1-E-1A	90	0.50
55	AL1-E-1B	270	0.50
56	AL1-E-2A	90	1.50
57	AL1-E-2B	270	1.50
58	AL1-E-3A	90	2.50
59	AL1-E-3B	270	2.50
Pipe Segment F (Branch Pipe - 26.7 mm OD)			
60	AL1-F-1A	90	0.50
61	AL1-F-1B	270	0.50
62	AL1-F-2A	90	1.50
63	AL1-F-2B	270	1.50
64	AL1-F-3A	90	2.50
65	AL1-F-3B	270	2.50
Total number of strain gauges installed on Alignment 1: 65			

[1]Refers to the location of the strain gauge around the circumference of the pipe, with 0° referring to the crown of the pipe and subsequent locations measured in the clockwise direction.
[2]Referes to the strain gauge location along the axial length of the pipeline alignment with respect to the top, or uphill end, of the alignment.

Alignment No. 2			
Strain Gauge Label and Location Along Alignment			
Strain Gauge No.		Strain Gauge Position[1] (°)	Distance From Top[2] (m)
Pipe Segment A (114.3 mm OD)			
1	AL2-A-1a	90	0.10
2	AL2-A-1b	270	0.10
3	AL2-A-2a	90	1.00
4	AL2-A-2b	270	1.00
5	AL2-A-3a	90	2.00
6	AL2-A-3b	270	2.00
7	AL2-A-4a	90	3.00
8	AL2-A-4b	270	3.00
9	AL2-A-5a	90	4.00
10	AL2-A-5b	270	4.00
11	AL2-A-6a	90	5.00
12	AL2-A-6b	270	5.00
13	AL2-A-7a	90	6.00
14	AL2-A-7b	270	6.00
Pipe Segment B (114.3 mm OD)			
15	AL2-B-1a	90	7.00
16	AL2-B-1b	270	7.00
17	AL2-B-2a	90	8.00
18	AL2-B-2b	270	8.00
19	AL2-B-3a	90	9.00
20	AL2-B-3b	270	9.00
21	AL2-B-4a	90	10.00
22	AL2-B-4b	270	10.00
23	AL2-B-5a	90	11.00
24	AL2-B-5b	270	11.00
25	AL2-B-6a	90	12.00
26	AL2-B-6b	270	12.00
Pipe Segment C (114.3 mm OD)			
27	AL2-C-1a	90	13.00
28	AL2-C-1b	270	13.00
29	AL2-C-2a	90	14.00
30	AL2-C-2b	270	14.00
31	AL2-C-3a	90	15.00
32	AL2-C-3b	270	15.00
33	AL2-C-4a	90	16.00
34	AL2-C-4b	270	16.00
35	AL2-C-5a	90	17.00
36	AL2-C-5b	270	17.00
37	AL2-C-6a	90	18.00
38	AL2-C-6b	270	18.00
Pipe Segment D (114.3 mm OD)			
39	AL2-D-1a	90	19.00
40	AL2-D-1b	270	19.00
41	AL2-D-2a	90	20.00
42	AL2-D-2b	270	20.00
43	AL2-D-3a	90	21.00
44	AL2-D-3b	270	21.00
45	AL2-D-4a	90	22.00
46	AL2-D-4b	270	22.00
47	AL2-D-5a	90	23.00
48	AL2-D5b	270	23.00
49	Al2-D-6a	90	24.00
50	AL2-D-6b	270	24.00
Total number of strain gauges installed on Alignment 2: 50			

[1]Refers to the location of the strain gauge around the circumference of the pipe, with 0° referring to the crown of the pipe and subsequent locations measured in the clockwise direction.

[2]Referes to the strain gauge location along the axial length of the pipeline alignment with respect to the top, or uphill end, of the alignment.

Alignment No. 3			
Strain Gauge Label and Location Along Alignment			
Strain Gauge No.		Strain Gauge Position[1] (°)	Distance From Top[2] (m)
Pipe Segment A (60.3 mm OD)			
1	AL3-A-1A	270	0.10
2	AL3-A-1B	0	0.10
3	AL3-A-1C	90	0.10
4	AL3-A-2A	270	1.00
5	AL3-A-2B	90	1.00
6	AL3-A-3A	270	3.00
7	AL3-A-3B	0	3.00
8	AL3-A-3C	90	3.00
9	AL3-A-4A	270	5.00
10	AL3-A-4B	90	5.00
Pipe Segment B (60.3 mm OD)			
11	AL3-B-1A	90	6.50
12	AL3-B-1B	270	6.50
13	AL3-B-2A	90	7.50
14	AL3-B-2B	270	7.50
15	AL3-B-3A	90	8.50
16	AL3-B-3B	270	8.50
17	AL3-B-4A	90	9.50
18	AL3-B-4B	270	9.50
19	AL3-B-5A	90	10.50
20	AL3-B-5B	270	10.50
21	AL3-B-6A	90	11.50
22	AL3-B-6B	270	11.50
Pipe Segment C (60.3 mm OD)			
23	AL3-C-1A	90	12.50
24	AL3-C-1B	270	12.50
25	AL3-C-2A	90	13.50
26	AL3-C-2B	270	13.50
27	AL3-C-3A	90	14.50
28	AL3-C-3B	270	14.50
29	AL3-C-4A	90	15.50
30	AL3-C-4B	270	15.50
31	AL3-C-5A	90	16.50
32	AL3-C-5B	270	16.50
33	AL3-C-6A	90	17.50
34	AL3-C-6B	270	17.50
Pipe Segment D (60.3 mm OD)			
35	AL3-D-1A	90	18.50
36	AL3-D-1B	270	18.50
37	AL3-D-2A	90	19.50
38	AL3-D-2B	270	19.50
39	AL3-D-3A	90	20.50
40	AL3-D-3B	270	20.50
41	AL3-D-4A	90	21.50
42	AL3-D-4B	270	21.50
43	AL3-D-5A	90	22.50
44	AL3-D-5B	270	22.50
45	AL3-D-6A	90	23.50
46	AL3-D-6B	270	23.50
Total number of strain gauges on Alignment 3: 46			

[1]Refers to the location of the strain gauge around the circumference of the pipe, with 0° referring to the crown of the pipe and subsequent locations measured in the clockwise direction.

[2]Referes to the strain gauge location along the axial length of the pipeline alignment with respect to the top, or uphill end, of the alignment.

Alignment No. 4			
Strain Gauge Label and Location Along Alignment			
Strain Gauge No.		Strain Gauge Position[1] (°)	Distance From Top[2] (m)
Pipe Segment A (60.3 mm OD)			
1	AL4-A-1A	90	0.10
2	AL4-A-1B	0	0.10
3	AL4-A-1C	270	0.10
4	AL4-A-2A	90	2.00
5	AL4-A-2B	0	2.00
6	AL4-A-2C	270	2.00
7	AL4-A-3A	90	5.00
8	AL4-A-3B	0	5.00
9	AL4-A-3C	270	5.00
Pipe Segment B (60.3 mm OD)			
10	AL4-B-1A	90	8.00
11	AL4-B-1B	0	8.00
12	AL4-B-1C	270	8.00
13	AL4-B-2A	90	11.00
14	AL4-B-2B	0	11.00
15	AL4-B-2C	270	11.00
Pipe Segment C (60.3 mm OD)			
16	AL4-C-1A	90	14.00
17	AL4-C-1B	0	14.00
18	AL4-C-1C	270	14.00
19	AL4-C-2A	90	17.00
20	AL4-C-2B	0	17.00
21	AL4-C-2C	270	17.00
Pipe Segment D (60.3 mm OD)			
22	AL4-D-1A	90	20.00
23	AL4-D-1B	0	20.00
24	AL4-D-1C	270	20.00
25	AL4-D-2A	90	23.00
26	AL4-D-2B	0	23.00
27	AL4-D-2C	270	23.00
Total number of strain gauges installed on Alignment 4: 27			

[1]Refers to the location of the strain gauge around the circumference of the pipe, with 0° referring to the crown of the pipe and subsequent locations measured in the clockwise direction.

[2]Referes to the strain gauge location along the axial length of the pipeline alignment with respect to the top, or uphill end, of the alignment.

Alignment No. 5			
Strain Gauge Label and Location Along Alignment			
Strain Gauge No.		Strain Gauge Position[1] (°)	Distance From Top[2] (m)
Pipe Segment A (114.3 mm OD)			
1	AL5-A-1A	270	0.10
2	AL5-A-1B	0	0.10
3	AL5-A-1C	90	0.10
4	AL5-A-2A	270	1.00
5	AL5-A-2B	0	1.00
6	AL5-A-2C	90	1.00
7	AL5-A-3A	270	2.95
8	AL5-A-3B	0	2.95
9	AL5-A-3C	90	2.95
10	AL5-A-4A	270	4.95
11	AL5-A-4B	0	4.95
12	AL5-A-4C	90	4.95
Pipe Segment B (114.3 mm OD)			
13	AL5-B-1A	270	7.00
14	AL5-B-1B	0	7.00
15	AL5-B-1C	90	7.00
16	AL5-B-2A	270	9.00
17	AL5-B-2B	0	9.00
18	AL5-B-2C	90	9.00
19	AL5-B-3A	270	11.00
20	AL5-B-3B	0	11.00
21	AL5-B-3C	90	11.00
Pipe Segment C (114.3 mm OD)			
22	AL5-C-1A	270	13.00
23	AL5-C-1B	0	13.00
24	AL5-C-1C	90	13.00
25	AL5-C-2A	270	15.00
26	AL5-C-2B	0	15.00
27	AL5-C-2C	90	15.00
28	AL5-C-3A	270	17.00
29	AL5-C-3B	0	17.00
30	AL5-C-3C	90	17.00
Pipe Segment D (114.3 mm OD)			
31	AL5-D-1A	270	19.00
32	AL5-D-1B	0	19.00
33	AL5-D-1C	90	19.00
34	AL5-D-2A	270	21.00
35	AL5-D-2B	0	21.00
36	AL5-D-2C	90	21.00
37	AL5-D-3A	270	23.00
38	AL5-D-3B	0	23.00
39	AL5-D-3C	90	23.00
Total number of strain gauges installed on Alignment 5: 39			

[1]Refers to the location of the strain gauge around the circumference of the pipe, with 0° referring to the crown of the pipe and subsequent locations measured in the clockwise direction.

[2]Referes to the strain gauge location along the axial length of the pipeline alignment with respect to the top, or uphill end, of the alignment.

Alignment No. 1, Segments A, E and F – Strain Gauge Labels and Locations Along Alignment

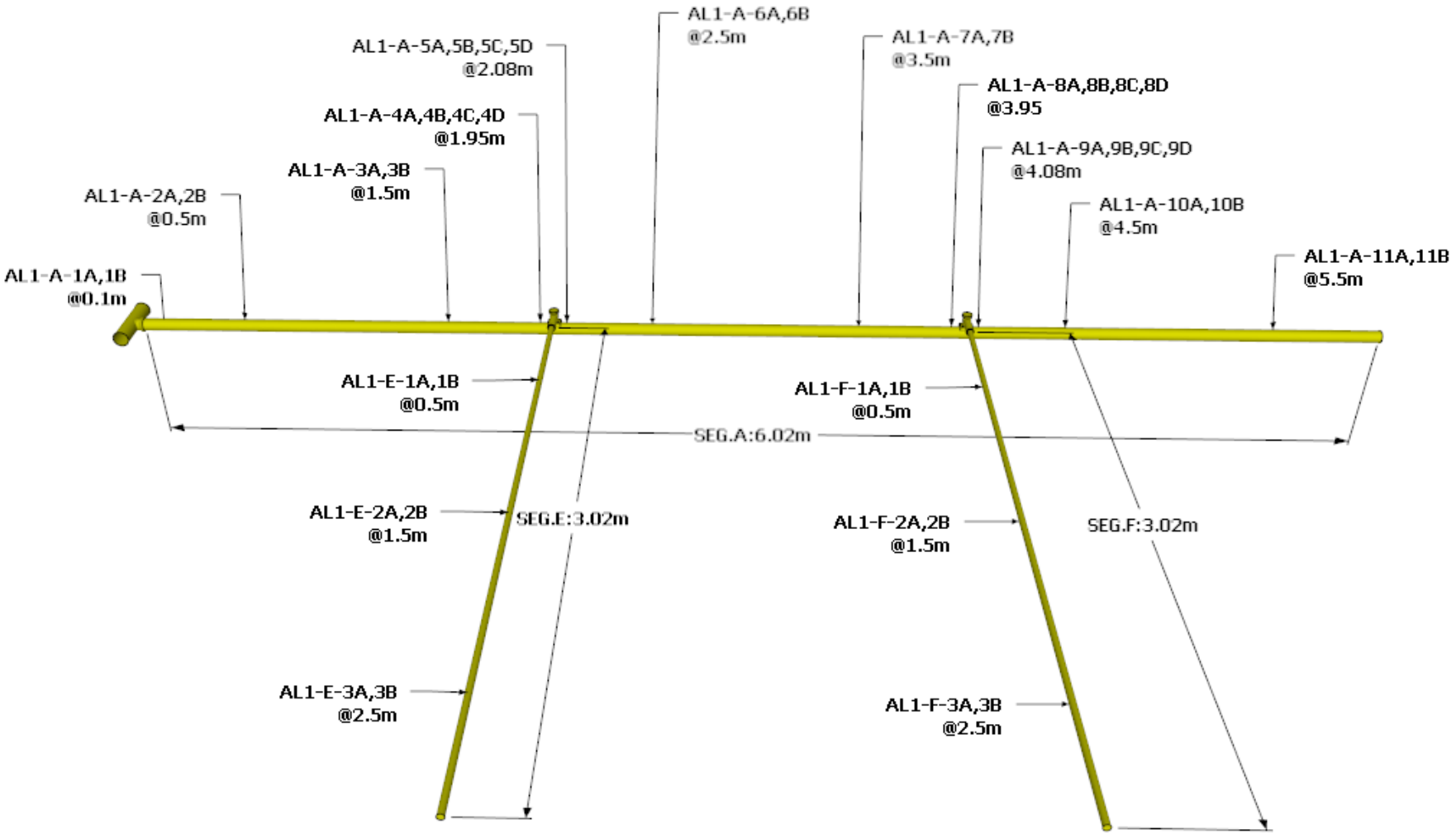

Alignment No. 1, Segments B, C and D – Strain Gauge Labels and Locations Along Alignment

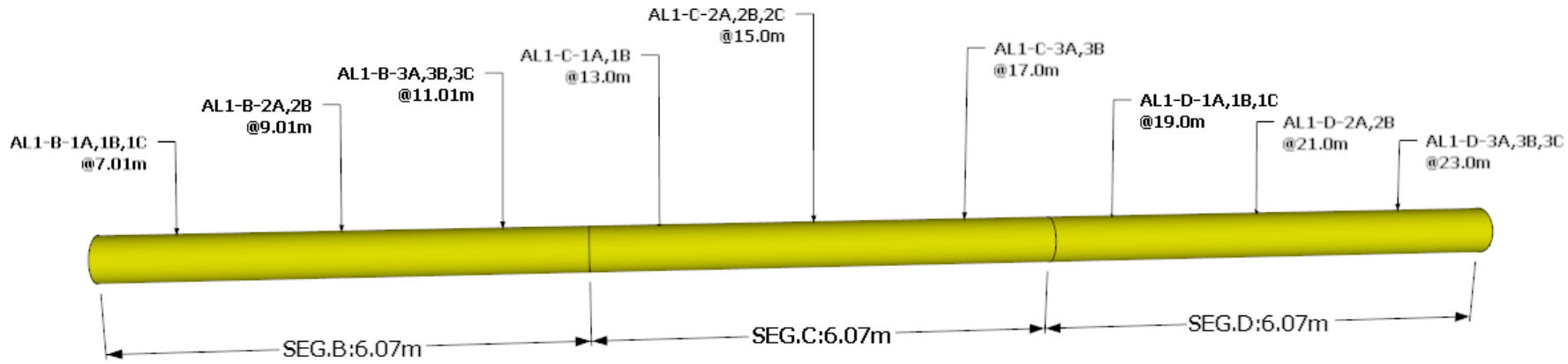

Strain Gauge Labeling in Cross Section

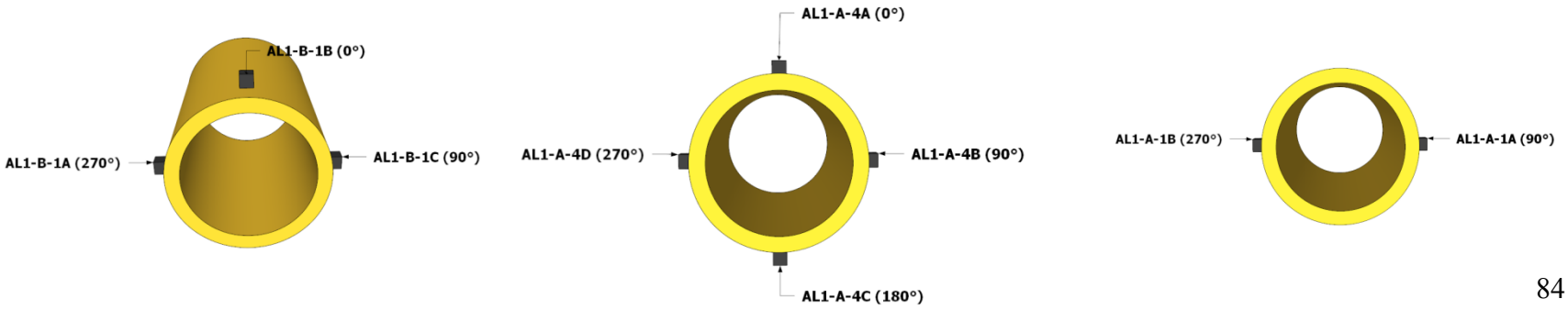

Alignment No. 2 – Strain Gauge Labels and Locations Along Alignment

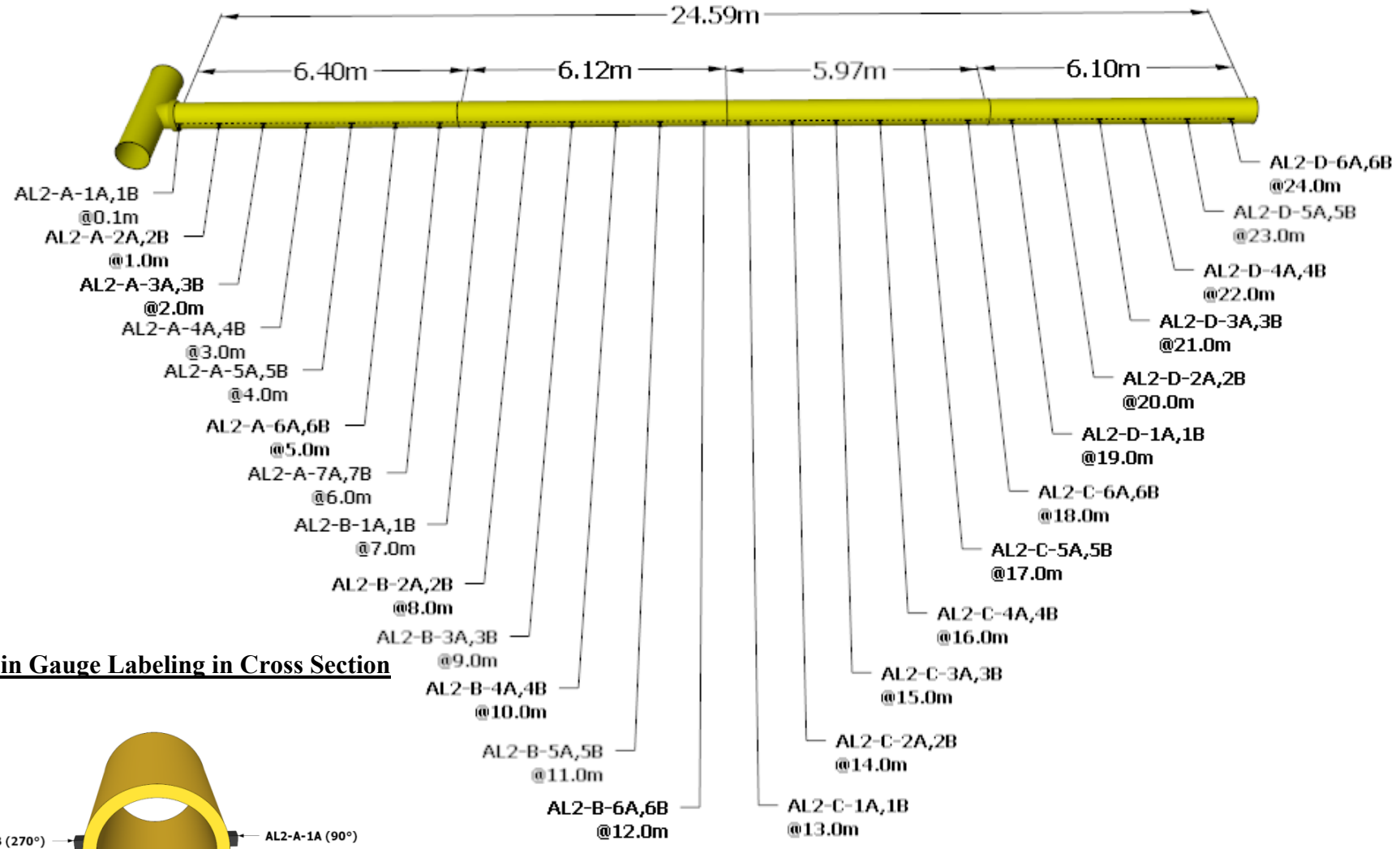

Strain Gauge Labeling in Cross Section

Alignment No. 3 – Strain Gauge Labels and Locations Along Alignment

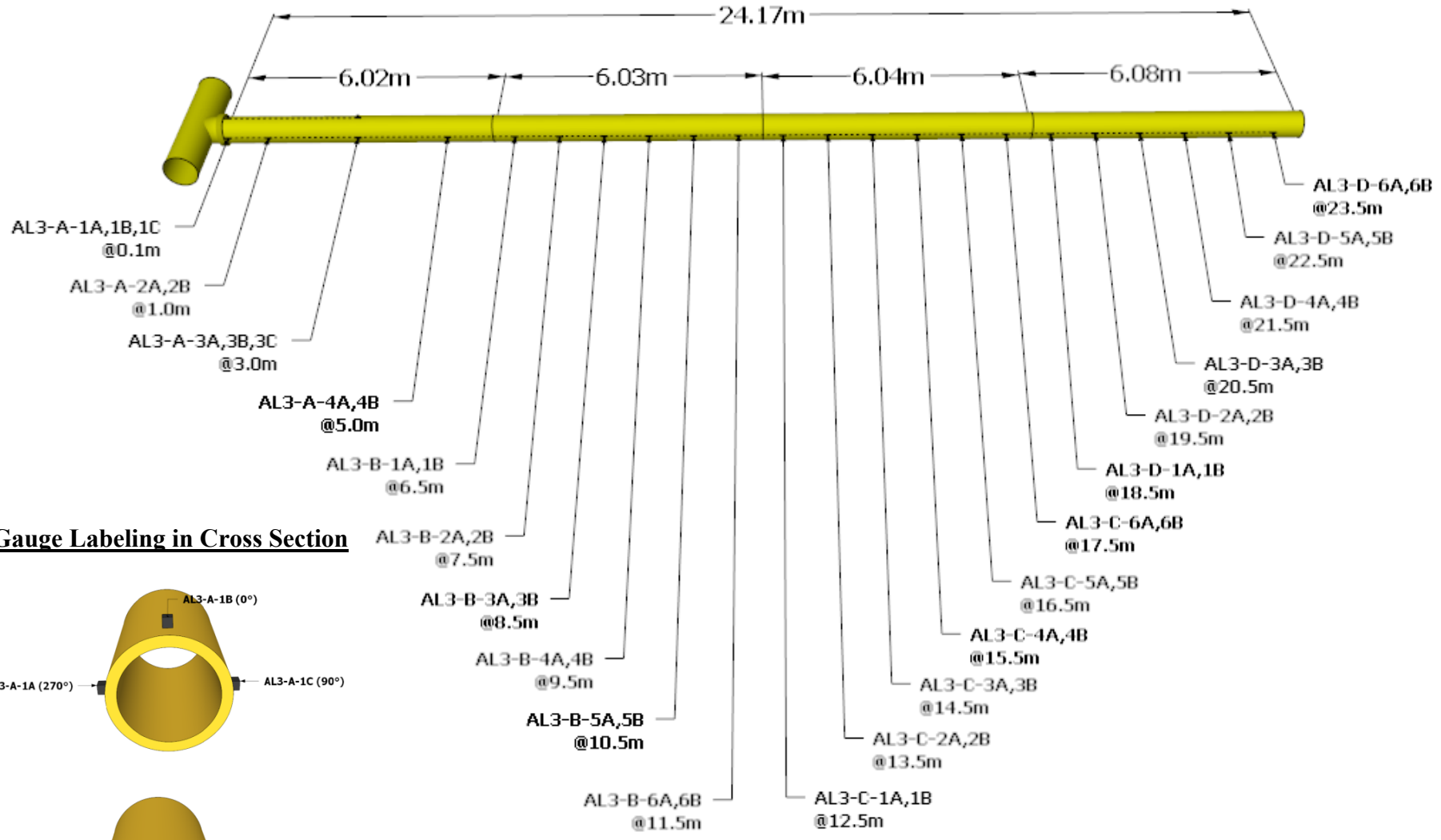

Strain Gauge Labeling in Cross Section

Alignment No. 4 – Strain Gauge Labels and Locations Along Alignment

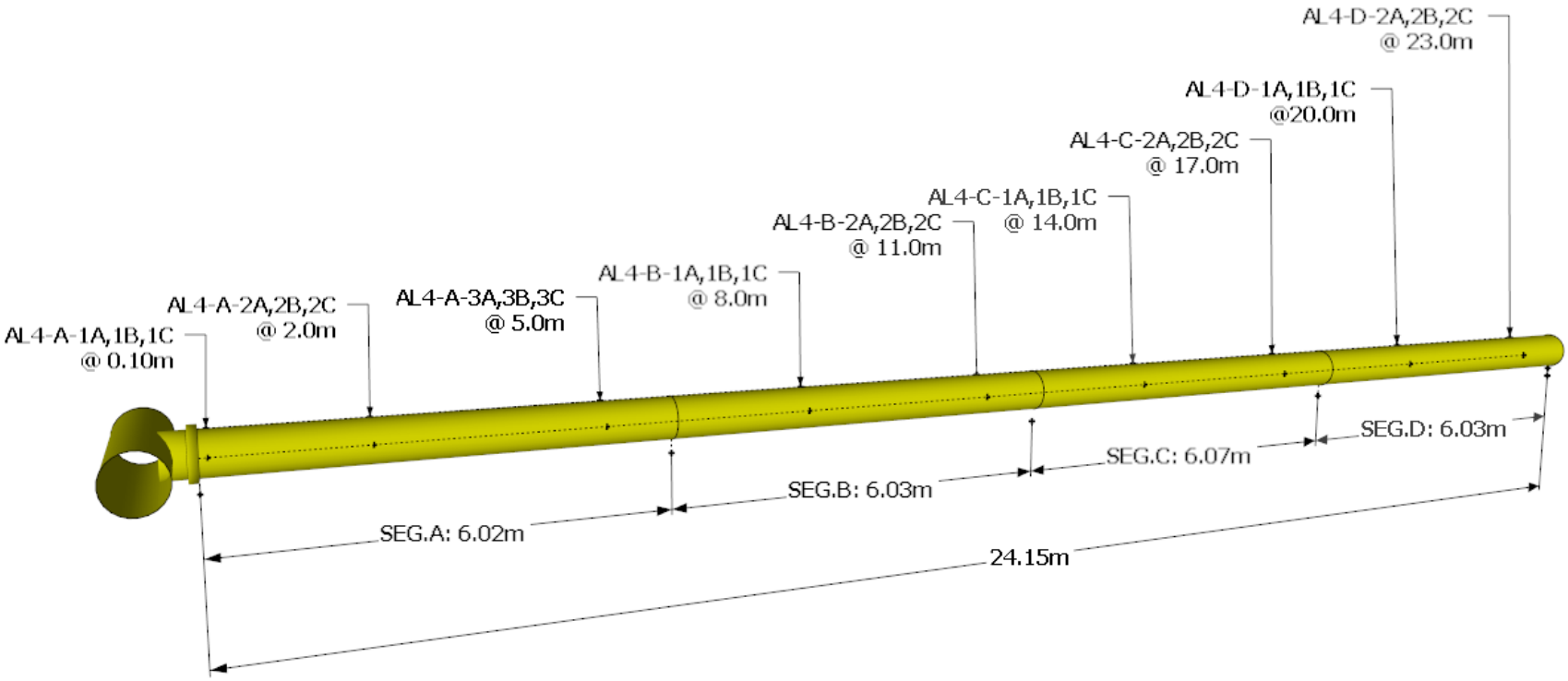

Strain Gauge Labeling in Cross Section

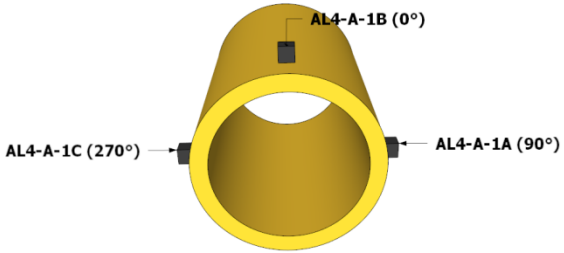

Alignment No. 5 – Strain Gauge Labels and Locations Along Alignment

Strain Gauge Labeling in Cross Section

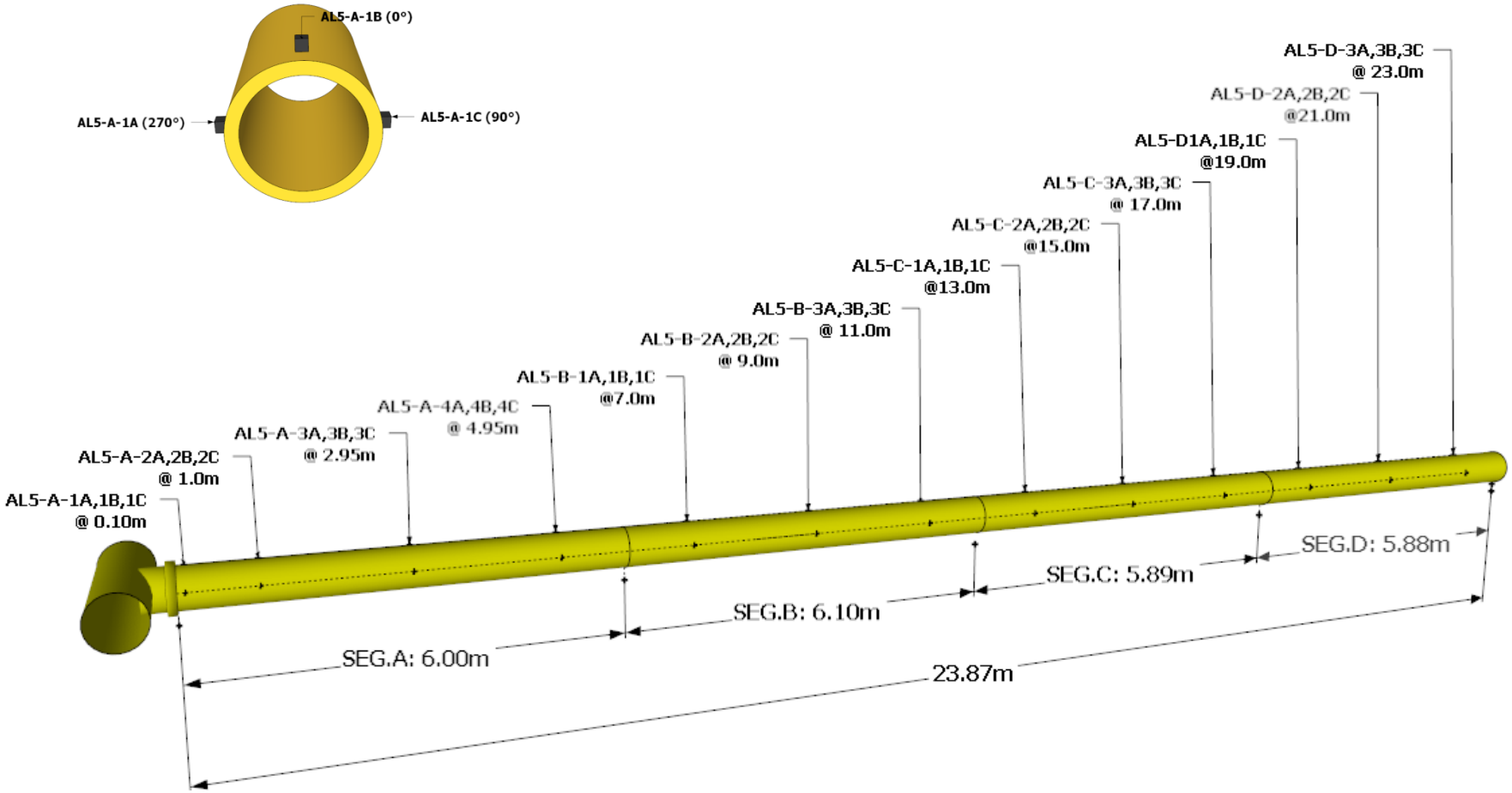

APPENDIX D

Detailed ground surface and pipeline survey monitoring point locations and topographic survey at the research site

Topographic survey of the research site before pipeline installations - April 27, 2013

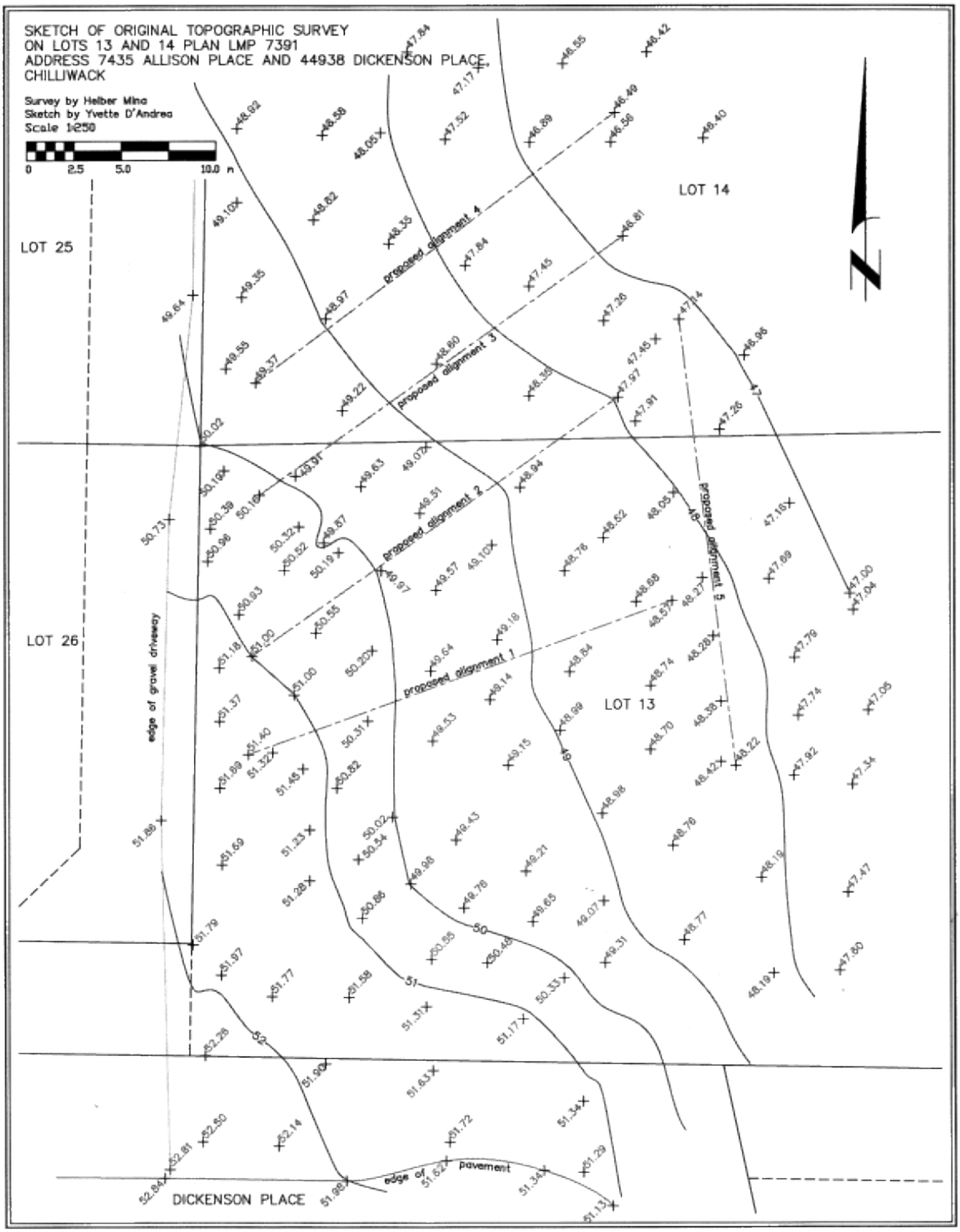

Topographic survey at the research site after pipeline installations & established survey monitoring points - May 31, 2013

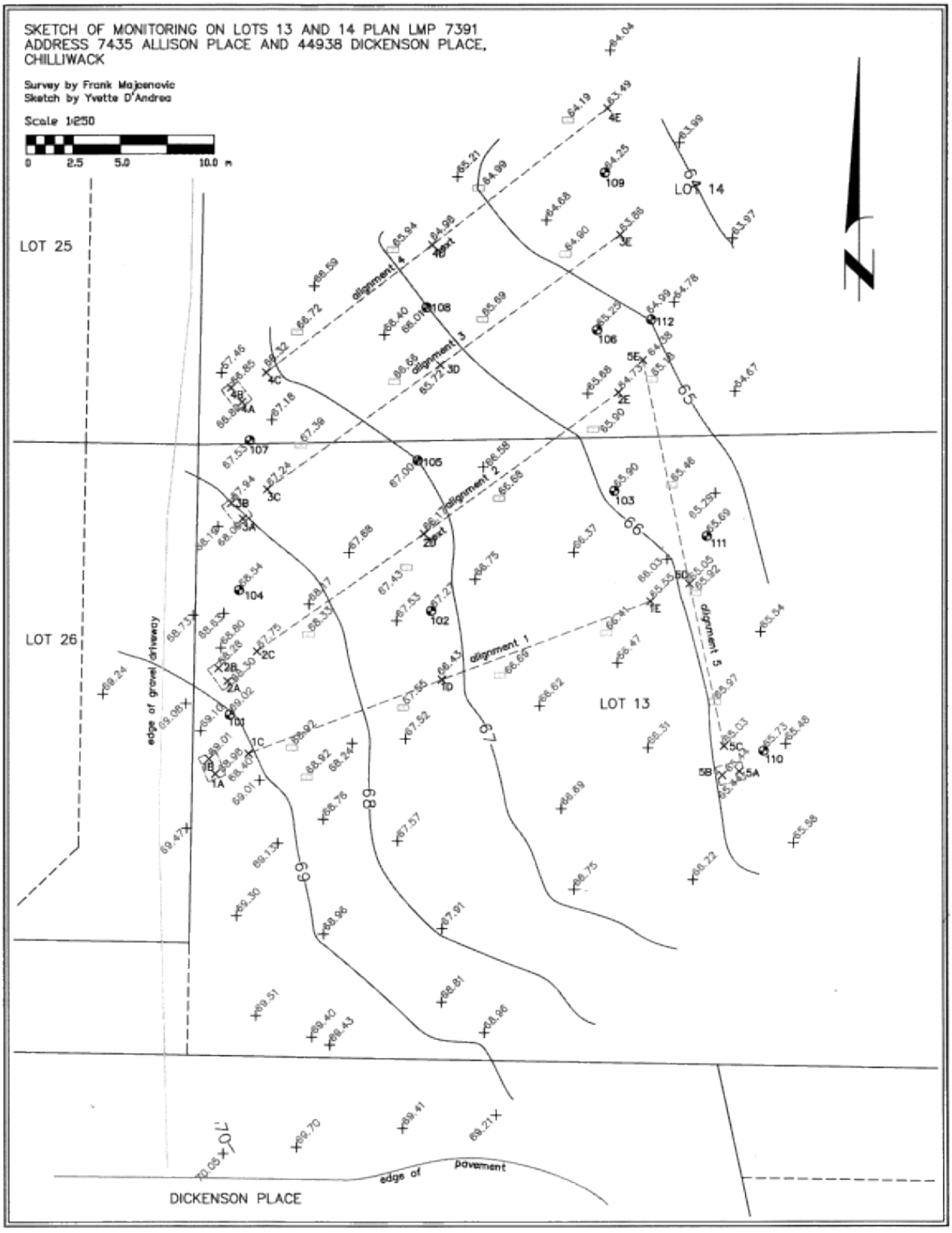

Summary of survey monitoring point labels established at the research site

Survey Monument Label	Location of Survey Monument at the Site
101	Ground surface monitoring point
102	Ground surface monitoring point
103	Ground surface monitoring point
104	Ground surface monitoring point
105	Ground surface monitoring point
106	Ground surface monitoring point
107	Ground surface monitoring point
108	Ground surface monitoring point
109	Ground surface monitoring point
110	Ground surface monitoring point
111	Ground surface monitoring point
112	Ground surface monitoring point
1A	Alignment 1 anchor monitoring point
1B	Alignment 1 anchor monitoring point
1C	Alignment 1 pipe monitoring point (top end)
1D	Alignment 1 pipe monitoring point (mid point)
1E	Alignment 1 pipe monitoring point (bottom end)
2A	Alignment 2 anchor monitoring point
2B	Alignment 2 anchor monitoring point
2C	Alignment 2 pipe monitoring point (top end)
2D	Alignment 2 pipe monitoring point (mid point)
2E	Alignment 2 pipe monitoring point (bottom end)
3A	Alignment 3 anchor monitoring point
3B	Alignment 3 anchor monitoring point
3C	Alignment 3 pipe monitoring point (top end)
3D	Alignment 3 pipe monitoring point (mid point)
3E	Alignment 3 pipe monitoring point (bottom end)
4A	Alignment 4 anchor monitoring point
4B	Alignment 4 anchor monitoring point
4C	Alignment 4 pipe monitoring point (top end)
4D	Alignment 4 pipe monitoring point (mid point)
4E	Alignment 4 pipe monitoring point (bottom end)
5A	Alignment 5 anchor monitoring point
5B	Alignment 5 anchor monitoring point
5C	Alignment 5 pipe monitoring point (top end)
5D	Alignment 5 pipe monitoring point (mid point)
5E	Alignment 5 pipe monitoring point (bottom end)

APPENDIX E

Experimental field data observations from May 23, 2013 to December 31, 2013

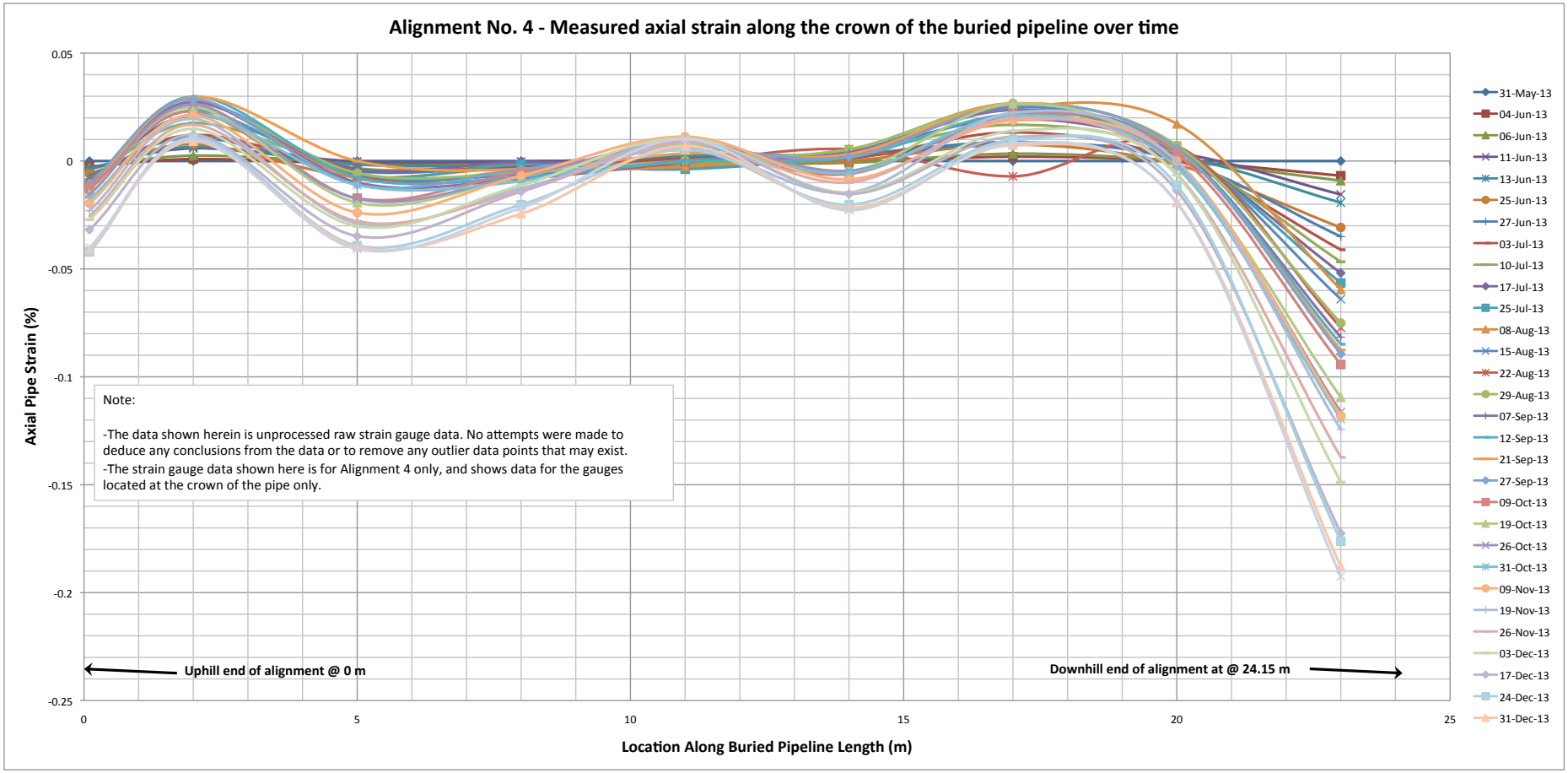
Alignment No. 4 - Measured axial strain along the crown of the buried pipeline over time
Axial Pipe Strain (%)
0.05
0
-0.05
-0.1
-0.15
-0.2
-0.25
0
5
10
15
20
25
Location Along Buried Pipeline Length (m)
Note:
-The data shown herein is unprocessed raw strain gauge data. No attempts were made to deduce any conclusions from the data or to remove any outlier data points that may exist.
-The strain gauge data shown here is for Alignment 4 only, and shows data for the gauges located at the crown of the pipe only.
Uphill end of alignment @ 0 m
Downhill end of alignment at @ 24.15 m
31-May-13
04-Jun-13
06-Jun-13
11-Jun-13
13-Jun-13
25-Jun-13
27-Jun-13
03-Jul-13
10-Jul-13
17-Jul-13
25-Jul-13
08-Aug-13
15-Aug-13
22-Aug-13
29-Aug-13
07-Sep-13
12-Sep-13
21-Sep-13
27-Sep-13
09-Oct-13
19-Oct-13
26-Oct-13
31-Oct-13
09-Nov-13
19-Nov-13
26-Nov-13
03-Dec-13
17-Dec-13
24-Dec-13
31-Dec-13

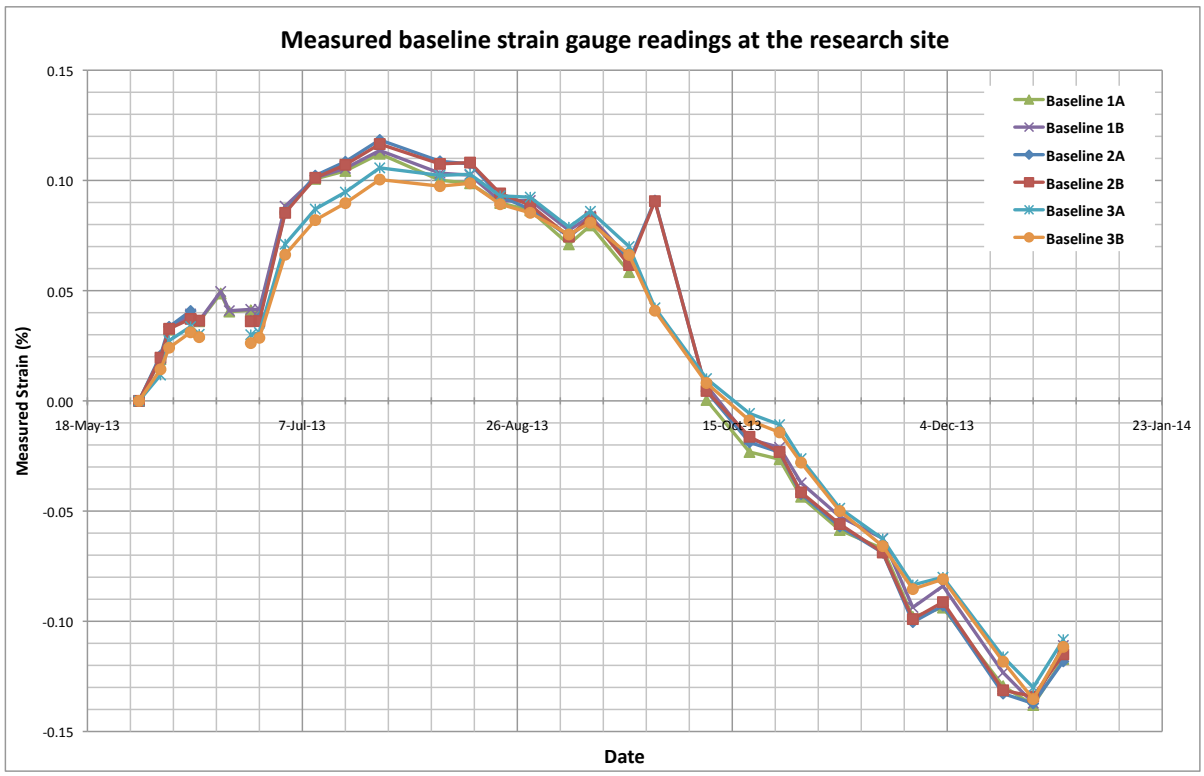
Measured baseline strain gauge readings at the research site
0.15
0.10
0.05
0.00
-0.05
-0.10
-0.15
Measured Strain (%)
18-May-13
7-Jul-13
26-Aug-13
15-Oct-13
4-Dec-13
23-Jan-14
Date
Baseline 1A
Baseline 1B
Baseline 2A
Baseline 2B
Baseline 3A
Baseline 3B

0

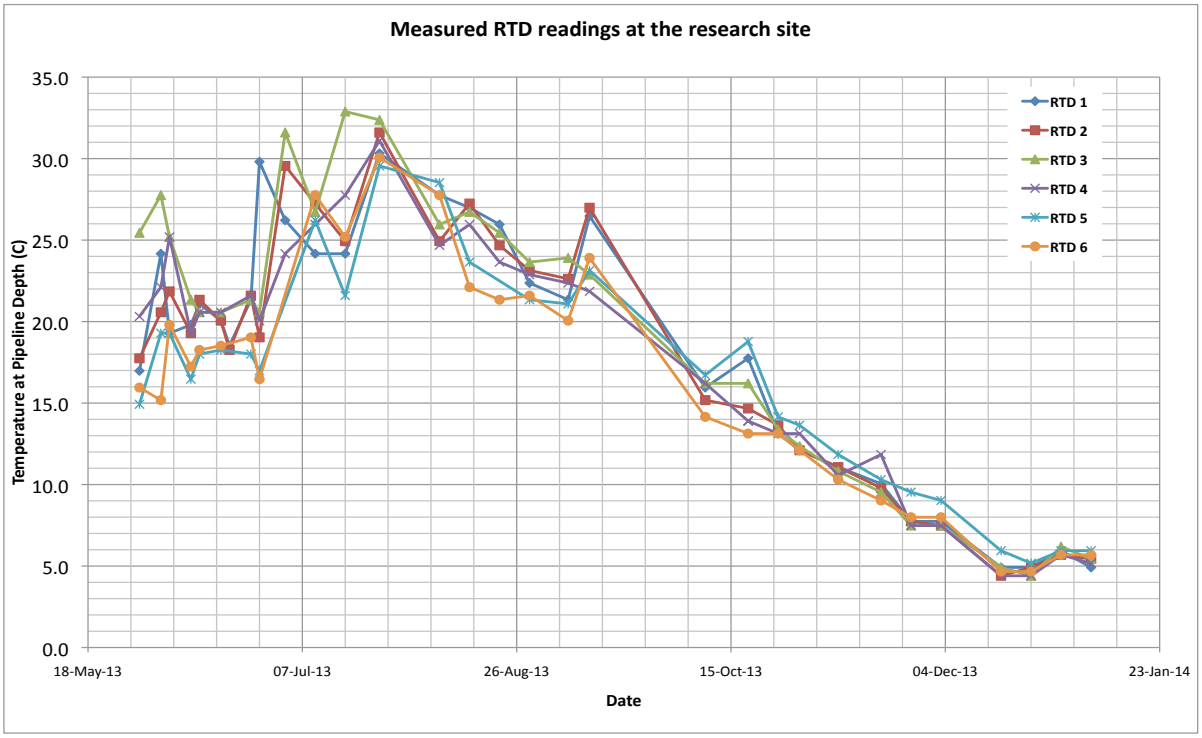
Measured RTD readings at the research site
35.0
30.0
25.0
20.0
15.0
10.0
5.0
0.0
Temperature at Pipeline Depth (C)
18-May-13
07-Jul-13
26-Aug-13
15-Oct-13
04-Dec-13
23-Jan-14
Date
RTD 1
RTD 2
RTD 3
RTD 4
RTD 5
RTD 6

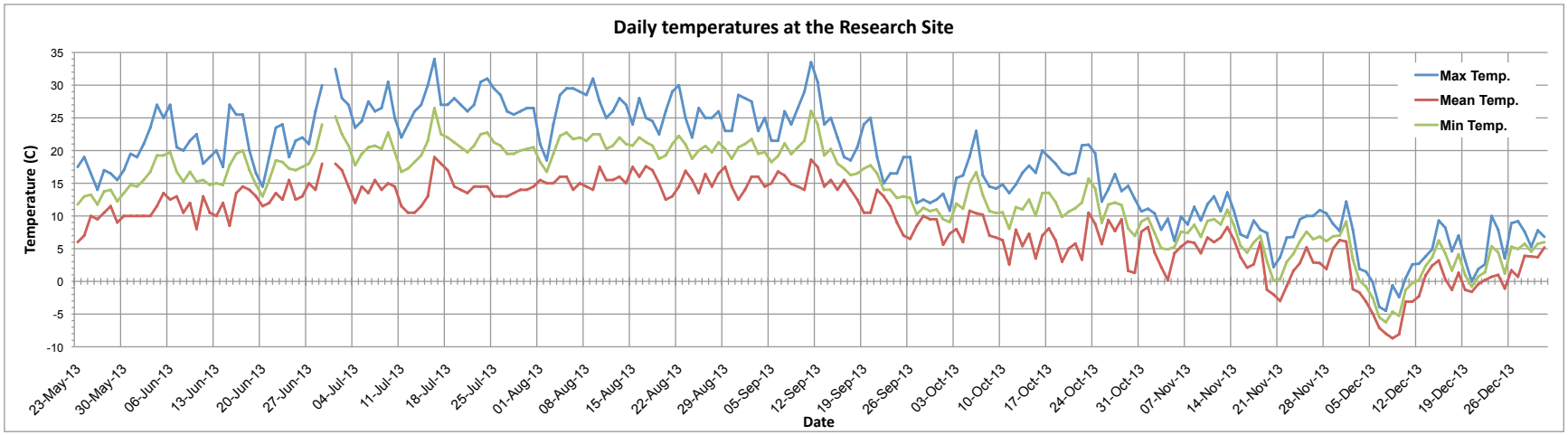
Daily temperatures at the Research Site
Temperature (C)
35
30
25
20
15
10
5
0
-5
-10
Max Temp.
Mean Temp.
Min Temp.
23-May-13
30-May-13
06-Jun-13
13-Jun-13
20-Jun-13
27-Jun-13
04-Jul-13
11-Jul-13
18-Jul-13
25-Jul-13
01-Aug-13
08-Aug-13
15-Aug-13
22-Aug-13
29-Aug-13
05-Sep-13
12-Sep-13
19-Sep-13
26-Sep-13
03-Oct-13
10-Oct-13
17-Oct-13
24-Oct-13
31-Oct-13
07-Nov-13
14-Nov-13
21-Nov-13
28-Nov-13
05-Dec-13
12-Dec-13
19-Dec-13
26-Dec-13
Date

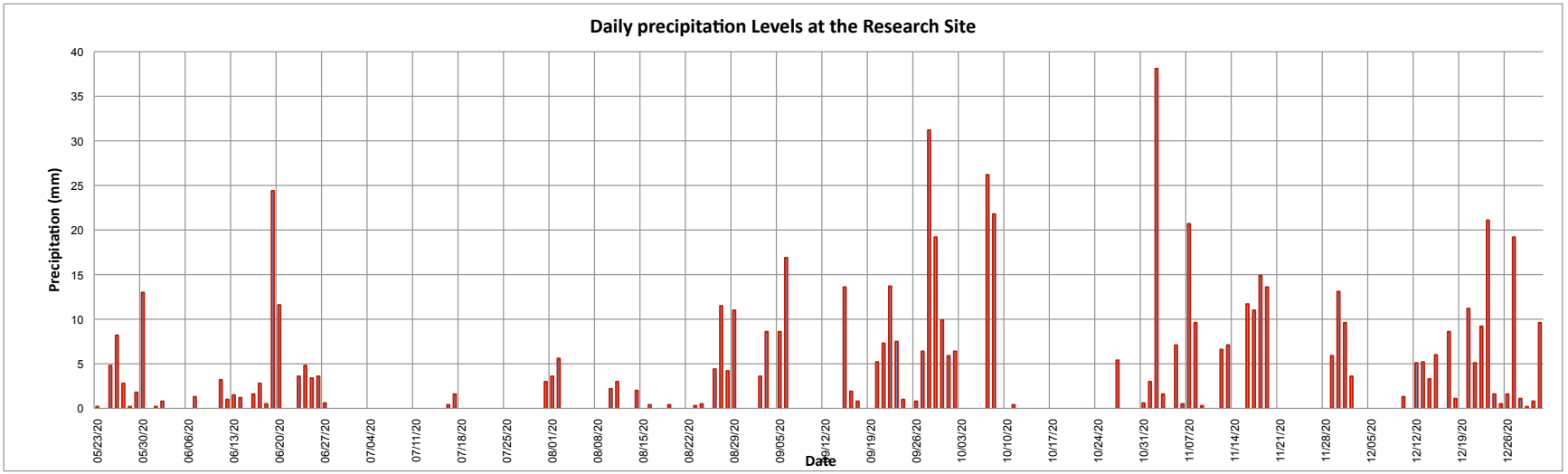
Daily precipitation Levels at the Research Site
Precipitation (mm)
40
35
30
25
20
15
10
5
0
05/23/20
05/30/20
06/06/20
06/13/20
06/20/20
06/27/20
07/04/20
07/11/20
07/18/20
07/25/20
08/01/20
08/08/20
08/15/20
08/22/20
08/29/20
09/05/20
09/12/20
09/19/20
09/26/20
10/03/20
10/10/20
10/17/20
10/24/20
10/31/20
11/07/20
11/14/20
11/21/20
11/28/20
12/05/20
12/12/20
12/19/20
12/26/20
Date

APPENDIX F

Results from thermal contraction laboratory tests on MDPE pipe specimens to estimate the strain gauge stiffening effect on local strain readings

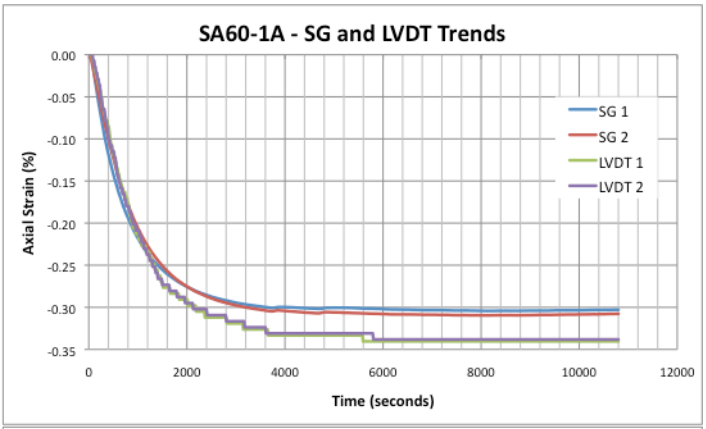
SA60-1A - SG and LVDT Trends
Axial Strain (%)
0.00
-0.05
-0.10
-0.15
-0.20
-0.25
-0.30
-0.35
0
2000
4000
6000
8000
10000
12000
Time (seconds)
SG 1
SG 2
LVDT 1
LVDT 2

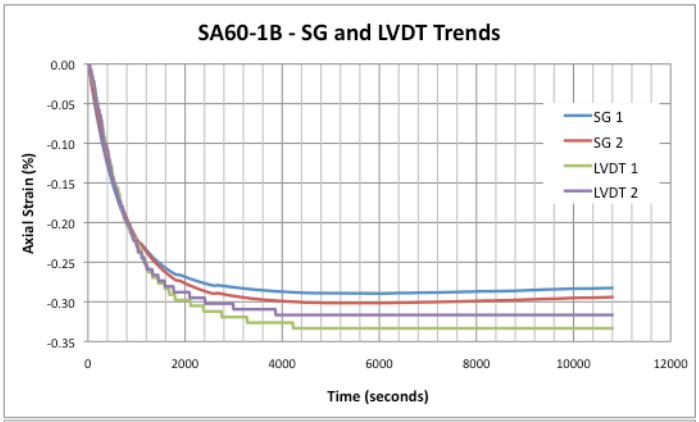
SA60-1B - SG and LVDT Trends
Axial Strain (%)
0.00
-0.05
-0.10
-0.15
-0.20
-0.25
-0.30
-0.35
0
2000
4000
6000
8000
10000
12000
Time (seconds)
SG 1
SG 2
LVDT 1
LVDT 2

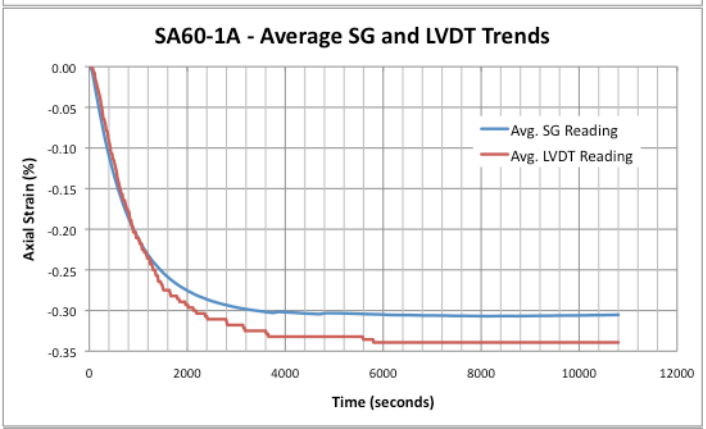
SA60-1A - Average SG and LVDT Trends
Axial Strain (%)
0.00
-0.05
-0.10
-0.15
-0.20
-0.25
-0.30
-0.35
0
2000
4000
6000
8000
10000
12000
Time (seconds)
Avg. SG Reading
Avg. LVDT Reading

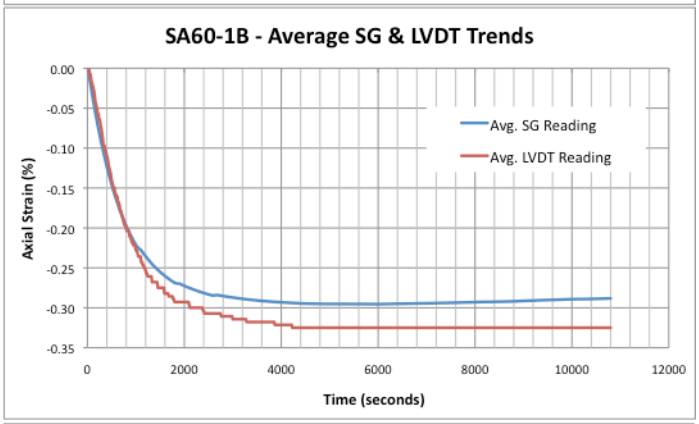
SA60-1B - Average SG & LVDT Trends
Axial Strain (%)
0.00
-0.05
-0.10
-0.15
-0.20
-0.25
-0.30
-0.35
0
2000
4000
6000
8000
10000
12000
Time (seconds)
Avg. SG Reading
Avg. LVDT Reading

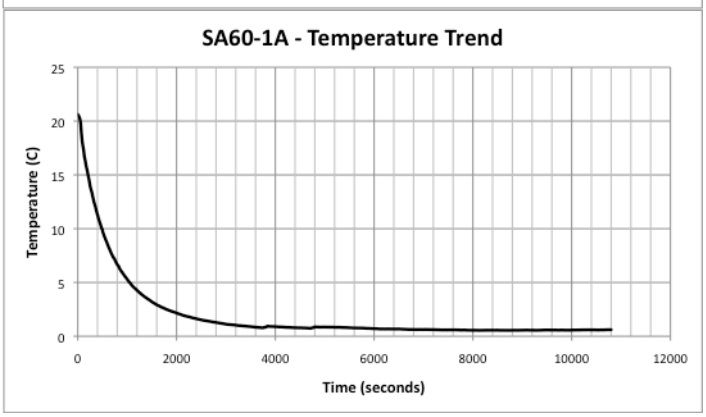
SA60-1A - Temperature Trend
Temperature (C)
25
20
15
10
5
0
0
2000
4000
6000
8000
10000
12000
Time (seconds)

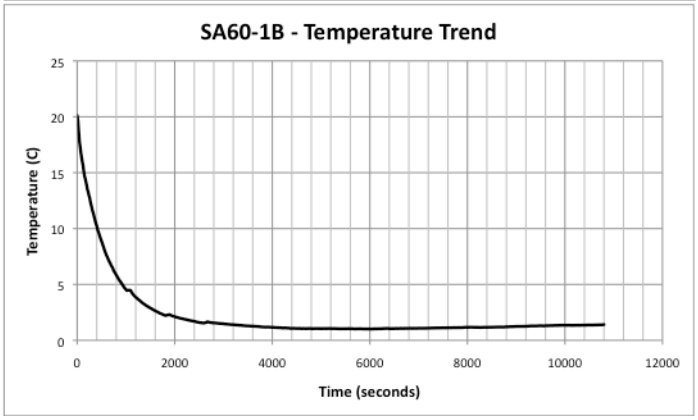
SA60-1B - Temperature Trend
Temperature (C)
25
20
15
10
5
0
0
2000
4000
6000
8000
10000
12000
Time (seconds)

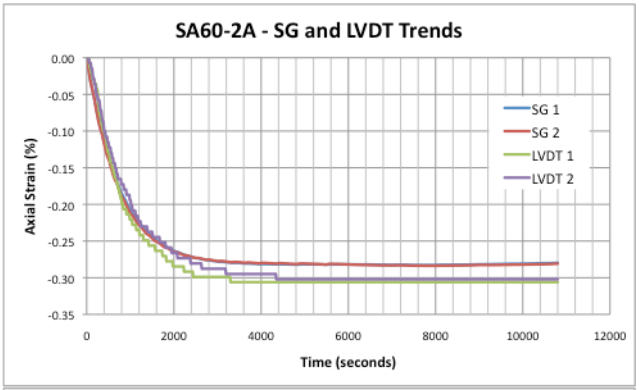
SA60-2A - SG and LVDT Trends
Axial Strain (%)
0.00
-0.05
-0.10
-0.15
-0.20
-0.25
-0.30
-0.35
0
2000
4000
6000
8000
10000
12000
Time (seconds)
SG 1
SG 2
LVDT 1
LVDT 2

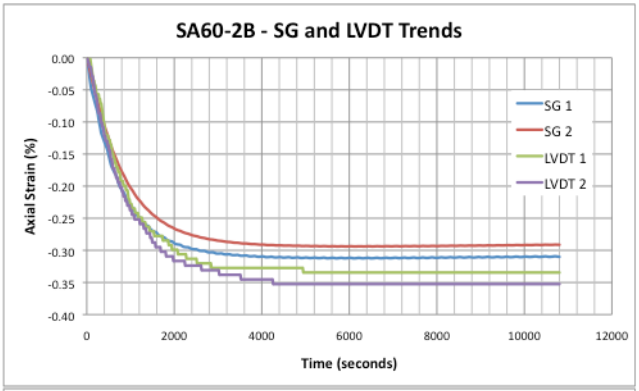
SA60-2B - SG and LVDT Trends
Axial Strain (%)
0.00
-0.05
-0.10
-0.15
-0.20
-0.25
-0.30
-0.35
-0.40
0
2000
4000
6000
8000
10000
12000
Time (seconds)
SG 1
SG 2
LVDT 1
LVDT 2

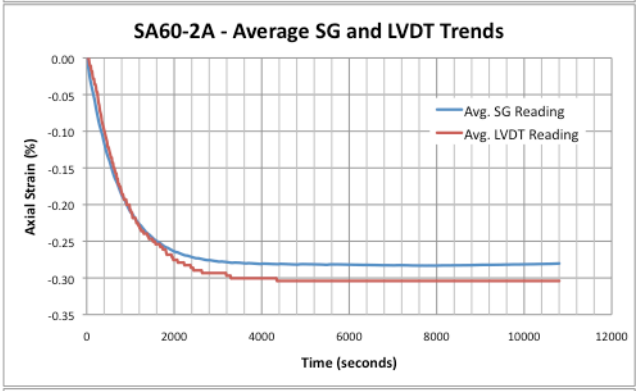
SA60-2A - Average SG and LVDT Trends
Axial Strain (%)
0.00
-0.05
-0.10
-0.15
-0.20
-0.25
-0.30
-0.35
0
2000
4000
6000
8000
10000
12000
Time (seconds)
Avg. SG Reading
Avg. LVDT Reading

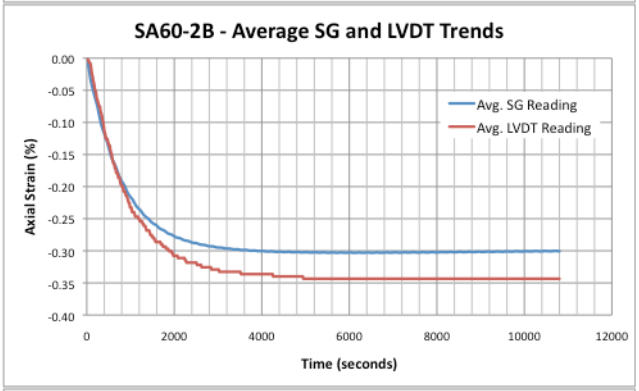
SA60-2B - Average SG and LVDT Trends
Axial Strain (%)
0.00
-0.05
-0.10
-0.15
-0.20
-0.25
-0.30
-0.35
-0.40
0
2000
4000
6000
8000
10000
12000
Time (seconds)
Avg. SG Reading
Avg. LVDT Reading

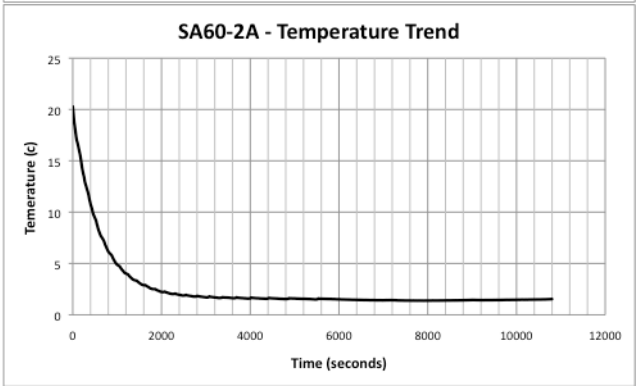
SA60-2A - Temperature Trend
Temerature (c)
25
20
15
10
5
0
0
2000
4000
6000
8000
10000
12000
Time (seconds)

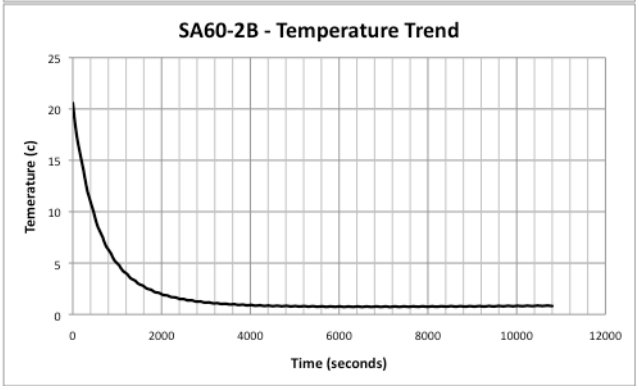
SA60-2B - Temperature Trend
Temerature (c)
25
20
15
10
5
0
0
2000
4000
6000
8000
10000
12000
Time (seconds)

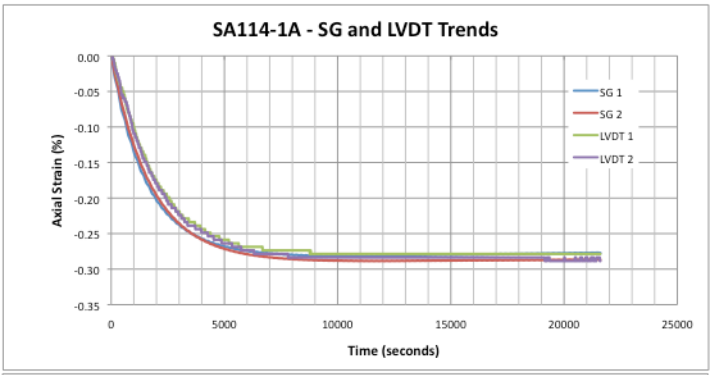
SA114-1A - SG and LVDT Trends
Axial Strain (%)
0.00
-0.05
-0.10
-0.15
-0.20
-0.25
-0.30
-0.35
0
5000
10000
15000
20000
25000
Time (seconds)
SG 1
SG 2
LVDT 1
LVDT 2

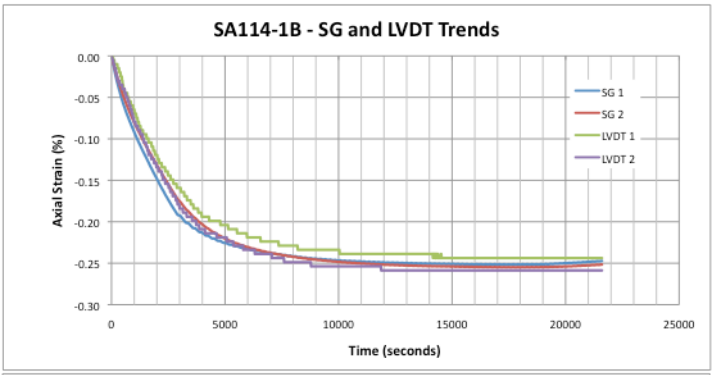
SA114-1B - SG and LVDT Trends
Axial Strain (%)
0.00
-0.05
-0.10
-0.15
-0.20
-0.25
-0.30
0
5000
10000
15000
20000
25000
Time (seconds)
SG 1
SG 2
LVDT 1
LVDT 2

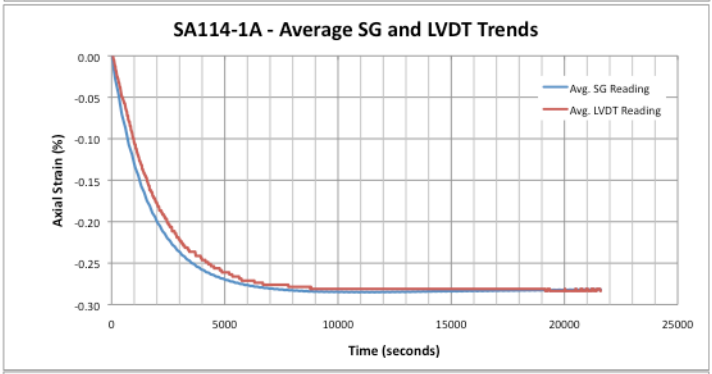
SA114-1A - Average SG and LVDT Trends
Axial Strain (%)
0.00
-0.05
-0.10
-0.15
-0.20
-0.25
-0.30
0
5000
10000
15000
20000
25000
Time (seconds)
Avg. SG Reading
Avg. LVDT Reading

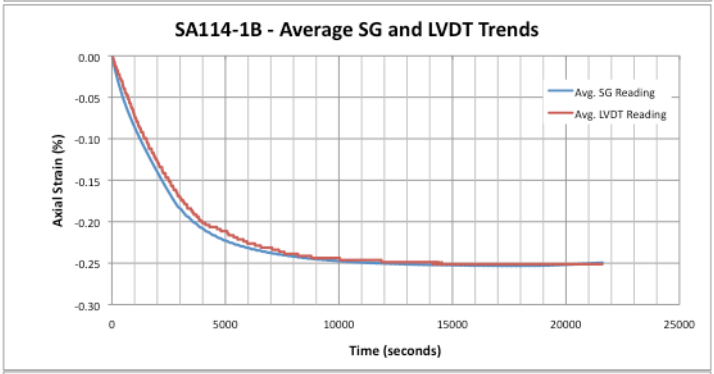
SA114-1B - Average SG and LVDT Trends
Axial Strain (%)
0.00
-0.05
-0.10
-0.15
-0.20
-0.25
-0.30
0
5000
10000
15000
20000
25000
Time (seconds)
Avg. SG Reading
Avg. LVDT Reading

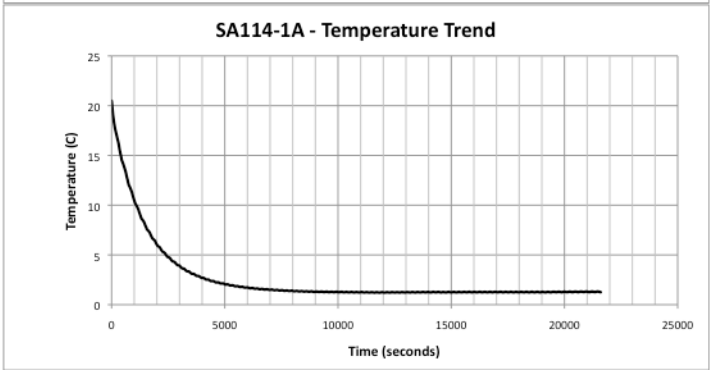
SA114-1A - Temperature Trend
Temperature (C)
25
20
15
10
5
0
0
5000
10000
15000
20000
25000
Time (seconds)

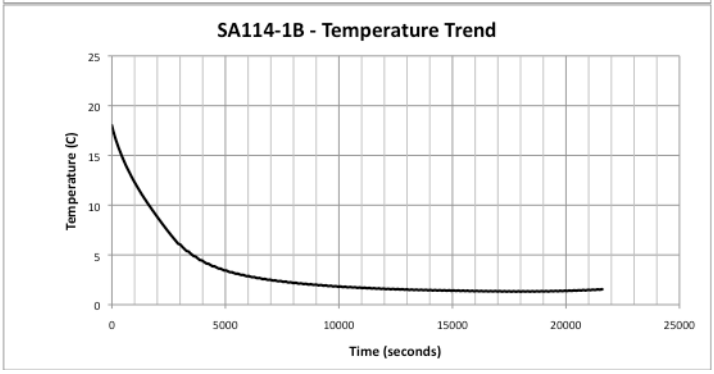
SA114-1B - Temperature Trend
Temperature (C)
25
20
15
10
5
0
0
5000
10000
15000
20000
25000
Time (seconds)

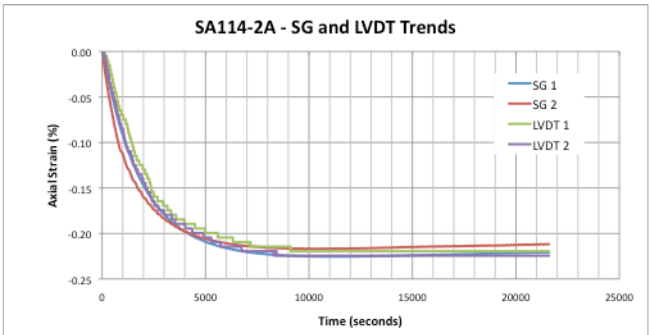
SA114-2A - SG and LVDT Trends
Axial Strain (%)
Time (seconds)
SG 1
SG 2
LVDT 1
LVDT 2

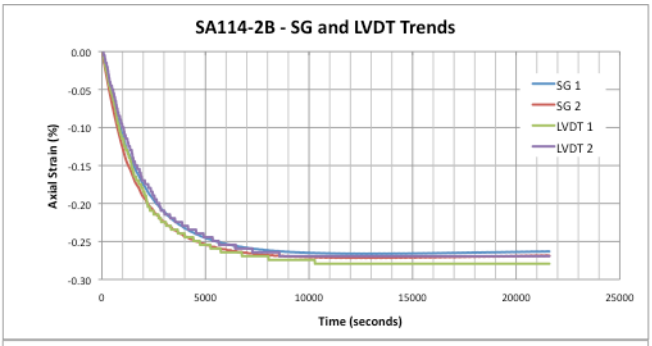
SA114-2B - SG and LVDT Trends
Axial Strain (%)
Time (seconds)
SG 1
SG 2
LVDT 1
LVDT 2

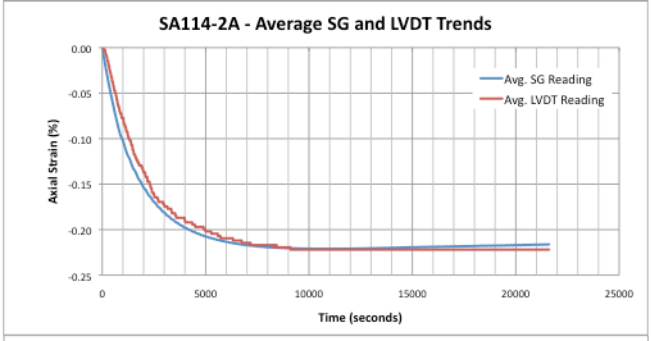
SA114-2A - Average SG and LVDT Trends
Axial Strain (%)
Time (seconds)
Avg. SG Reading
Avg. LVDT Reading

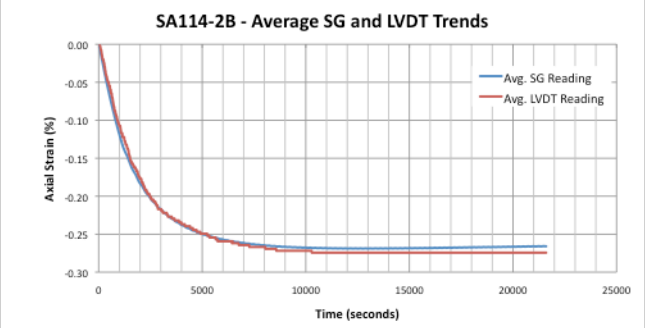
SA114-2B - Average SG and LVDT Trends
Axial Strain (%)
Time (seconds)
Avg. SG Reading
Avg. LVDT Reading

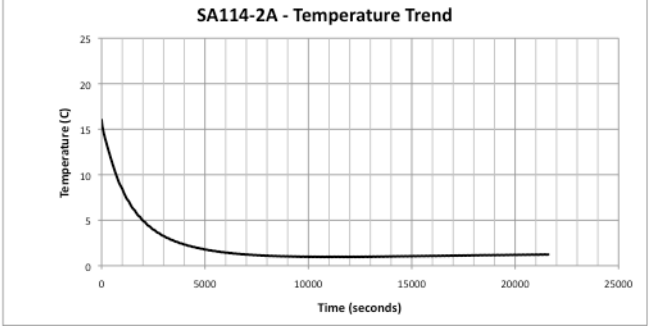
SA114-2A - Temperature Trend
Temperature (C)
Time (seconds)

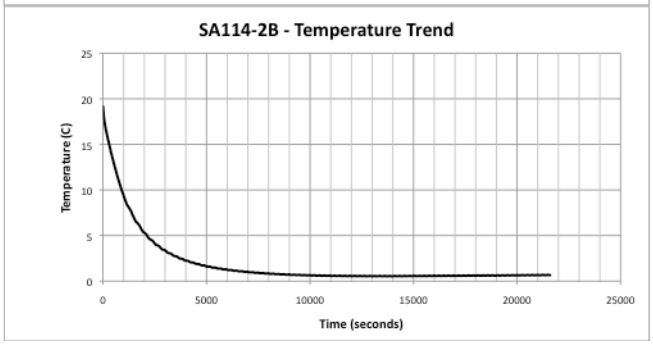
SA114-2B - Temperature Trend
Temperature (C)
Time (seconds)